



Counterparty Risk Modelling of Fixed Income Derivatives

by

Sijing Wang

Thesis submitted for the degree of

Doctoral of Philosophy

ICMA Centre

Henley Business School

University of Reading

October 2016

Abstract

The interdependency between the evolution of counterparty credit quality and the underlying risk factor(s) driving the value of a derivative contract has led to wrong way/right way risk, which could have a significant impact on the exposure and CVA profiles of OTC derivatives portfolios. Traditional approaches in modelling counterparty credit risk are mainly classified into Merton-type structural models and reduced form models. However, the former suffers from the drawback that the default probabilities generated from the model are not consistent with the market implied ones while the latter fails to offer a reasonable economic rationale and is of limited asset-credit correlation structures.

This thesis is dedicated to the modelling of wrong way/right way risk of fixed income derivatives based on the Bessel bridge approach proposed by Davis and Pistorius (2010). I begin with a brief review of the existing literature on counterparty credit risk modelling with a focus on structural and reduced-form approaches and pointing out the advantages and disadvantages of both methods. Then in the second part of the thesis, we go through the technical details of inverse first-passage time problem of the credit index process and Bessel bridge approach. We apply the unilateral version of the default framework to an FX-Hull-White hybrid setting for the exchange rate and correlated interest rates to establish a joint FX-credit unilateral default model. An extension to the bilateral version of the joint FX-credit default model without identifying the joint distribution density function of the two credit index processes conditional on default is presented in the third part of the thesis and extensive numerical analysis are conducted in the expected positive exposure profiles of a cross currency swap contract for various sets of FX-credit and default correlation sce-

narios. The impact of wrong way/right way risk illustrated are plausible . For the final main topic of thesis, we work on CVA of Bermudan swaptions. A multi-curve interest rate framework with stochastic basis spreads are developed, into which the unilateral Bessel bridge approach based joint interest rate-credit model is integrated and least-square Monte-Carlo simulation is applied to compute CVA with the presence of wrong way/right way risk.

Declaration of Original Authorship

I, Sijing Wang confirm that this thesis, titled "Counterparty Risk Modelling of Fixed Income Derivatives" is my own work and the use of all material from other sources has been properly and fully acknowledged.

Acknowledgements

In carrying out the work presented in this thesis I have had the opportunity to be supervised by both Dr Emese Lazar and Dr Martijn Pistorius, and I would like to express my gratitude to each of them for their help and support. This work was carried out under the terms of a fully sponsored PhD studentship at the ICMA Centre, University of Reading. I would like to thank Dr Alfonso Dufour, director of the PhD program at ICMA Centre for making this opportunity available to me, which has given me an invaluable experience for which I am truly grateful. During the course of my PhD studies I have had the opportunity to meet many people with whom I have had beneficial discussions, and to make many friends, both among staff and students at ICMA Centre-too many to name-but all of whom I would like to thank. I have also benefited from participation in the conferences and workshops of the European quantitative finance community, and from useful feedback concerning presentations of my work by participants at the International Finance and Banking Society Conference in Barcelona, Spain (2016), the Quantitative Finance and Risk Symposium in Rhodes Island, Greece (2016), the International Financial Engineering and Banking Society Conference in Malaga, Spain (2016), 14th Paris December Finance Meeting (upcoming 2016) and the European Summer School in Financial Mathematics in Saint Petersburg, Russia (2016). I would especially like to express my thanks to my parents for their constant support, encouragement, and unreserved love.

Table of Contents

Abstract	ii
Acknowledgments	v
Table of Contents	ix
List of Tables	xi
List of Figures	xx
1 Introduction	1
1.1 Motivation	1
1.2 Review of Counterparty Risk Modelling Framework	3
1.2.1 Structural Default Models	3
1.2.2 Reduced-Form Default Models	5
1.3 Original Contributions	6
1.4 General Valuation of Counterparty Credit Risk	7

1.4.1	Risk-Neutral Framework in the Credit Derivatives Market	7
1.4.2	Unilateral Counterparty Risk	8
1.4.3	Bilateral Counterparty Risk	10
1.4.4	Counterparty Risk Measures	11
2	Unilateral Counterparty Risk Modelling of FX Derivatives	15
2.1	Chapter Overview	15
2.2	IFPT Problem and Main Results	18
2.3	Bessel Bridge Approach for Wrong Way Risk Modelling	21
2.3.1	Credit Index Process Conditional on Default	21
2.3.2	Unilateral Joint Asset-Credit Modelling via Bessel bridges	26
2.4	Unilateral Joint FX-Credit Default Model	28
2.4.1	FX-Hull-White Hybrid Model	28
2.4.2	Exchange Rate Dynamics Conditional on Default	32
2.4.3	Calibration of Multi-Currency Framework	35
2.4.4	Calibration of Risk-Neutral Default Time Distribution	41
2.4.5	Bootstrapping of Survival Curves	43
2.5	Numerical Tests	45
2.5.1	Comparison with Hull and White (2001)	46
2.5.2	FX Forward	47

2.5.3	Cross Currency Swap	48
2.5.4	Cross Currency Swap Valuation Formula	49
2.5.5	Case Study I	50
2.5.6	Case Study II	53
2.6	Conclusions	54
3	Bilateral Counterparty Risk Modelling of Cross Currency Swaps	58
3.1	Chapter Overview	58
3.2	Bilateral Joint Asset-Credit Modelling via Bessel bridges	61
3.3	Application to Foreign Exchange Setting	65
3.3.1	Calibration of Risk-Neutral Default Time Distribution	65
3.3.2	Exchange Rate Dynamics Conditional on First-to-Default	67
3.4	Numerical Results	70
3.4.1	Case Study I	71
3.4.2	Case Study II	72
3.4.3	Case Study III	76
3.4.4	Conclusion	82
4	Bermudan Swaption CVA and Wrong Way Risk	84
4.1	Chapter Overview	84
4.2	Credit Value Adjustment	92

4.3	Multi-Curve Framework with Stochastic Basis Spreads	93
4.3.1	Assumptions and Notations	94
4.3.2	Model Dynamics	95
4.3.3	Caplet Pricing	97
4.3.4	A Example of Calibration to Market Data	99
4.4	Pricing Bermudan Swaption with Least Square Method	100
4.4.1	Bermudan Swaption	100
4.4.2	Least Squares Method	102
4.5	Joint Interest Rate-Credit Model via Bessel Bridges	106
4.5.1	Counterparty Risk Modelling via Bessel Bridges	106
4.6	Numerical Results	108
4.6.1	Setup	108
4.6.2	EPE and PFE	110
4.6.3	CVA	112
4.7	Conclusion	114
5	Conclusion	117
A	Histograms of EPEs and ENEs in Chapter 3	119

List of Tables

2.4.1 ATM Yen cap and ATM Dollar cap implied volatility quotes on 28th April 2014. Data Source: Bloomberg	36
2.4.2 ATM USDJPY FX call option implied volatility quotes on 28th April 2014. Data Source: Bloomberg	41
2.4.3 Market CDS term structure of Nomura International on 28th April 2014. . .	43
3.3.1 Market CDS term structures of Daiwa Securities and Nomura Securities on 28th April 2014. Data Source: Bloomberg	66
3.4.1 Summary of the correlation scenarios, numerical results and the standard error of unilateral and unilateral adjusted EPE simulations.	72
3.4.2 Summary of the correlation scenarios, numerical results and the standard errors of unilateral and unilateral adjusted EPE simulations.	74
3.4.3 Summary of the correlation scenarios, numerical results and the standard errors of unilateral adjusted ENE simulations.	76
3.4.4 Summary of the correlation scenarios, numerical results and the standard errors of unilateral adjusted EPE simulations.	78
3.4.5 Summary of the correlation scenarios, numerical results and the standard errors of unilateral and unilateral adjusted ENE simulations.	80

4.3.1 ATM Dollar cap implied volatility quotes on 28th April 2014. Data Source:	
Bloomberg	99
4.6.1 Market CDS term structures of Citigroup on 28th April 2014. Data Source:	
Bloomberg	109

List of Figures

2.4.1	Implied hazard function calibrated to 8 CDS quotes on Nomura International for maturities ranging from 6 months to 10 years.	43
2.4.2	Implied volatilities of the credit index process calibrated to 8 CDS quotes on Nomura International for maturities ranging from 6 months to 10 years.	44
2.4.3	Interpolated default probability curve generated from CDS quotes of Nomura International on 28th April 2014.	45
2.5.1	Implied Default barrier generated from CDS quotes of Nomura International on 28th April 2014, based on Hull and White (2001) approach.	47
2.5.2	Histograms of simulated exposure of 5-year USDJPY FX forward contract with strike $K = 95$ at $T = 5Y$ when $\rho_{S,Y} = -0.5$ and $\rho_{S,Y} = -0.3$	52
2.5.3	Histograms of simulated exposure of 5-year USDJPY FX forward contract with strike $K = 95$ at $T = 5Y$ when $\rho_{S,Y} = 0.3, 0.5$	52
2.5.4	Histograms of simulated exposure of 5-year USDJPY FX forward contract with strike $K = 95$ at $T = 5Y$ when $\rho_{S,Y} = 0$	52
2.5.5	EPEs and PFEs of the 5-year USDJPY FX forward contract across correlation scenarios ($\rho_{S,Y} = -0.5, -0.3, 0, +0.3, +0.5$).	53

2.5.6	EPEs of the 5-year USDJPY fixed-for-fixed cross currency swap computed on a quarterly basis across exchange rate-credit correlation scenarios.	55
2.5.7	PFEs 97.5% of the 5-year USDJPY fixed-for-fixed cross currency swap computed on a quarterly basis across exchange rate-credit correlation scenarios.	56
2.5.8	PFEs 2.5% of the 5-year USDJPY fixed-for-fixed cross currency swap computed on a quarterly basis across exchange rate-credit correlation scenarios.	57
3.2.1	Sample paths of investor and counterparty credit index processes, conditional on counterparty default at time 2Y.	63
3.3.1	Implied hazard rate and credit index volatility term structure from par CDS spreads of Daiwa Securities observed on 28th April 2014.	66
3.3.2	Implied hazard rate and credit index volatility term structure from par CDS spreads of Nomura Securities observed on 28th April 2014.	66
3.4.1	EPE profile of a 5-year fixed-for-fixed USDJPY cross currency swap from the point of view of Daiwa Securities conditional on first-to-default of Nomura Securities at $t = 2.5$ (years). Trade date: 28th April 2014, yen payer: Daiwa Securities, dollar payer: Nomura Securities, $K_{¥} = 1.38\%$, $K_{\$} = 1.5\%$, $S(0) = 102.5$, $N_0^{¥} = 1$, $\rho_{I,C} = 0.3$, $\rho_{I,S} = 0$, $\rho_{C,S} = \{-0.5, -0.3, 0, 0.3, 0.5\}$. Table 3.4.1 is the corresponding summary of the correlation scenarios, numerical results and the standard errors of EPE simulations.	72

3.4.2	<p>Unilateral adjusted EPE profile of a 5-year fixed-for-fixed USDJPY cross currency swap from the point of view of Daiwa Securities conditional on first-to-default of Nomura Securities at $t = 2.5$ (years). Trade date: 28th April 2014, yen payer: Daiwa Securities, dollar payer: Nomura Securities, $K_{¥} = 1.38\%$, $K_{\\$} = 1.5\%$, $S(0) = 102.5$, $N_0^{¥} = 1$, $\rho_{I,S} = 0$, $\rho_{C,S} = \{-0.5, -0.3, 0, 0.3, 0.5\}$, $\rho_{I,C} = \{0, 0.3, 0.5, 0.75\}$. Table 3.4.2 is the corresponding summary of the correlation scenarios, numerical results and the standard errors of EPE simulations.</p>	73
3.4.3	<p>Unilateral adjusted ENE profile of a 5-year fixed-for-fixed USDJPY cross currency swap from the point of view of Daiwa Securities conditional on first-to-default of Nomura Securities at $t = 2.5$ (years). Trade date: 28th April 2014, yen payer: Daiwa Securities, dollar payer: Nomura Securities, $K_{¥} = 1.38\%$, $K_{\\$} = 1.5\%$, $S(0) = 102.5$, $N_0^{¥} = 1$, $\rho_{I,S} = 0$, $\rho_{C,S} = \{-0.5, -0.3, 0, 0.3, 0.5\}$, $\rho_{I,C} = \{0, 0.3, 0.5, 0.75\}$. Table 3.4.3 is the corresponding summary of the correlation scenarios, numerical results and the standard errors of ENE simulations.</p>	75
3.4.4	<p>Bilateral EPE of a 5-year fixed-for-fixed USDJPY cross currency swap at $t = 2.5$ (years) observed on 28th April 2014. $K_{¥} = 1.38\%$, $K_{\\$} = 1.5\%$, $S(0) = 102.5$, $N_0^{¥} = 1$, $\rho_{I,S} = 0$, $\rho_{C,S} = \{-0.5, -0.3, 0, 0.3, 0.5\}$, $\rho_{I,C} = \{0, 0.3, 0.5, 0.75\}$.</p>	77
3.4.5	<p>Unilateral adjusted EPE profile of a 5-year fixed-for-fixed USDJPY cross currency swap from the point of view of Daiwa Securities conditional on first-to-default of Nomura Securities at $t = 2.5$ (years). Trade date: 28th April 2014, yen payer: Daiwa Securities, dollar payer: Nomura Securities, $K_{¥} = 1.38\%$, $K_{\\$} = 1.5\%$, $S(0) = 102.5$, $N_0^{¥} = 1$, $\rho_{C,S} = 0$, $\rho_{I,S} = \{-0.5, -0.3, 0, 0.3, 0.5\}$, $\rho_{I,C} = \{0, 0.3, 0.5, 0.75\}$. Table 3.4.4 is the corresponding summary of the correlation scenarios, numerical results and the standard errors of EPE simulations.</p>	79

3.4.6	Unilateral adjusted ENE profile of a 5-year fixed-for-fixed USDJPY cross currency swap from the point of view of Daiwa Securities conditional on first-to-default of Daiwa Securities at $t = 2.5$ (years). Trade date: 28th April 2014, yen payer: Daiwa Securities, dollar payer: Nomura Securities, $K_{¥} = 1.38\%$, $K_{\$} = 1.5\%$, $S(0) = 102.5$, $N_0^{¥} = 1$, $\rho_{I,S} = 0$, $\rho_{C,S} = \{-0.5, -0.3, 0, 0.3, 0.5\}$, $\rho_{I,C} = \{0, 0.3, 0.5, 0.75\}$. Table 3.4.5 is the corresponding summary of the correlation scenarios, numerical results and the standard errors of ENE simulations.	81
3.4.7	Bilateral EPE of a 5-year fixed-for-fixed USDJPY cross currency swap at $t = 2.5$ (years) observed on 28th April 2014. $K_{¥} = 1.38\%$, $K_{\$} = 1.5\%$, $S(0) = 102.5$, $N_0^{¥} = 1$, $\rho_{C,S} = 0$, $\rho_{I,S} = \{-0.5, -0.3, 0, 0.3, 0.5\}$, $\rho_{I,C} = \{0, 0.3, 0.5, 0.75\}$	82
4.1.1	The notional amounts (in trillions of US dollars) outstanding of OTC derivatives by risk category from BIS semi-annual survey, June 1998 through December 2013.	85
4.1.2	3-month Libor-OIS spread since June 2008	86
4.1.3	Libor rates of tenor 1M, 3M, 6M, 12M since the crisis	87
4.6.1	Implied hazard rate and credit index volatility term structures from par CDS spreads of Citigroup observed on 28th April 2014.	109
4.6.2	The 3M USD forward Libor-OIS spread on 28th April 2014. Data Source: Bloomberg	110
4.6.3	The EPE of a cash-settled Bermudan swaption with 5-year maturity and 1-year lockout period on 28th April 2014. $K = 1\%$, $N = \$100000$, $\rho_{C,S} = \{-0.5, -0.4, -0.2, 0, 0.2, 0.4, 0.5\}$	111

4.6.4	The EPE of a cash-settled Bermudan swaption with 10-year maturity and 1-year lockout period on 28th April 2014. $K = 1\%$, $N = \$100000$, $\rho_{C,S} = \{-0.5, -0.4, -0.2, 0, 0.2, 0.4, 0.5\}$	111
4.6.5	The EPE of a cash-settled Bermudan swaption with 10-year maturity and 5-year lockout period on 28th April 2014. $K = 1\%$, $N = \$100000$, $\rho_{C,S} = \{-0.5, -0.4, -0.2, 0, 0.2, 0.4, 0.5\}$	112
4.6.6	The 97.5% PFE of a cash-settled Bermudan swaption with 5-year maturity and 1-year lockout period on 28th April 2014. $K = 1\%$, $N = \$100000$, $\rho_{C,S} = \{-0.5, -0.4, -0.2, 0, 0.2, 0.4, 0.5\}$	112
4.6.7	The 97.5% PFE of a cash-settled Bermudan swaption with 10-year maturity and 1-year lockout period on 28th April 2014. $K = 1\%$, $N = \$100000$, $\rho_{C,S} = \{-0.5, -0.4, -0.2, 0, 0.2, 0.4, 0.5\}$	113
4.6.8	The 97.5% PFE of a cash-settled Bermudan swaption with 10-year maturity and 5-year lockout period on 28th April 2014. $K = 1\%$, $N = \$100000$, $\rho_{C,S} = \{-0.5, -0.4, -0.2, 0, 0.2, 0.4, 0.5\}$	113
4.6.9	The CVA of a cash-settled Bermudan swaption with 5-year maturity and 1-year lockout period on 28th April 2014. $K = 1\%$, $N = \$100000$, $\rho_{C,S} = \{-0.5, -0.4, -0.2, 0, 0.2, 0.4, 0.5\}$	114
4.6.10	The CVA of a cash-settled Bermudan swaption with 10-year maturity and 1-year lockout period on 28th April 2014. $K = 1\%$, $N = \$100000$, $\rho_{C,S} = \{-0.5, -0.4, -0.2, 0, 0.2, 0.4, 0.5\}$	115
4.6.11	The CVA of a cash-settled Bermudan swaption with 10-year maturity and 5-year lockout period on 28th April 2014. $K = 1\%$, $N = \$100000$, $\rho_{C,S} = \{-0.5, -0.4, -0.2, 0, 0.2, 0.4, 0.5\}$	115

A.0.1	Histograms of the exposures of the 5-year fixed-for-fixed USDJPY cross currency swap from the point of view of Daiwa Securities conditional on first-to-default of Nomura Securities at $t = 2.5$ (years). Unilateral Case: $\rho_{C,S} = -0.5$. Bilateral Case: $\rho_{C,S} = -0.5, \rho_{I,S} = 0, \rho_{I,C} = \{0, 0.3, 0.5, 0.75\}$	119
A.0.2	Histograms of the exposures of the 5-year fixed-for-fixed USDJPY cross currency swap from the point of view of Daiwa Securities conditional on first-to-default of Nomura Securities at $t = 2.5$ (years). Unilateral Case: $\rho_{C,S} = -0.3$. Bilateral Case: $\rho_{C,S} = -0.3, \rho_{I,S} = 0, \rho_{I,C} = \{0, 0.3, 0.5, 0.75\}$	120
A.0.3	Histograms of the exposures of a 5-year fixed-for-fixed USDJPY cross currency swap conditional on first-to-default of Nomura Securities at $t = 2.5$ (years) observed on 28th April 2014. Unilateral Case: $\rho_{C,S} = 0$. Bilateral Case: $\rho_{C,S} = 0, \rho_{I,S} = 0, \rho_{I,C} = \{0, 0.3, 0.5, 0.75\}$	121
A.0.4	Histograms of the exposures of a 5-year fixed-for-fixed USDJPY cross currency swap conditional on first-to-default of Nomura Securities at $t = 2.5$ (years) observed on 28th April 2014. Unilateral Case: $\rho_{C,S} = 0.3$. Bilateral Case: $\rho_{C,S} = 0.3, \rho_{I,S} = 0, \rho_{I,C} = \{0, 0.3, 0.5, 0.75\}$	121
A.0.5	Histograms of the exposures of a 5-year fixed-for-fixed USDJPY cross currency swap conditional on first-to-default of Nomura Securities at $t = 2.5$ (years) observed on 28th April 2014. Unilateral Case: $\rho_{C,S} = 0.5$. Bilateral Case: $\rho_{C,S} = 0.5, \rho_{I,S} = 0, \rho_{I,C} = \{0, 0.3, 0.5, 0.75\}$	122
A.0.6	Histograms of the exposures of a 5-year fixed-for-fixed USDJPY cross currency swap conditional on first-to-default of Daiwa Securities at $t = 2.5$ (years) observed on 28th April 2014. $\rho_{C,S} = -0.5, \rho_{I,S} = 0, \rho_{I,C} = \{0, 0.3, 0.5, 0.75\}$	122

A.0.7	Histograms of the exposures of a 5-year fixed-for-fixed USDJPY cross currency swap conditional on first-to-default of Nomura Securities at $t = 2.5$ (years) observed on 28th April 2014. $\rho_{C,S} = -0.3, \rho_{I,S} = 0, \rho_{I,C} = \{0, 0.3, 0.5, 0.75\}$	122
A.0.8	Histograms of the exposures of a 5-year fixed-for-fixed USDJPY cross currency swap conditional on first-to-default of Nomura Securities at $t = 2.5$ (years) observed on 28th April 2014. $\rho_{C,S} = 0, \rho_{I,S} = 0, \rho_{I,C} = \{0, 0.3, 0.5, 0.75\}$	123
A.0.9	Histograms of the exposures of a 5-year fixed-for-fixed USDJPY cross currency swap conditional on first-to-default of Daiwa Securities at $t = 2.5$ (years) observed on 28th April 2014. $\rho_{C,S} = 0, \rho_{I,S} = -0.3, \rho_{I,C} = \{0, 0.3, 0.5, 0.75\}$	123
A.0.10	Histograms of the exposures of a 5-year fixed-for-fixed USDJPY cross currency swap conditional on first-to-default of Daiwa Securities at $t = 2.5$ (years) observed on 28th April 2014. $\rho_{C,S} = 0, \rho_{I,S} = 0, \rho_{I,C} = \{0, 0.3, 0.5, 0.75\}$	123
A.0.11	Histograms of the exposures of a 5-year fixed-for-fixed USDJPY cross currency swap conditional on first-to-default of Daiwa Securities at $t = 2.5$ (years) observed on 28th April 2014. $\rho_{C,S} = 0, \rho_{I,S} = -0.5, \rho_{I,C} = \{0, 0.3, 0.5, 0.75\}$	124
A.0.12	Histograms of the exposures of a 5-year fixed-for-fixed USDJPY cross currency swap conditional on first-to-default of Daiwa Securities at $t = 2.5$ (years) observed on 28th April 2014. $\rho_{C,S} = 0, \rho_{I,S} = -0.3, \rho_{I,C} = \{0, 0.3, 0.5, 0.75\}$	124

A.0.13 Histograms of the exposures of a 5-year fixed-for-fixed USDJPY cross currency swap conditional on first-to-default of Daiwa Securities at $t = 2.5$ (years) observed on 28th April 2014. $\rho_{C,S} = 0, \rho_{I,S} = 0, \rho_{I,C} = \{0, 0.3, 0.5, 0.75\}$	124
A.0.14 Histograms of the exposures of a 5-year fixed-for-fixed USDJPY cross currency swap conditional on first-to-default of Daiwa Securities at $t = 2.5$ (years) observed on 28th April 2014. $\rho_{C,S} = 0, \rho_{I,S} = 0.3, \rho_{I,C} = \{0, 0.3, 0.5, 0.75\}$	125
A.0.15 Histograms of the exposures of a 5-year fixed-for-fixed USDJPY cross currency swap conditional on first-to-default of Daiwa Securities at $t = 2.5$ (years) observed on 28th April 2014. $\rho_{C,S} = 0, \rho_{I,S} = 0.5, \rho_{I,C} = \{0, 0.3, 0.5, 0.75\}$	125
A.0.16 Histograms of the exposures of a 5-year fixed-for-fixed USDJPY cross currency swap conditional on first-to-default of Daiwa Securities at $t = 2.5$ (years) observed on 28th April 2014. Unilateral Case: $\rho_{I,S} = -0.5$. Bilateral Case: $\rho_{C,S} = 0, \rho_{I,S} = -0.5, \rho_{I,C} = \{0, 0.3, 0.5, 0.75\}$	125
A.0.17 Histograms of the exposures of a 5-year fixed-for-fixed USDJPY cross currency swap conditional on first-to-default of Daiwa Securities at $t = 2.5$ (years) observed on 28th April 2014. Unilateral Case: $\rho_{I,S} = -0.3$. Bilateral Case: $\rho_{C,S} = 0, \rho_{I,S} = -0.3, \rho_{I,C} = \{0, 0.3, 0.5, 0.75\}$	126
A.0.18 Histograms of the exposures of a 5-year fixed-for-fixed USDJPY cross currency swap conditional on first-to-default of Daiwa Securities at $t = 2.5$ (years) observed on 28th April 2014. Unilateral Case: $\rho_{I,S} = 0$. Bilateral Case: $\rho_{C,S} = 0, \rho_{I,S} = 0, \rho_{I,C} = \{0, 0.3, 0.5, 0.75\}$	126

A.0.19 Histograms of the exposures of a 5-year fixed-for-fixed USDJPY cross currency swap conditional on first-to-default of Daiwa Securities at $t = 2.5$ (years) observed on 28th April 2014. Unilateral Case: $\rho_{I,S} = 0.3$. Bilateral Case: $\rho_{C,S} = 0, \rho_{I,S} = 0.3, \rho_{I,C} = \{0, 0.3, 0.5, 0.75\}$ 127

A.0.20 Histograms of the exposures of a 5-year fixed-for-fixed USDJPY cross currency swap conditional on first-to-default of Daiwa Securities at $t = 2.5$ (years) observed on 28th April 2014. Unilateral Case: $\rho_{C,S} = 0.5$. Bilateral Case: $\rho_{C,S} = 0, \rho_{I,S} = 0.5, \rho_{I,C} = \{0, 0.3, 0.5, 0.75\}$ 127

Chapter 1

Introduction

1.1 Motivation

Counterparty risk is the risk taken by an investor entering into financial transactions with one (or more) counterparties, varying among sovereign entities, corporates, hedge funds, insurance companies having a relevant default probability. It can be seen as an integration of two sources of risks: credit risk, which reflects the likelihood of not only counterparty default but also one's own default, and market risk, which determines the size of either the investor's exposure upon default of the counterparty or vice and versa. The bilateral nature of default and the uncertainty of future exposure in OTC derivatives transactions are the two features that differentiate counterparty risk from traditional form of credit risk, where sovereigns and banks are assumed to be almost default-free and mainly corporate loans and bonds with fixed economic loss upon default are considered. The volume of outstanding OTC derivatives has grown exponentially over the past 20 years. These derivatives have played an important role in the financial markets in terms of transferring risk and creating connections among markets and market participants. However, the privately negotiated feature between counterparties of OTC derivatives leaves these contracts subject to counterparty risk when a party to an OTC derivatives contract may fail to perform on its contractual

obligations, causing losses to the other party. High-profile defaults of Bear Stearns and Lehman Brothers during the financial crisis have intensified concerns about counterparty risk embedded in OTC bank-to-bank and bank-to-corporate derivatives transactions and the ever-increasing interconnectedness within the financial system has significantly complicated risk quantification. Furthermore, from the regulatory perspective, Basel III Accord mentions that in addition to the default risk capital requirements for counterparty credit risk determined based on the standardised or internal ratings-based (IRB) approaches for credit risk (specified in Basel II), a bank must add a capital charge to cover the risk of mark-to-market losses on the expected counterparty risk (such losses being known as credit value adjustments, CVA) to OTC derivatives. In particular, banks must demonstrate, at least quarterly, that the stress period coincides with a period of increased CDS or other credit spreads (deterioration in credit qualities) - such as loan or corporate bond spreads - for a representative selection of the bank's counterparties with traded credit spreads and how it would affect the counterparty exposure model calibration and capital calculation, which makes the valuation and hedging of CVA with wrong way risk a strategic issue.

It is usually assumed in the conventional approach to measuring counterparty risk that the credit quality of the counterparties involved in the transaction is independent of the underlying asset value driving the counterparty exposure. However, lessons from the Asian financial crisis and the US sub-prime mortgage crisis have led to a consensus that major systemic or economic shocks can be exacerbated by potential counterparty related funding stress and subsequent credit quality deterioration. Therefore it is of great importance for risk modellers to quantify the impact of dependency between credit and market risk factors, which requires joint modelling of the credit quality of counterparties as well as underlying asset values.

The effect of asset-credit correlation is most commonly manifested in the form of wrong way risk (WWR), which arises when the value of the exposure to a certain counterparty is adversely correlated with the credit quality of that counterparty. Specifically, in our work we focus on general or conjectural wrong way risk, where the credit quality of

the counterparty may for non-specific reasons be held to be correlated with macroeconomic factors that also affect the value of derivatives transactions. An example of transaction with wrong way risk can be a USD/Baht cross currency swap contract (where the USD/Baht pair is quoted as x units of Thai Baht per US dollar) executed in March 1997 between a US bank with investment grade credit rating and a poorly capitalized Thai bank with high level of dollar denominated debt on its balance sheet. In March 1998, the Asia financial crisis triggered sharp swings in the FX market which resulted in severe declines in the value of baht against dollar. The rising debt servicing cost led to the deterioration of the Thai bank's credit quality while the currency movement increased the US bank's exposure to the Thai bank dramatically. In this case, even if you hold the Thai Baht denominated notional as a source of collateral, the value of the notional falls rapidly while your counterparty exposure is actually increasing due to the depreciation of Thai Baht, and hence the notional alone is insufficient in compensating your loss should the counterparty default. The reciprocal case where the value of the exposure is positively correlated with the credit quality of the counterparty is referred to as right way risk (RWR). An example of transaction can be that a bank sells a call option written on its own stock. Negative outlook or downgrade of the bank's credit status will be reflected in the drop of bank's share price, which could reduce the value of the call option and hence the bank's exposure to the option buyer.

1.2 Review of Counterparty Risk Modelling Framework

Established methods on modelling counterparty risk primarily fall into two categories: i) Merton-type/structural approach; ii) reduced-form approach. We now give an overview of the existing literatures on the two approaches.

1.2.1 Structural Default Models

First, the structural default approach initiated by Merton (1974), where a firm defaults if, at the time of servicing the debt, its asset value is below its outstanding debt value. The

Merton's model is later extended by Black and Cox (1976) who allow default to occur at any time throughout the life of the contract and model the time of default as the first time the ratio of firm's share price and the its debt value falls below a deterministic time-dependent barrier. The case of an exogenously specified constant default barrier is also considered (see, for example, Kim et al. (1993); Longstaff and Schwartz (1995)). Under the first-passage time framework, the value of the firm's equity can be regarded as a call option written on the firm's asset and struck at its debt value that is knocked-out at time of default. Modelling the debt by a zero-coupon bond with deterministic interest rate and the equity value by a geometric Brownian motion with constant drift and volatility, the default time distribution is equal to that of the first-passage time of a Brownian motion below the default barrier. Dependence between entities can be simply incorporated and an economic rationale behind default is offered as the model is linked to a company's fundamentals.

Further extensions of the first-passage time model to multi-dimensional versions are led by Zhou (2001a); Patras (2006); Haworth et al. (2008); Valuzis (2008) and several other researchers, where correlated lognormal dynamics for two firms' balance sheets are specified and analytical formulas for their joint survival probability distribution are derived using the eigenvalue expansion technique. However, the classical Brownian motion asset value model fails to explain high short-term CDS spreads observed in the market as the predictability of default event under such model leads to almost zero near term default probability for non-distressed firms. Improvements surrounding this issue have considered including non-linear or random default barrier (see, for example, Avellaneda and Zhu (2001); Brigo and Tarengi (2005); Brigo and Morini (2006); Brigo et al. (2011b)) and jump diffusion into asset value dynamics (see, for example, Zhou (2001b); Sepp (2006); Lipton and Sepp (2009); Fiorani et al. (2010); Lipton and Savescu (2012, 2013)). Furthermore, the class of Lévy processes is also being explored to replace the Brownian motion when modelling of asset value (see, for example, Cariboni and Schoutens (2007); Baxter (2007); Ballotta and Fusai (2014)).

1.2.2 Reduced-Form Default Models

The second major family of joint asset-credit models belong to the reduced form approach where default is modelled through an exogenous stochastic intensity process independent of the information arising from the default-free market. Leung and Kwok (2005) model default intensities as deterministic constants with default indicators of other names as feeds. The exponential triggers of the default times are taken to be independent and default correlation results from the cross feeds, although there is no explicit modelling of credit spread volatility and as a result may underestimate CVA. Brigo and Pallavicini (2008) propose CIR stochastic intensity processes, which are used for default intensities dynamics of the counterparty and the underlying reference entity and default correlation is modelled with a Gaussian copula function. They find that both default correlation and credit spread volatilities have a relevant and structured impact on the adjustment. The approach is further applied by Brigo and Chourdakis (2009) for the counterparty risk valuation of energy-commodity swaps and by Brigo and Capponi (2010) who extend it to the bilateral CVA valuation of CDS portfolios and derive a symmetric mathematical expression for the CVA where the two counterparties will agree on the value of CVA. Another category of research focuses on modelling wrong way risk by correlating the driving risk factors with the default intensity process, Pykhtin (2012) presents an algorithm that converts the unconditional distribution of netting-set-level exposure generated by an arbitrary Monte Carlo simulation process to an exposure at default (EAD) measure that consistently incorporates general WWR under the asymptotic single risk factor (ASRF) framework. Lipton and Shelton (2012) present an affine jump-diffusion framework for calculating the prices of credit default swaps (CDSs) with and without credit value adjustments (CVA) to account for counterparty risk. Closed-form expressions for the CVA in this framework are obtained in the limit of pure diffusion, and an expansion of the Green function in powers of the jump intensity is applicable in the general case. They show that in order to generate sufficient correlation to capture this so-called wrong-way risk, simultaneous jumps in the credit spreads of buyer, seller and reference entity are required. Other notable literatures include Ghamami and Goldberg (2014), Ghamami and Carr (2015); Li and Mercurio (2015). Alternative methods for wrong way

risk modelling such as scenario weighting (see, for example, Turlakov (2013); Glasserman and Yang (2015)) or adjusting default probability in the independence based CVA formula (see, for example Hull and White (2012) that captures wrong way risk by expressing the stochastic intensity of a counterparty default time in terms of the financial institution's credit exposure to the counterparty) are also proposed.

1.3 Original Contributions

In this thesis, we focus on the counterparty risk modelling of fixed income derivatives, with a particular emphasis on explicitly modelling and quantifying the impact of wrong way/right way risk on counterparty exposure profiles and CVAs. In Chapter 2, we present a unilateral version of a structural default model for modelling counterparty risk of FX forwards and cross currency swaps using the Bessel bridge approach proposed by Davis and Pistorius (2010). By combining the multi-currency framework with the unilateral default model, we establish a joint FX-credit default model that is able to capture the impact of exchange rate-credit correlation on the counterparty exposure measured by various risk metrics such as expected positive exposures and potential future exposures. The FX-credit correlation can be easily incorporated onto the driving Brownian motions of the exchange rate. Furthermore, the stochastic nature of the interest rate processes allows for the introduction of additional correlation structures between the interest rate and counterparty credit qualities and the model is tractable for the counterparty risk modelling of other FX-rates hybrid derivatives.

In Chapter 3, we extend our model to the bilateral version of the FX-credit default framework. Following Chapter 1, the credit index processes of two counterparties are introduced and their respective default times are modelled as inverse first-passage time problems. However, instead of trying to identify joint default distribution of the two counterparties conditional on the first-to-default counterparty through sophisticated numerical methods and jointly simulate the two credit index processes. We take a simpler yet efficient approach

by simulating the assumed first-to-default counterparty in terms of three-dimensional Bessel bridges and extract the path of the non-default counterparty through their correlated Brownian motions. Even though the joint conditional default probabilities cannot be explicitly derived, our approach is flexible in simulating counterparty exposures. Extensive numerical analysis are carried out and studied on the impact of the various correlation scenarios between the counterparty credit quality and the exchange rate, the investor credit quality and the exchange rate and the default correlation between the two counterparties.

In the final chapter, we work on Bermudan swaption CVAs with the presence of wrong way/right way risks. We establish a multi-curve interest rate framework with stochastic basis spreads, which is in line with post-crisis market practice in the treatment of interest rate modelling. Furthermore, we successfully integrate the Bessel bridge default model where wrong way/right way risk can be modelled explicitly into the multi-curve interest rate framework and come up with an approximation for the CVA of Bermudan swaptions. The model is robust and computationally efficient to capture the impact of wrong way/right way risk on the expected positive exposures and CVAs of Bermudan swaptions.

1.4 General Valuation of Counterparty Credit Risk

We begin by introducing the general valuation of counterparty credit risk in the unilateral and bilateral default cases. Let us refer to the two parties engaging in a generic derivative transaction subject to default risk as investor ("I") and counterparty ("C") and address valuation as seen from the point of view of the investor so that the cash flow received by investor will be positive whereas cash flows paid by investor will be seen as negative.

1.4.1 Risk-Neutral Framework in the Credit Derivatives Market

We place ourselves in a probability space $(\Omega, \mathcal{F}, \{\mathcal{F}_t\}_{t \geq 0}, \mathbb{Q})$, where $\{\mathcal{F}_t\}_{t \geq 0}$ is the filtration modelling the whole market information flow and we assume there exists a risk-neutral

measure \mathbb{Q}^1 . Let us denote by T the maturity of the transaction, by $\Pi(t, T)$ the money market account $B(t)$ discounted contractual cashflows until maturity subject to no default and by $V(t, T)$ the default-free value of the contract known with certainty at current time t , which can also be written as $V(t, T) = \mathbb{E}^{\mathbb{Q}}[\Pi(t, T)|\mathcal{F}_t]$. For more details, refer to Schönbucher (2003).

To set up a risk-neutral framework, we denote default time as τ , the survival indicator function $I(t) = 1$ if $\tau > t$ and $I(t) = 0$ if $\tau \leq t$. The default-free zero-coupon bonds (ZCB) with all maturities $T > t$ are defined as

$$P(t, T) = \text{price of ZCB paying 1 at } T. \quad (1.1)$$

and the defaultable zero-coupon bonds with all maturities $T > t$ are defined as

$$P^D(t, T) = \text{price of defaultable ZCB if } \tau > t. \quad (1.2)$$

To ensure no-arbitrage we must require that the defaultable zero-coupon bond is always worth less than its corresponding default-free zero-coupon bond. And the bond prices are a decreasing, non-negative function of maturity T . A risk-neutral probability of an event A at time T is simply the state price of a security that pays 1 at time T if A occurs, which is $\mathbb{E}^{\mathbb{Q}}[DF(T) * \mathbf{1}_A]$, where DF is the money market account discount factor. Standard procedure on how to convert from real world probability measure to risk-neutral measure based on Girsanov theorem will not be detailed here.

1.4.2 Unilateral Counterparty Risk

Suppose that the investor is default-free while the counterparty is defaultable² and denote τ_C the default time of the counterparty and $\Pi^D(t, T)$ the contractual cash flows until maturity discounted back to time t and subject to counterparty default risk, then we have the default-

¹In the credit derivatives market, there may not be a unique risk-neutral measure

²It does not only refer to bankruptcy. The cross of barrier zero refers to any credit event specified in the CDS contract that the model is calibrated to

risky value of the contract $V^D(t, T)$ at time t conditional on $\{t < \tau_C \leq T\}$:

$$\begin{aligned}
 V^D(t, T) &= \mathbb{E}^{\mathbb{Q}}[\Pi^D(t, T)|\mathcal{F}_t] = \mathbb{E}^{\mathbb{Q}}[\Pi(t, T)|\mathcal{F}_t] \\
 &\quad - (1 - R_C)\mathbb{E}^{\mathbb{Q}}[\mathbb{E}^{\mathbb{Q}}[\mathbf{1}_{\{t < \tau_C = s \leq T\}}D(t, s)V(s, T)^+|\mathcal{F}_s]|\mathcal{F}_t] \\
 &= \mathbb{E}^{\mathbb{Q}}[\Pi(t, T)|\mathcal{F}_t] \\
 &\quad - (1 - R_C)\mathbb{E}^{\mathbb{Q}}[\mathbf{1}_{\{t < \tau_C \leq T\}}D(t, \tau_C)V(\tau_C, T)^+|\mathcal{F}_t]
 \end{aligned} \tag{1.3}$$

where $V^+ = \max(0, V)$, $D(t, s)$ is the stochastic discount factor at time t with maturity s and R_C ³ is the recovery rate that is exchanged as a proportion of the net present value of the contract upon default of the counterparty. The second component in equation 1.3 is the adjustment to the default-free value of the contract accounting for counterparty default. For proof of the formula, see Brigo and Masetti (2006).

Similarly, we can also consider the case where the investor is defaultable while the counterparty is default-free with analogous notations, then the corresponding default-risky value $V^D(t, T)$ at time t conditional on $\{t < \tau_I \leq T\}$ is :

$$\begin{aligned}
 V^D(t, T) &= \mathbb{E}^{\mathbb{Q}}[\Pi^D(t, T)|\mathcal{F}_t] = \mathbb{E}^{\mathbb{Q}}[\Pi(t, T)|\mathcal{F}_t] \\
 &\quad + (1 - R_I)\mathbb{E}^{\mathbb{Q}}[\mathbb{E}^{\mathbb{Q}}[\mathbf{1}_{\{t < \tau_I = s \leq T\}}D(t, s)V(s, T)^-|\mathcal{F}_s]|\mathcal{F}_t] \\
 &= \mathbb{E}^{\mathbb{Q}}[\Pi(t, T)|\mathcal{F}_t] \\
 &\quad + (1 - R_I)\mathbb{E}^{\mathbb{Q}}[\mathbf{1}_{\{t < \tau_I \leq T\}}D(t, \tau_I)V(\tau_I, T)^-|\mathcal{F}_t]
 \end{aligned} \tag{1.4}$$

where $V^- = \max(0, -V)$ and R_I is the recovery rate that is exchanged as a proportion of the net present value of the contract upon default of the investor. The second component in equation 1.4 can be seen as the investor's gain in the transaction owing to its own default.

³The recovery rate here ignores the difficulty involved in the real world determination of recovery in credit derivatives, e.g. CDS, like time delays, dealer polls and delivery options. For simplicity, we assume constant recovery rates in the thesis throughout.

1.4.3 Bilateral Counterparty Risk

Unilateral counterparty risk neglects the fact that an investor may default prior to the counterparty and that the counterparty may also default prior to the investor before the contract expires worthless, in whichever case the latter default event will become irrelevant. Furthermore, the investor or the counterparty may actually gain from their own possible default. For more details on the symmetric argument, see, for example, Brigo et al. (2011c).

We define stopping time

$$\tau = \min\{\tau_I, \tau_C\} \quad (1.5)$$

as the first-to-default time of both the investor and the counterparty. If $\tau > T$, neither the investor or the counterparty has defaulted throughout the life of the contract. If $t < \tau \leq T$, then either the investor or the counterparty has defaulted and the corresponding default-risky value of the contract $V^D(t, T)$ at time t is

$$\begin{aligned} V^D(t, T) &= \mathbb{E}^{\mathbb{Q}}[\Pi^D(t, T)|\mathcal{F}_t] = \mathbb{E}^{\mathbb{Q}}[\Pi(t, T)|\mathcal{F}_t] \\ &\quad + (1 - R_I)\mathbb{E}^{\mathbb{Q}}[\mathbb{E}^{\mathbb{Q}}[\mathbf{1}_{\{\tau_I = s \leq \min\{T, \tau_C\}\}} D(t, s) V(s, T)^- | \mathcal{F}_s] | \mathcal{F}_t] \\ &\quad - (1 - R_C)\mathbb{E}^{\mathbb{Q}}[\mathbb{E}^{\mathbb{Q}}[\mathbf{1}_{\{\tau_C = s \leq \min\{T, \tau_I\}\}} D(t, s) V(s, T)^+ | \mathcal{F}_s] | \mathcal{F}_t] \\ &= \mathbb{E}^{\mathbb{Q}}[\Pi(t, T)|\mathcal{F}_t] \\ &\quad + (1 - R_I)\mathbb{E}^{\mathbb{Q}}[D(t, \tau_I)\mathbf{1}_{\{\tau_I \leq \min\{T, \tau_C\}\}} V(\tau_I, T)^- | \mathcal{F}_t] \\ &\quad - (1 - R_I)\mathbb{E}^{\mathbb{Q}}[D(t, \tau_C)\mathbf{1}_{\{\tau_C \leq \min\{T, \tau_I\}\}} V(\tau_C, T)^+ | \mathcal{F}_t]. \end{aligned} \quad (1.6)$$

The second and the third components of equation 1.6 together form the bilateral price adjustments, which could change sign due to the offsetting nature when the credit quality of the investor worsens while that of the counterparty improves. The value of the contract subject to bilateral default risk can be expressed in terms of the default-free value plus a long position in a zero strike European put option on $V(\tau, T)$ minus a short position in a zero strike European call option on $V(\tau, T)$. It can be observed from this formula that if there's no default throughout the life of the transaction the problem reduces to the risk-neutral val-

uation of the contract in a default-free setting. For proof of the formula, see Brigo and Capponi (2010).

In general, the credit exposure to a particular counterparty arises not from a single transaction but several ones. For any particular market scenario, some of these transactions will have positive, and others negative value. In the event of counterparty bankruptcy or any other relevant event of default specified in the relevant agreement if accelerated (i.e. effected), all transactions or all of a given type are netted (i.e. set off against each other) at market value or, if otherwise specified in the contract or if it is not possible to obtain a market value, at an amount equal to the loss suffered by the non-defaulting party in replacing the relevant contract. The alternative would allow the liquidator to choose which contracts to enforce and which not to (and thus potentially "cherry pick"). There are international jurisdictions where the enforceability of netting in bankruptcy has not been legally tested. Netting is usually considered at portfolio of trades and it's out of the scope of this thesis as we consider counterparty risk at single trade level.

1.4.4 Counterparty Risk Measures

Next, we introduce several statistical quantities that have been frequently used in measuring counterparty risk. First of all, the potential future exposure (PFE) computed at time t of the defaultable contract value $V^D(t)$ is defined as:

$$PFE(\alpha, t) = \inf\{x : \mathbb{P}(V^D(t) \leq x) \geq \alpha\}, \quad (1.7)$$

where α is the specified level of the confidence interval (usually at 95% or 97.5%) and \mathbb{P} is the probability distribution of $V^D(t)$. Based on equation 1.6, we refer to Cesari et al. (2009) and introduce two fundamental bilateral counterparty risk measures being widely used in the financial industry to monitor risks of financial institutions.

Second, the unilateral adjusted modified expected positive exposure (EPE^{mod}) condi-

tional on earlier counterparty default at time $\tau_C = s > 0$, defined as

$$EPE_s^{mod} = \frac{1}{P(t, s)} \mathbb{E}^{\mathbb{Q}}[D(t, s)V(s, T)^+ | \mathcal{F}_s]. \quad (1.8)$$

similarly, the unilateral adjusted modified expected negative exposure (ENE^{mod}) conditional on earlier investor default at time $\tau_I = s > 0$, defined as

$$ENE_s^{mod} = \frac{1}{P(t, s)} \mathbb{E}^{\mathbb{Q}}[D(t, s)V(s, T)^- | \mathcal{F}_s]. \quad (1.9)$$

To further reflect the possible change of sign nature of bilateral counterparty risk exposure, we define the bilateral expected positive exposure (BEPE) from the point of view of the investor as

$$BEPE_s^{mod} = EPE_s^{mod} - ENE_s^{mod}, \quad (1.10)$$

which can later be used to quantify the impact of asset-credit correlation and default correlation on the investor's effective exposure towards the counterparty.

Notice that the modified versions of EPEs and ENEs are introduced such that we can quantify the impact of asset-credit correlation and default correlation on the future exposure of the contract. Furthermore, both measures are defined under the risk-neutral measure to allow for potential hedges and the computation of CVA, DVA and bilateral CVA. However, these two measures can also be calculated under the real measure using historical analysis in risk management applications. For more information regarding choice of measure, the reader is referred to, for example, Cesari et al. (2009).

The structure of the remainder of the thesis is organized as follows. In Chapter 2, we introduce in detail the Bessel bridge approach where the counterparty default time is modelled in terms of an inverse first-passage time (IFPT) problem and how the credit index process is specified such that the default time distribution is calibrated exactly to the market CDS quotes of certain counterparty. In particular, the conditional law of the credit index process upon default is shown to be equal to that of the corresponding three-dimensional

Bessel bridge process, which can be then efficiently simulated in terms of three independent Brownian bridges. The asset price dynamics conditional on default can be subsequently expressed directly in terms of the credit index process such that the asset-credit correlation is explicitly incorporated and the joint simulation of the asset price and credit index process can be conducted in a computationally efficient manner. We integrate the unilateral default model into a stochastic foreign exchange setting, where the correlation between FX rate and interest rates are also considered, to establish a unilateral joint FX-credit default model. We then apply our framework to FX forward and cross currency swap contracts and calculate their expected positive exposure and potential future exposure profiles for various asset-credit correlation scenarios. Numerical examples are presented to illustrate the impact of wrong way/right way risk throughout the life of the contracts.

Chapter 3 extends the unilateral joint FX-credit default model to the bilateral case where not only the counterparty but the investor can also default. In this context, the model is further developed such that the correlation between the counterparty credit quality and the exchange rate, the correlation between the investor credit quality and the exchange rate and the default correlation between the two parties are explicitly incorporated. We apply the model to study the expected positive/negative exposures of cross currency swaps upon default at a particular time for various wrong way/right way and default correlation scenarios.

In Chapter 4, we study Bermudan swaption CVA with presence of wrong way risk. A multi-curve interest rate framework for the valuation of interest rate swaps by modelling the overnight-index-swap (OIS) rate and the Xibor⁴-OIS spreads explicitly is built partly based on Mercurio and Xie (2012), where Xibor (interbank money market rate) is a generic notation for Libor-like interest rates. Specifically, standard Hull-White short rate model is used to model OIS rate and 1-factor lognormal model is used to model the basis spreads. Since the OIS (overnight index swap rate) is considered to be a better proxy of risk-free rate compared to Xibor, which has credit risk and liquidity risk premiums and hence is

⁴A generic notation for interbank offer rate in various markets.

higher than risk-free rates, we believe it's reasonable to assume positive Xibor-OIS spreads. Although the Euribor-OIS spread briefly went negative in 2009 due to the crisis, we consider such scenario to be rare and counterintuitive and hence do not consider such scenario in this thesis. Finally, least-square regression based approach is used to obtain the optimal exercise boundary of the Bermudan swaptions. Since the basis spreads are a proxy of credit risk premium, the asset-credit correlation is imposed on the evolution of the basis spreads with a given tenor and the counterparty credit quality, from which a joint interest rate-credit default model is established based on Bessel bridge approach. . Numerical examples on expected positive exposure profiles and CVAs with various wrong way/right way correlation scenarios are studied to illustrate the impact of wrong way/right way risk on Bermudan swaption CVAs.

Chapter 2

Unilateral Counterparty Risk

Modelling of FX Derivatives

2.1 Chapter Overview

As mentioned in the previous chapter, in many of the derivatives transactions, the evolution of the counterparty credit quality is correlated with the underlying asset price(s) and hence should be treated as a source of risk that is to be taken into account when valuing a transaction or calculating counterparty exposures. In this chapter, a joint FX-credit unilateral default framework where wrong way/right way correlation is explicitly modelled is developed partially based on the theoretical foundations established in Davis and Pistorius (2010). The model follows a similar economic rationale of the traditional Merton-type approach where the evolution of counterparty credit quality is modelled in terms of a distance-to-default process and default can actually be observed.

The traditional Merton-type approach assumes that a firm's asset value is driven by a lognormal diffusion and the firm defaults at the time of debt maturity if the notional of the debt exceeds the asset value. His ideas were extended by several researchers, notably by Black and Cox (1976), who propose the idea of continuous default barrier such that default

can occur at any time throughout the life of the contract. Due to the predictability of default event in these approaches, the probability of a non-distressed firm defaulting in the near term is often close to zero. To address this, the subsequent structural default approaches model credit spread volatility and incorporate curvilinear barriers (see, for example, Hull and White (2001) and Blanchet-Scalliet et al. (2011)). One desirable feature of these first-passage time approaches is that default event of a counterparty is observable, which is in line with market intuition as the credit quality of a counterparty evolves gradually and hence the asset-credit correlation can be naturally incorporated. However, the default barrier is explicitly specified and consequently either numerical methods are applied to solve for the default barrier or analytically solvable lognormal dynamics with constant parameters are introduced and as a result, their models cannot fit the term structure of CDS spreads implied by the market exactly, thus often incurring a bias in their risk calculation.

Hull and White (2001) approach the problem by modelling the time of default as the first time the Brownian motion driving the asset value hits a specified time-dependent barrier and show that the barrier can be chosen such that the model is calibrated exactly to the market CDS spreads. This approach is also characterized as the inverse first-passage time (IFPT) problem where given a certain distribution the time-dependent barrier needs to be numerically retrieved such that the first hitting time of a stochastic process across the barrier follows that distribution. Numerical solutions of this generally non-linear boundary have been developed by Cheng et al. (2006) who apply free-boundary-problem-techniques, Zucca and Sacerdote (2009) who analyse a Monte Carlo approximation method and a method based on the discretization of the Volterra integral equation satisfied by the boundary derived in Peskir (2002) and Jaimungal et al. (2009) who utilize integral equation theories. Chen et al. (2011) prove the existence and uniqueness of the IFPT of an arbitrary continuous distribution function for a diffusion process with smooth and bounded coefficients and a strictly positive volatility function. A related "smoothed" version of the IFPT problem is also studied in Ettinger et al. (2014), where for any prescribed life-time they prove the unique existence of a continuously differentiable boundary for which a standard Brownian motion killed at a rate that is given function of this boundary has the prescribed life-time.

Since the application of numerical methods can sometimes be computationally intensive and for a certain class of distribution functions no closed-form solution is available, Davis and Pistorius (2010) consider a variation of the problem by replacing the time-dependent barrier with a flat barrier equal to zero and derive an explicit solution to an inverse first-passage time problem of a linear time-inhomogeneous Brownian motion to zero for any default time distribution having a density. They show that with an appropriate specification of the initial distribution and the time-dependent drift and volatility being taken proportional to the hazard rate of the given distribution the model is calibrated exactly to the market CDS quotes. They show further that the law of asset value conditional on first-passage occurring at a particular time in the future can be identified in terms of time-changed three-dimensional Bessel bridge processes, by which the asset value conditional on default is directly driven among others. The Lévy extension of this approach is developed in Davis and Pistorius (2015). On the hand, although the reduced-form models can be calibrated exactly to the survival probabilities implied from CDS quotes, the asset-credit correlations that can be modelled is of very limited scope and the lack of economic interpretation make them unappealing.

The model we propose follows the framework proposed by Davis and Pistorius (2010) that retains the structural default modelling advantages that distance-to-default is explicitly modelled such that the evolution of the counterparty credit quality is observable; and meanwhile our model is capable of being calibrated exactly to the market implied survival probabilities of a certain counterparty. However, in spite of the rich literatures on counterparty risk modelling of single name CDSs and single currency interest rate swaps whose counterparty exposures are mainly driven by a single source of underlying, i.e. the CDS spread of the reference entity for the former and Xibor rates for the latter. Few of them pay attention to hybrid derivatives especially cross currency swaps whose counterparty exposures are driven by the exchange rate, cross currency basis spread, domestic and foreign periodic interest rate payments combined with the possible correlations between each of the two, which could make the modelling of wrong way risk much more complicated. Furthermore, asset-credit dependency is frequently treated as an implicit requirement though there

has been a genuine interest after the financial crisis in detecting and measuring its effect explicitly. The main contribution of this chapter is to provide a joint FX-credit structural default model to explicitly capture wrong way risk of cross currency swaps. To place a specific focus on counterparty risk modelling, we simplify the matter by containing ourselves within the pre-crisis single curve interest rate framework when it comes to the pricing of FX derivatives, under which we construct a multi-currency model composed of one-factor lognormal exchange rate dynamics correlated with domestic and foreign interest rates specified by one-factor Hull-White (1FHW) models respectively. The exchange rate dynamics conditional on default are derived and expressed directly in terms of the distance-to-default process, which can be efficiently simulated as a three-dimensional Bessel bridge process. Finally, we conduct case studies on two hypothetical cross currency swap contracts traded between a US financial institution assumed to be default-free and Nomura International assumed to be defaultable. Monte Carlo simulation is applied to compute EPEs and PFEs of the contract for various exchange rate-credit correlation scenarios to quantify the impact of wrong way/right way risk on the counterparty exposure. It can be shown that wrong way/right way risk could have significant impact on the counterparty exposure calculation.

2.2 IFPT Problem and Main Results

In this section, we briefly go through the theory of IFPT problem and summarize the results obtained in Davis and Pistorius (2010).

For a given cumulative distribution function P with density f defined on the positive half line, the canonical inverse first-passage time problem is formulated to search for a boundary $b(t) : \mathbb{R}^+ \rightarrow [-\infty, +\infty]$ such that the first-passage time τ_b^Y of a real valued Markov process Y with right-continuous left-limit paths and initial distribution μ across

$b(t)$ follows the given distribution P :

$$P(\tau_b^Y \leq t) = P(t), \quad t \in (0, +\infty),$$

$$\tau_b^Y = \inf\{t \in (0, +\infty) : Y(t) \in (-\infty, b(t))\}.$$

As mentioned in the previous chapter, the identification of the boundary $b(t)$ often involves numerical schemes, hence a modification of the formulation is considered in Davis and Pistorius (2010) with the following definition:

Definition 2.2.1. *For a continuous probability distribution function P with density f on \mathbb{R}^+ and a given Markov process X with right-continuous and left limit paths, the inverse first-passage time problem is to find a probability measure μ on $(\mathbb{R}^+, \mathcal{B}(\mathbb{R}^+))$ and an increasing continuous function $I : \mathbb{R}^+ \rightarrow [0, +\infty]$ such that for the time-changed process $Y = X \circ I = \{(X \circ I)(t), t \in \mathbb{R}^+\}$ the first-passage time into the negative half-line $(-\infty, 0)$ follows distribution P :*

$$P(\tau_0^Y \leq t) = P(t), \quad t \in (0, +\infty),$$

$$\tau_0^Y = \inf\{t \in (0, +\infty) : Y(t) \in (-\infty, 0)\}.$$

Let $(\Omega, \mathcal{F}, \mathbb{P})$ be the probability space, a specific family of linear Gaussian processes starting from an independent random point $A \sim F$ is considered in their work:

$$Y(t) = A + \int_0^t \nu \sigma^2(s) ds + \int_0^t \sigma(s) dW(s), \quad Y(0) = A, \quad t > 0, \quad \nu \neq 0, \quad (2.1)$$

where $\sigma : \mathbb{R}^+ \rightarrow \mathbb{R}$ is a function such that

$$I(t) := \int_0^t \sigma^2(s) ds < \infty, \quad t > 0 \quad (2.2)$$

and Y is in law equal to the time-changed Brownian motion $\{X(I(t)), t \geq 0\}$:

$$X(t) = A + \nu t + W(t). \quad (2.3)$$

The randomization of A is embedded into Y such that conditional on $Y(0) = A$ the distribution P of the first time Y crosses the zero should satisfy the following:

$$P(t) = \mathbb{P}[\tau_0^Y \leq t] = \int_0^\infty \mathbb{P}[\tau_0^Y \leq t | A = a] F(da). \quad (2.4)$$

It is shown that by taking the Laplace-Stieltjes transform of P in t :

$$\mathcal{L}P(q) = \int_0^\infty \mathbb{E}^\mathbb{P}[e^{-q\tau_0^Y} | A = a] F(da) = \int_0^\infty e^{-a\Phi(q)} F(da), \quad \Phi(q) = \nu + \sqrt{\nu^2 + 2q}, \quad (2.5)$$

given that $q = \phi(\theta) = \frac{1}{2}\theta^2 - \nu\theta$, F must satisfy

$$\mathcal{L}P(\phi(\theta)) = \mathcal{L}F(\theta), \quad (2.6)$$

which indicates that the left-hand side of equation 2.6 is strictly monotone as a function of θ . They show that randomization can be defined in terms of a two-parameter family of probability distributions $\{F_\lambda^{(\nu)}\}$ that is employed for the embedding of the exponential distribution with parameter $\lambda > 0$:

$$\frac{F_\lambda^{(\nu)}(dx)}{dx} = \begin{cases} 2\lambda x e^{-x\sqrt{2\lambda}}, & \nu = -\sqrt{2\lambda}, \\ \frac{2\lambda}{\theta_+ - \theta_-} (e^{\theta_+ x} - e^{\theta_- x}), & \nu < -\sqrt{2\lambda}, \end{cases}$$

where $\theta_\pm = \nu \pm \sqrt{\nu^2 - 2\lambda}$, an explicit solution of Y is found through the specification of its time-dependent drift and volatility function in the following theorem:

Theorem 2.2.1. *Suppose that P is a continuous probability distribution function with density f , define the hazard function*

$$\gamma(t) = \frac{f(t)}{1 - P(t)} \quad (2.7)$$

and for a fixed $\lambda > 0$, specify σ^2 as

$$\sigma^2(t) = \frac{\gamma(t)}{\lambda}, \quad (2.8)$$

then $\mathbb{P}(\tau_0^Y \leq t) = P(t)$ for all $t \in (0, \infty)$.

Proof. For proof see Davis & Pistorius (2010). □

In the application of counterparty risk modelling, the default event of an institution can be modelled as the first hitting time of its credit index process Y across zero. By taking the implied volatility function of the credit index process to be proportional to the hazard rate function of the institution's risk-neutral default probability distribution, which is itself implied from market CDSs, the default model is ensured to exactly match the given CDS quotes.

2.3 Bessel Bridge Approach for Wrong Way Risk Modelling

Given the specification of the credit index process in the previous section, we now introduce the Bessel bridge approach proposed in Davis and Pistorius (2010) to obtaining the conditional distributions of the credit index process and the driving underlying asset price process upon default and how wrong way risk is explicitly embedded in the underlying asset price dynamics directly in terms of the credit index process.

2.3.1 Credit Index Process Conditional on Default

First of all, the identification of the law of credit index process conditional on hitting the zero barrier at time $\tau_0^Y = s > 0$ involves the application of the Doob h -transform of Y . To achieve this, it is the prerequisite to introduce the Cameron-Martin-Girsanov change of measure theory as follows:

Theorem 2.3.1 (Cameron-Martin-Girsanov Theorem). *Let $(X(t), \Omega, \mathcal{F}, \{\mathcal{F}(t) = \sigma(\{X(q) : q \leq t\})\}, \mathbb{P})$ relate to the space for Brownian motion on \mathbb{R}^n . Suppose that $c(t)$ is an*

$\{\mathcal{F}(t^+)\}$ previsible \mathbb{R}^n -valued process such that

$$\zeta(t) = \exp\left(\int_0^t c(q)dX(q) - \frac{1}{2} \int_0^t |c(q)|^2 dq\right) \quad (2.9)$$

defines a martingale ζ if $c(t)$ is a bounded process. Then there exists a unique measure \mathbb{Q} on (Ω, \mathcal{F}) such that

$$\frac{d\mathbb{Q}}{d\mathbb{P}}|_{\mathcal{F}(t)} = \zeta(t), \quad \forall t > 0, \quad (2.10)$$

and under \mathbb{Q}

$$\tilde{X}(t) = X(t) - \int_0^t c(q)dq \quad (2.11)$$

defines a Brownian motion relative to $\{\mathcal{F}(t^+)\}$.

Proof. For proof see Rogers and Williams (2000, Chapter IV.6). □

Now suppose that $(X(t), \Omega, \mathcal{F}, \{\mathcal{F}(t)\}) = \sigma(\{X(q) : q \leq t\}, \mathbb{P})$ is a Brownian motion starting from zero under the state space \mathbb{R} , we define the Brownian transition density p as

$$p(t, t+t'; u, v) = P(X(t+t') = v | X(t) = u) \quad (2.12)$$

and a strictly positive space-time regular $h : \mathbb{R}^+ \times \mathbb{R} \rightarrow (0, \infty)$ as

$$h(t, u) = P(X(T) \in \mathbb{R} | X(t) = u), \quad t \leq T, \quad (2.13)$$

where $h(0, 0) = 1$ is assumed without loss of generality. The conditioned semi-group $\hat{p}(t, t+t'; u, v) = P(X(t+t') = v | X(t) = u, X(T) \in \mathbb{R})$ is easily computed from p and

h :

$$\hat{p}(t, t+t'; u, v) = \frac{P(X(t+t') = v; X(T) \in \mathbb{R} | X(t) = u)}{P(X(T) \in \mathbb{R} | X(t) = u)} = p(t, t+t'; u, v) \frac{h(t+t', v)}{h(t, u)}. \quad (2.14)$$

In fact, $\hat{p}(t, t+t'; u, v)$ is indeed a Markov kernel satisfying

$$\int_v \hat{p}(t, t+t'; u, v) dv = 1 \quad (2.15)$$

if, for $t \geq 0, t' > 0, u \in \mathbb{R}$,

$$h(t, u) = \int_v p(t, t+t'; u, v) h(t+t', v) dv = E[h(t+t', X(t+t')) | X(t) = u]. \quad (2.16)$$

This leads to the change of measure from \mathbb{P} to \mathbb{Q} on (Ω, \mathcal{F}) where the Radon-Nikodym derivative is

$$\frac{d\mathbb{Q}}{d\mathbb{P}}|_{\mathcal{F}(t)} = Z(t) \equiv h(t, X(t)) \quad (2.17)$$

and the coordinate process \tilde{X} under \mathbb{Q} is a non-homogeneous Markov process with transition density \hat{p} . Apply Itô's lemma to the \mathbb{P} -martingale $Z(t)$, we have:

$$dZ(t) = \frac{1}{h(0,0)} \{h'(t, X(t))dX(t) + [\dot{h}(t, X(t)) + \frac{1}{2}h''(t, X(t))]dt\}, \quad (2.18)$$

where a dot denotes a derivative with respect to t and a prime denotes a derivative with respect to X . Since $Z(t)$ is a \mathbb{P} -martingale, the drift term in equation 2.18 must vanish, along with equation 2.17, we have

$$dZ(t) = Z(t) \frac{h'(t, X(t))}{h(t, X(t))} dX(t). \quad (2.19)$$

Based on Theorem 2.3.1, it can be concluded that the coordinate process $\tilde{X}(t)$ under \mathbb{Q} :

$$\tilde{X}(t) = X(t) - \int_0^t \frac{h'(q, X(q))}{h(q, X(q))} dq \quad (2.20)$$

is a \mathbb{Q} -Brownian motion. For more details, please refer to Rogers and Williams (2000).

The Cameron-Martin-Girsanov theorem is applied in Davis and Pistorius (2010), where the conditional distribution of the credit index process Y hitting the zero barrier at time $s > 0$, $P(\tau_0^Y = s | Y(0) = A)$, can be seen as the Doob h -transform of a time-changed Brownian motion starting from $A > 0$ with the h -function given by

$$h_Y(I(t), A) = P(\tau_0^Y \in s - dt | Y(0) = A) / dt = \frac{\sigma^2(s)A}{\sqrt{2\pi(I(s) - I(t))^3}} e^{-\frac{(A + \nu I(t))^2}{2(I(s) - I(t))}}, \quad t \in (0, s), \quad (2.21)$$

with $I(t) = \int_0^t \sigma^2(q) dq$ such that there exists a non-homogeneous Markov process $\eta = (\eta(t), t \in [0, s])$, for any set $L \in \mathcal{F}_t^Y$, the sigma field generated by $\{Y(q)\}_{q \leq t}$, we have $P^h(\eta(t) \in L | \eta(0) = A) = P(Y(t) \in L | Y(0) = A)$, where the Radon-Nikodym derivative is

$$\frac{d\mathbb{P}^h}{d\mathbb{P}} \Big|_{\mathcal{F}^Y(t)} = \frac{h_Y(I(s) - I(t), Y(t))}{h_Y(0, A)}. \quad (2.22)$$

Since

$$\frac{h'_Y(I(t), Y(t))}{h_Y(I(t), Y(t))} = \left[\frac{1}{Y(t)} - \frac{Y(t)}{I(s) - I(t)} \right] \sigma^2(t), \quad (2.23)$$

we have an SDE for η of the form:

$$d\eta(t) = \left[\frac{1}{\eta(t)} - \frac{\eta(t)}{I(s) - I(t)} \right] \sigma^2(t) dt + dW(t), \quad t \in (0, s), \quad (2.24)$$

$$\eta(0) = A,$$

where $A \sim F_\lambda^{(\nu)}$ and is independent of W , a standard Brownian motion. Furthermore, to

identify the distribution of η , the following definition is introduced:

Definition 2.3.1 (Bessel Process). Fix an integer $d \geq 2$, let $W = \{(W_1, \dots, W_d), \mathcal{F}(t)\}_{0 \leq t < \infty}$ and $\{\mathbb{P}^x\}_{x \in \mathbb{R}^d}$ be a d -dimensional Brownian family on some measurable space (Ω, \mathcal{F}) . The process $R = \{R(t) = \|W(t)\|, R(0) = \|x\|, \mathcal{F}(t)\}_{0 \leq t < \infty}$:

$$R(t) \triangleq \sqrt{(W_1(t))^2 + \dots + (W_d(t))^2}, \quad t \in [0, \infty), \quad (2.25)$$

together with the family of measures $\{\hat{\mathbb{P}}^r\}_{r \geq 0} \triangleq \{\mathbb{P}^{r,0,\dots,0}\}_{r \geq 0}$ on (Ω, \mathcal{F}) is called a Bessel family with dimension d . For fixed $r \geq 0$, R on $(\Omega, \mathcal{F}, \hat{\mathbb{P}}^r)$ is a Bessel process with dimension d starting at r .

Next, if we replace W with a d -dimensional Brownian bridge $Z = \{(Z_1, \dots, Z_d), \tilde{\mathcal{F}}(t)\}_{0 \leq t < \infty}$ defined in $\{\mathbb{P}^y\}_{y \in \mathbb{R}^d}$ starting from $y \in \mathbb{R}^d$:

$$Z(t) = \frac{y(s-t)}{s} + B(t) - \frac{t}{s}B(s), \quad t \in [0, s], \quad (2.26)$$

where B is a d -dimensional Brownian motion. The resulting process $\tilde{R} = \{\tilde{R}(t) = \|Z(t)\|, \tilde{\mathcal{F}}(t)\}_{0 \leq t < \infty}$:

$$\tilde{R}(t) \triangleq \sqrt{(Z_1(t))^2 + \dots + (Z_d(t))^2}, \quad t \in [0, s], \quad (2.27)$$

is called a d -dimensional Bessel bridge. Let $d = 3$, by applying Ito's lemma to \tilde{R} , it can be shown that the three-dimensional Bessel bridge satisfies the SDE of the form:

$$d\tilde{R}(t) = \left[\frac{1}{\tilde{R}(t)} - \frac{\tilde{R}(t)}{s-t} \right] dt + dW(t), \quad (2.28)$$

where W is a 3-dimensional Brownian motion. Combined with the SDE satisfied by η , it is proved in Davis and Pistorius (2010) that η is actually in law equal to the corresponding

time-changed 3-dimensional Bessel bridge ($\tilde{R}(I(t))$, $t \in [0, s)$):

$$d\tilde{R}(I(t)) = \left[\frac{1}{\tilde{R}(I(t))} - \frac{\tilde{R}(I(t))}{I(s) - I(t)} \right] \sigma^2(t) dt + dW(t), \quad t \in (0, s), \quad (2.29)$$

$$\tilde{R}(I(0)) = A, \quad A \sim F_\lambda^{(\nu)}.$$

Since η is in law equal to Y conditional on $\tau_0^Y = s > 0$, the credit index process Y solves the following SDE:

$$dY(t) = \left(\frac{1}{Y(t)} - \frac{Y(t)}{\int_t^s \sigma^2(q) dq} \right) \sigma^2(t) dt + \sigma(t) dB(t), \quad t \in (0, s), \quad Y(0) = A, \quad (2.30)$$

where $A \sim F_\lambda^{(\nu)}$ is independent of B . Based on Bertoin et al. (1999), the path of Y can then be simulated as ($\tilde{R}(I(t))$, $t \in [0, s]$) by replacing $s \rightarrow I(s)$, $t \rightarrow I(t)$, $dt \rightarrow \sigma^2(t)dt$ and exploiting the relation between the three-dimensional Bessel bridge and Brownian bridges as follows:

$$Y(t) = \tilde{R}(t) = \sqrt{\left(\frac{A(s-t)}{s} + Z_1(t) \right)^2 + Z_2^2(t) + Z_3^2(t)}, \quad (2.31)$$

where Z_i , $i = 1, 2, 3$, are independent $0 \rightarrow 0$ Brownian bridges:

$$dZ_i(t) = -\frac{Z_i(t)}{s-t} dt + dB_i(t) \quad (2.32)$$

and B_i are independent Brownian motions.

2.3.2 Unilateral Joint Asset-Credit Modelling via Bessel bridges

Next, the focus is turned to the establishment of a joint asset-credit model to quantify wrong way/right way risk. To achieve this, characterization of the joint probability distribution of the stochastic process $(Y(t), S(t)$, $t \leq s$) conditional on default ($\tau_0^Y = s > 0$) is required, where S is the asset value dynamics.

Based on Davis and Pistorius (2010), the conditional law of asset value dynamics is

identified by correlating its driving Brownian motion with the credit index process Y as follows. Denote $W = \{(W_1, \dots, W_d), \mathcal{F}(t)\}_{0 \leq t < \infty}$ as a d -dimensional Brownian motion with correlation matrix $\Sigma = (\rho^{ij})_{i,j=1}^d$ defined on a filtered probability space $(\Omega, \mathcal{F}, \{\mathcal{F}_t\}_{t \geq 0}, \mathbb{P})$. For time horizon $T > s$, we model the corresponding d -dimensional asset value process $S = (S_1, \dots, S_d)$ as the Ito-diffusion driven by W :

$$\frac{dS_i(t)}{S_i(t)} = \mu_i(t)dt + \sum_{j=1}^d v_{ij}(t)dW_j(t), \quad S(0) = s(0), \quad (2.33)$$

for $\{\mathcal{F}_t\}_{t \geq 0}$ -adapted processes $\mu_i(t)$ and $v_{ij}(t)$, $\sum_{i,j} \int_0^T \{|\mu_i(t)| + |v_{ij}(t)|^2\} dt < \infty$, \mathbb{P} -a.s. Let the Brownian motion W correlate with the Brownian motion driving the credit index process, $B(t)$, $[B, W_i] = \rho_i t$, $t \geq 0$, which can also be expressed as

$$B(t) = \int_0^t \frac{1}{\sigma(s)} dY(s) - \nu \int_0^t \sigma(s) ds. \quad (2.34)$$

Denote $\rho = (\rho_1, \dots, \rho_d)$ as the row-vector of correlations and $Q = (Q^{ik})_{i,k=1}^d$ as the Cholesky decomposition of the matrix $\Sigma - \rho\rho'$, it is shown that W may be expressed in terms of $d + 1$ independent Brownian motions B, B_*, \dots, B_d :

$$W_i(t) = \rho_i B(t) + \sum_{k=1}^d Q^{ik} B_k(t) \quad (2.35)$$

and subsequently the asset value dynamics can be expressed directly in terms of $Y(t)$:

$$\frac{dS_i(t)}{S_i(t)} = [\mu_i(t) - \nu\sigma(t)\rho_i]dt + \frac{1}{\sigma(t)} \sum_{j=1}^d v_{ij}(t)\rho_j dY(t) + \sum_{j,k=1}^d v_{ij}(t)Q^{jk} dB_k(t), \quad S_i(0) = s_i(0). \quad (2.36)$$

Therefore, the asset-credit correlation effect is captured by linking the credit index process and the asset price process, where wrong way/right way risk can be quantified with a chosen risk metric calculated by jointly simulating Y and S given a set of asset-credit correlation scenarios.

2.4 Unilateral Joint FX-Credit Default Model

In this section, we present a multi-currency framework with correlated interest rates for the valuation of FX derivatives and calibrate it to the market quotes of interest rate caps and FX call options. We then integrate the counterparty default model with Bessel bridges into the multi-currency framework to establish a unilateral joint FX-credit default model, where the credit index process is calibrated to the market CDS quotes.

2.4.1 FX-Hull-White Hybrid Model

First of all, we follow similarly to Brigo and Alfonsi (2005) and consider the short rate process as the sum of a deterministic function and a mean-reverting Markovian process. As a specific example, we restrict ourselves to the USDJPY FX framework. We define probability spaces $(\Omega, \mathcal{F}, \{\mathcal{F}_t\}_{t \geq 0}, \mathbb{Q}^{\$})$ and $(\Psi, \mathcal{G}, \{\mathcal{G}_t\}_{t \geq 0}, \mathbb{Q}^{\yen})$, where $\{\mathcal{F}_t\}_{t \geq 0}$ and $\{\mathcal{G}_t\}_{t \geq 0}$ are the filtrations modelling the US and Japanese market information respectively, $\mathbb{Q}^{\$}$ and \mathbb{Q}^{\yen} are the US and Japanese risk-neutral measures generated by their money market accounts numeraires defined below:

$$B_{\$}(t) = e^{\int_0^t r_{\$}(s) ds}, \quad B_{\yen}(t) = e^{\int_0^t r_{\yen}(s) ds}, \quad t \geq 0, \quad (2.37)$$

where $\{r_{\$}(t)\}_{t \geq 0}$ and $\{r_{\yen}(t)\}_{t \geq 0}$ are stochastic interest rate processes adapted to $\{\mathcal{F}_t\}_{t \geq 0}$ and $\{\mathcal{G}_t\}_{t \geq 0}$. The dollar and yen discount factors are then expressed as:

$$D_{\$}(t) = \frac{1}{B_{\$}(t)}, \quad D_{\yen}(t) = \frac{1}{B_{\yen}(t)} \quad (2.38)$$

and the values of dollar and yen zero-coupon bonds (ZCBs) for maturity T at time t are

$$P_{\$}(t, T) = E^{\mathbb{Q}^{\$}}[e^{-\int_t^T r_{\$}(s) ds} | \mathcal{F}_t], \quad P_{\yen}(t, T) = E^{\mathbb{Q}^{\yen}}[e^{-\int_t^T r_{\yen}(s) ds} | \mathcal{G}_t], \quad (2.39)$$

which serve as numeraires of US and Japanese T -forward measures $\mathbb{Q}^{T\$}$ and $\mathbb{Q}^{T\yen}$.

Under the specified probability spaces, the corresponding short rate processes are given as follows:

$$r_{\$}(t) = \theta_{\$}(t) + y_{\$}(t), \quad r_{\$}(0) > 0, \quad (2.40)$$

$$r_{¥}(t) = \theta_{¥}(t) + y_{¥}(t), \quad r_{¥}(0) > 0, \quad (2.41)$$

$$dy_{\$}(t) = -ay_{\$}(t)dt + \sigma_{\$}dW_{\$}^{\mathbb{Q}^{\$}}(t), \quad \sigma_{\$} > 0, \quad y_{\$}(0) = 0, \quad (2.42)$$

$$dy_{¥}(t) = -by_{¥}(t)dt + \sigma_{¥}dW_{¥}^{\mathbb{Q}^{¥}}(t), \quad \sigma_{¥} > 0, \quad y_{¥}(0) = 0, \quad (2.43)$$

where $\theta_{\$}(t)$ and $\theta_{¥}(t)$ are deterministic functions fitted to the initial term structures of dollar and yen interest rates, $W_{\$}^{\mathbb{Q}^{\$}}(t)$ and $W_{¥}^{\mathbb{Q}^{¥}}(t)$ are standard Brownian motions under $\mathbb{Q}^{\$}$ and $\mathbb{Q}^{¥}$, a and b determine the speed of mean reversion and $\sigma_{\$}$ and $\sigma_{¥}$ are the diffusion coefficients. It's important to note that the theoretical possibility of having negative interest rates under Hull-White model is a clear drawback; however such probability is almost negligible in practice.

For the USDJPY exchange rate process $S(t)$, we follow Frey and Sommer (1996) and Sippel and Ohkoshi (2002), assuming that it follows lognormal dynamics under $\mathbb{Q}^{¥}$:

$$\frac{dS(t)}{S(t)} = (r_{¥}(t) - r_{\$}(t))dt + \sigma_S dW_S^{\mathbb{Q}^{¥}}(t), \quad S(0) > 0, \quad (2.44)$$

where $W_S^{\mathbb{Q}^{¥}}(t)$ is a Brownian motion under $\mathbb{Q}^{¥}$ and σ_S is the implied FX volatility. Since the instrument we consider in the thesis is cross currency swap, a linear product with no volatility skew exposure, such exchange rate specification is more tractable and feasible for implementation purposes. More sophisticated FX models with stochastic volatility component may be more realistic from an FX perspective but will not improve our setup in a meaningful way.

For convenience, we consider all the dynamics under $\mathbb{Q}^{¥}$, where we need to derive the risk-neutral dynamics of $y_{\$}(t)$ under $\mathbb{Q}^{¥}$. Given the short rate dynamics specified as above, it can be observed that $\{r_{\$}(t)\}_{t \geq 0}$ and $\{r_{¥}(t)\}_{t \geq 0}$ are both linear in their state variables $y_{\$}(t)$ and $y_{¥}(t)$ respectively. First of all, we introduce the following result.

Lemma 2.4.1. *The prices of dollar and yen zero coupon bonds at time t with maturity T are:*

$$P_{\$}(t, T, y_{\$}(t)) = \exp\{A_{\$}(t, T) - C_{\$}(t, T)y_{\$}(t)\}, \quad (2.45)$$

$$P_{¥}(t, T, y_{¥}(t)) = \exp\{A_{¥}(t, T) - C_{¥}(t, T)y_{¥}(t)\}, \quad (2.46)$$

where

$$A_{\$}(t, T) = \log \frac{P_{\$}(0, T)}{P_{\$}(0, t)} + \frac{\sigma_{\$}^2}{2a^3} \left[-\frac{3}{2} + 2e^{-a(T-t)} - \frac{1}{2}e^{-2a(T-t)} + 2(e^{-at} - e^{-aT}) - \frac{1}{2}(e^{-2at} - e^{-2aT}) \right],$$

$$A_{¥}(t, T) = \log \frac{P_{¥}(0, T)}{P_{¥}(0, t)} + \frac{\sigma_{¥}^2}{2b^3} \left[-\frac{3}{2} + 2e^{-b(T-t)} - \frac{1}{2}e^{-2b(T-t)} + 2(e^{-bt} - e^{-bT}) - \frac{1}{2}(e^{-2bt} - e^{-2bT}) \right],$$

$$C_{\$}(t, T) = \frac{1 - e^{-a(T-t)}}{a},$$

$$C_{¥}(t, T) = \frac{1 - e^{-b(T-t)}}{b}.$$

Proof. For the proof see Pelsser (2000, Chapter 5). \square

Furthermore, by applying the Heath-Jarrow-Morton arbitrage-free argument from Heath et al. (1992), we have the following result.

Lemma 2.4.2. *The dollar and yen zero coupon bond prices $P_{\$}(t, T, y_{\$}(t))$ and $P_{¥}(t, T, y_{¥}(t))$ with maturity T at time t satisfy the following SDEs:*

$$\frac{dP_{\$}(t, T, y_{\$}(t))}{P_{\$}(t, T, y_{\$}(t))} = r_{\$}(t)dt - \sigma_{\$}C_{\$}(t, T)dW_{\$}^{\mathbb{Q}^{\$}}(t), \quad (2.47)$$

$$\frac{dP_{¥}(t, T, y_{¥}(t))}{P_{¥}(t, T, y_{¥}(t))} = r_{\$}(t)dt - \sigma_{¥}C_{¥}(t, T)dW_{¥}^{\mathbb{Q}^{¥}}(t). \quad (2.48)$$

Proof. For proof see Musiela and Rutkowski (2006, Chapter 4). \square

Now assume that the risk-neutral dynamics of the dollar zero coupon bond price $P_{\$}(t, T, y_{\$}(t))$ under $\mathbb{Q}^{¥}$ is specified as

$$\frac{dP_{\$}(t, T, y_{\$}(t))}{P_{\$}(t, T, y_{\$}(t))} = \mu(t)dt - \sigma_{\$}C_{\$}(t, T)dW_{\$}^{\mathbb{Q}^{¥}}(t), \quad (2.49)$$

where $\mu(t)$ is a time-dependent deterministic function currently unknown and $W_{\$}^{Q^{\yen}}(t)$ is a standard Brownian motion under Q^{\yen} . Lemma 2.4.3 provides the risk-neutral dynamics of $y_{\$}(t)$ under Q^{\yen} :

Lemma 2.4.3. *Under the yen risk-neutral measure Q^{\yen} , the yen denominated asset $S(t)P_{\$}(t, T, y_{\$}(t))$ discounted by $B_{\yen}(t)$:*

$$\tilde{S}(t) = \frac{S(t)P_{\$}(t, T, y_{\$}(t))}{B_{\yen}(t)} \quad (2.50)$$

should be a martingale. By using Ito's product rule the drift of the dollar zero coupon bond price dynamics under Q^{\yen} can be expressed as

$$\mu(t) = r_{\$}(t) - \sigma_{\$}\sigma_S\rho_{S,\$} \quad (2.51)$$

and hence

$$dy_{\$}(t) = (-ay_{\$}(t) - \sigma_{\$}\sigma_S\rho_{S,\$})dt + \sigma_{\$}dW_{\$}^{Q^{\yen}}(t), \quad (2.52)$$

where $dW_{\$}^{Q^{\yen}}(t) = dW_{\$}^{Q^{\$}}(t) + \sigma_S\rho_{S,\$}dt$.

Proof. For proof see Shreve (2004, Chapter 9). □

Finally, since the exchange rate process is correlated with both the dollar and yen short rate processes:

$$dW_S^{Q^{\yen}}(t)dW_{\yen}^{Q^{\yen}}(t) = \rho_{S,\yen}dt, \quad \rho_{S,\yen} \in (-1, 1), \quad (2.53)$$

$$dW_{\$}^{Q^{\yen}}(t)dW_S^{Q^{\yen}}(t) = \rho_{S,\$}dt, \quad \rho_{S,\$} \in (-1, 1), \quad (2.54)$$

$$dW_{\$}^{Q^{\yen}}(t)dW_{\yen}^{Q^{\yen}}(t) = \rho_{\$, \yen}dt, \quad \rho_{\$, \yen} \in (-1, 1), \quad (2.55)$$

and the full correlation matrix of the Brownian motions $W_S^{Q^{\yen}}(t)$, $W_{\$}^{Q^{\yen}}(t)$, $W_{\yen}^{Q^{\yen}}(t)$ is given by

$$M = \begin{pmatrix} 1 & \rho_{S,\$} & \rho_{S,\yen} \\ \rho_{S,\$} & 1 & \rho_{\$, \yen} \\ \rho_{S,\yen} & \rho_{\$, \yen} & 1 \end{pmatrix}.$$

To guarantee that the correlation matrix is positive semi-definite, the following constraints are imposed on the three correlation parameters:

$$\begin{aligned} \rho_{S,\yen}\rho_{\$, \yen} - \sqrt{1 - \rho_{S,\yen}^2 - \rho_{\$, \yen}^2 + \rho_{S,\yen}^2\rho_{\$, \yen}^2} &\leq \rho_{S,\$} \leq \rho_{S,\yen}\rho_{\$, \yen} + \sqrt{1 - \rho_{S,\yen}^2 - \rho_{\$, \yen}^2 + \rho_{S,\yen}^2\rho_{\$, \yen}^2}, \\ \rho_{S,\$}\rho_{\$, \yen} - \sqrt{1 - \rho_{S,\$}^2 - \rho_{\$, \yen}^2 + \rho_{S,\$}^2\rho_{\$, \yen}^2} &\leq \rho_{S,\yen} \leq \rho_{S,\$}\rho_{\$, \yen} + \sqrt{1 - \rho_{S,\$}^2 - \rho_{\$, \yen}^2 + \rho_{S,\$}^2\rho_{\$, \yen}^2}, \\ \rho_{S,\yen}\rho_{S,\$} - \sqrt{1 - \rho_{S,\yen}^2 - \rho_{S,\$}^2 + \rho_{S,\yen}^2\rho_{S,\$}^2} &\leq \rho_{\$, \yen} \leq \rho_{S,\yen}\rho_{S,\$} + \sqrt{1 - \rho_{S,\yen}^2 - \rho_{S,\$}^2 + \rho_{S,\yen}^2\rho_{S,\$}^2}. \end{aligned}$$

2.4.2 Exchange Rate Dynamics Conditional on Default

Under our multi-currency framework, we assume a non-zero correlation between the exchange rate process S and the credit index process Y and it can be shown that conditional on default the former can be expressed directly in terms of the latter.

Given the specification of the multi-currency framework with correlated short rates in the previous section, the integral form solution of S under \mathbb{Q}^\yen at time $t \geq 0$ for a future time point $T > t$ can be expressed as:

$$S(T) = S(t) \exp\left\{\int_t^T [r_\yen(s) - r_\$(s)]ds + \sigma_S[W_S^{\mathbb{Q}^\yen}(T) - W_S^{\mathbb{Q}^\yen}(t)]\right\}, \quad (2.56)$$

where

$$\begin{aligned} \int_t^T r_\yen(s)ds &= \ln \frac{P_\yen(0, t)}{P_\yen(0, T)} + y_\yen(t)C_\yen(t, T) + \frac{1}{2}[V_\yen(0, T) - V_\yen(0, t)] + \sigma_\yen \int_t^T C_\yen(s, T)dW_\yen^{\mathbb{Q}^\yen}(s), \\ \int_t^T r_\$(s)ds &= \ln \frac{P_\$(0, t)}{P_\$(0, T)} + y_\$(t)C_\$(t, T) + \frac{1}{2}[V_\$(0, T) - V_\$(0, t)] - \int_t^T \sigma_\$ \sigma_S \rho_{\$, \yen} C_\$(s, T)ds \\ &\quad + \sigma_\$ \int_t^T C_\$(s, T)dW_\$^{\mathbb{Q}^\yen}(s), \end{aligned}$$

with $V_{\text{¥}}(t, T)$ and $V_{\text{§}}(t, T)$ expressed as

$$\begin{aligned} V_{\text{¥}}(t, T) &= \frac{\sigma_{\text{¥}}^2}{b^2} \left[T - t + \frac{2}{b} e^{-b(T-t)} - \frac{1}{2b} e^{-2b(T-t)} - \frac{3}{2b} \right], \\ V_{\text{§}}(t, T) &= \frac{\sigma_{\text{§}}^2}{a^2} \left[T - t + \frac{2}{a} e^{-a(T-t)} - \frac{1}{2a} e^{-2a(T-t)} - \frac{3}{2a} \right]. \end{aligned}$$

On the other hand, the evolution of the credit quality of the counterparty is modelled as the credit index process Y :

$$Y(T) = A + \int_0^T \nu \sigma^2(s) ds + \int_0^T \sigma(s) dW^{\mathbb{Q}^{\text{¥}}}(s), \quad Y(0) = A, \quad T > 0, \quad (2.57)$$

where $A \sim F_{\lambda}^{(\nu)}$ and $W^{\mathbb{Q}^{\text{¥}}}(t)$ is a standard Brownian motion under $\mathbb{Q}^{\text{¥}}$. Since $W^{\mathbb{Q}^{\text{¥}}}$ can be expressed by Y as

$$W^{\mathbb{Q}^{\text{¥}}}(T) = \int_0^T \frac{1}{\sigma(s)} dY(s) - \nu \int_0^T \sigma(s) ds, \quad (2.58)$$

the dependency between the exchange rate process S and the credit index process Y can be incorporated by correlating $W^{\mathbb{Q}^{\text{¥}}}$ with $W_S^{\mathbb{Q}^{\text{¥}}}$ such that $\langle W^{\mathbb{Q}^{\text{¥}}}, W_S^{\mathbb{Q}^{\text{¥}}} \rangle_T = \rho_{S,Y} T$, $\rho_{S,Y} \in (-1, 1)$. Furthermore, since the exchange rate process is correlated with the two short rate processes as specified in the previous section by the estimated full correlation matrix, we can now expand the matrix to incorporate the correlation structure between the Brownian motions $\tilde{\mathbf{W}}(t) = [W_S^{\mathbb{Q}^{\text{¥}}}(t), W_{\text{§}}^{\mathbb{Q}^{\text{¥}}}(t), W_{\text{¥}}^{\mathbb{Q}^{\text{¥}}}(t), W^{\mathbb{Q}^{\text{¥}}}(t)]^\top$:

$$d\tilde{\mathbf{W}}(t)(d\tilde{\mathbf{W}}(t))^\top = \begin{pmatrix} 1 & \rho_{S,\text{§}} & \rho_{S,\text{¥}} & \rho_{S,Y} \\ \rho_{S,\text{§}} & 1 & \rho_{\text{§},\text{¥}} & 0 \\ \rho_{S,\text{¥}} & \rho_{\text{§},\text{¥}} & 1 & 0 \\ \rho_{S,Y} & 0 & 0 & 1 \end{pmatrix}.$$

It is important to note that the positive semi-definite condition of the correlation matrix must be satisfied, which requires that the determinants of the matrix and all of its leading principal minor matrices must be non-negative and therefore the following constraint needs

to be imposed on $\rho_{S,Y}$:

$$-\sqrt{\frac{1 - \rho_{S,\$}^2 - \rho_{S,\yen}^2 - \rho_{\$, \yen}^2 + 2\rho_{S,\$}\rho_{S,\yen}\rho_{\$, \yen}}{1 - \rho_{\$, \yen}^2}} \leq \rho_{S,Y} \leq \sqrt{\frac{1 - \rho_{S,\$}^2 - \rho_{S,\yen}^2 - \rho_{\$, \yen}^2 + 2\rho_{S,\$}\rho_{S,\yen}\rho_{\$, \yen}}{1 - \rho_{\$, \yen}^2}}. \quad (2.59)$$

We can then express the Brownian motions $(W_S^{\mathbb{Q}^\yen}, W_S^{\mathbb{Q}^\$}, W_\yen^{\mathbb{Q}^\yen}, W_\$^{\mathbb{Q}^\yen})$ in terms of a linear transformation of four independent standard Brownian motions $(W_1^{\mathbb{Q}^\yen}, W_2^{\mathbb{Q}^\yen}, W_3^{\mathbb{Q}^\yen}, W_4^{\mathbb{Q}^\yen})$:

$$\begin{aligned} W_S^{\mathbb{Q}^\yen}(T) &= \rho_{S,Y}W_1^{\mathbb{Q}^\yen}(T) + \sqrt{1 - \rho_{S,Y}^2}W_2^{\mathbb{Q}^\yen}(T), \\ W_\yen^{\mathbb{Q}^\yen}(T) &= \rho_1W_1^{\mathbb{Q}^\yen}(T) + \rho_2W_2^{\mathbb{Q}^\yen}(T), \\ W_\$^{\mathbb{Q}^\yen}(T) &= \rho_3W_1^{\mathbb{Q}^\yen}(T) + \rho_4W_2^{\mathbb{Q}^\yen}(T) + \rho_5W_3^{\mathbb{Q}^\yen}(T), \end{aligned} \quad (2.60)$$

where

$$\begin{aligned} \rho_1 &= \frac{\rho_{S,\yen}}{\sqrt{1 - \rho_{S,Y}^2}}, \quad \rho_2 = \sqrt{1 - \frac{\rho_{S,\yen}^2}{1 - \rho_{S,Y}^2}}, \quad \rho_3 = \frac{\rho_{S,\$}}{\sqrt{1 - \rho_{S,Y}^2}}, \\ \rho_4 &= \frac{\rho_{\$, \yen}(1 - \rho_{S,Y}^2) - \rho_{S,\yen}\rho_{S,\$}}{\sqrt{(1 - \rho_{S,Y}^2 - \rho_{S,\yen}^2)(1 - \rho_{S,Y}^2)}}, \quad \rho_5 = \sqrt{1 - \rho_4^2 - \frac{\rho_{S,\$}^2}{1 - \rho_{S,Y}^2}}. \end{aligned} \quad (2.61)$$

The Brownian motion driving the exchange rate process under measure \mathbb{Q}^\yen conditional on default can be further expressed directly in terms of the credit index process¹. Given equation 2.58, we have

$$W_S^{\mathbb{Q}^\yen}(T) = \int_0^T \frac{\rho_{S,\yen}}{\sigma(s)} dY(s) - \nu\rho_{S,\yen} \int_0^T \sigma(s) ds + \sqrt{1 - \rho_{S,Y}^2}W_1^{\mathbb{Q}^\yen}(T), \quad (2.62)$$

¹To clarify, empirical evidence (for example, Russian default in 1997) suggests that there's a negative correlation between the exchange rate (especially among emerging market currencies) and the credit quality of a company. Usually a depreciating currency leads to the deterioration in the credit quality of a large corporate entity, which happens almost simultaneously. Our modelling objective is to capture the negative correlation between the two suggested by empirical evidence, rather than the causation, and we're not stating that deteriorating credit quality leads to a weakening currency, as it is usually the other way round.

combining equation 2.60, the exchange rate process $S(T)$ can be rearranged as

$$\begin{aligned}
 S(T) &= S(t) \exp\{M_{\mathbb{Y}}(t, T) - M_{\mathbb{S}}(t, T) - \frac{1}{2}(\sigma_S)^2(T-t) + \int_t^T [\sigma_{\mathbb{S}}\sigma_S\rho_{S,\mathbb{S}}C_{\mathbb{S}}(s, T) - \nu\sigma_S\rho_{S,Y}\sigma(s)]ds\} \\
 &\quad + \sigma_S\sqrt{1-\rho_{S,Y}^2}W_1^{\mathbb{Q}^{\mathbb{Y}}}(T-t) + \sigma_{\mathbb{Y}}\int_t^T C_{\mathbb{Y}}(s, T)dW_{\mathbb{Y}}^{\mathbb{Q}^{\mathbb{Y}}}(s) - \sigma_{\mathbb{S}}\int_t^T C_{\mathbb{S}}(s, T)dW_{\mathbb{S}}^{\mathbb{Q}^{\mathbb{Y}}}(s) \\
 &\quad + \int_t^T \frac{\sigma_S\rho_{S,Y}}{\sigma(s)}dY(s) \\
 &= S(t) \exp\{M_{\mathbb{Y}}(t, T) - M_{\mathbb{S}}(t, T) - \frac{1}{2}(\sigma_S)^2(T-t) + \int_t^T [\sigma_{\mathbb{S}}\sigma_S\rho_{S,\mathbb{S}}C_{\mathbb{S}}(s, T) - \nu\sigma_S\rho_{S,Y}\sigma(s)]ds\} \\
 &\quad + \sigma^S\sqrt{1-\rho_{S,Y}^2}W_1^{\mathbb{Q}^{\mathbb{Y}}}(T-t) + \sigma_{\mathbb{Y}}\int_t^T C_{\mathbb{Y}}(s, T)d[\rho_1W_1^{\mathbb{Q}^{\mathbb{Y}}}(s) + \rho_2W_2^{\mathbb{Q}^{\mathbb{Y}}}(s)] \\
 &\quad - \sigma_{\mathbb{S}}\int_t^T C_{\mathbb{S}}(s, T)d[\rho_3W_1^{\mathbb{Q}^{\mathbb{Y}}}(s) + \rho_4W_2^{\mathbb{Q}^{\mathbb{Y}}}(s) + \rho_5W_3^{\mathbb{Q}^{\mathbb{Y}}}(s)] + \int_t^T \frac{\sigma_S\rho_{S,Y}}{\sigma(s)}dY(s) \\
 &= S(t) \exp\{M_{\mathbb{Y}}(t, T) - M_{\mathbb{S}}(t, T) - \frac{1}{2}(\sigma_S)^2(T-t) + \int_t^T [\sigma_{\mathbb{S}}\sigma_S\rho_{S,\mathbb{S}}C_{\mathbb{S}}(s, T) - \nu\sigma_S\rho_{S,Y}\sigma(s)]ds\} \\
 &\quad + \int_t^T [\sigma_S\sqrt{1-\rho_{S,Y}^2} + \rho_1\sigma_{\mathbb{Y}}C_{\mathbb{Y}}(s, T) - \rho_3\sigma_{\mathbb{S}}C_{\mathbb{S}}(s, T)]dW_1^{\mathbb{Q}^{\mathbb{Y}}}(s) \\
 &\quad + \int_t^T [\rho_2\sigma_{\mathbb{Y}}C_{\mathbb{Y}}(s, T) - \rho_4\sigma_{\mathbb{S}}C_{\mathbb{S}}(s, T)]W_2^{\mathbb{Q}^{\mathbb{Y}}}(s) - \int_t^T \rho_5\sigma_{\mathbb{S}}C_{\mathbb{S}}(s, T)dW_3^{\mathbb{Q}^{\mathbb{Y}}}(s) + \int_t^T \frac{\sigma_S\rho_{S,Y}}{\sigma(s)}dY(s),
 \end{aligned} \tag{2.63}$$

where

$$\begin{aligned}
 M_{\mathbb{Y}}(t, T) &= \ln \frac{P_{\mathbb{Y}}(0, t)}{P_{\mathbb{Y}}(0, T)} + y_{\mathbb{Y}}(t)C_{\mathbb{Y}}(t, T) + \frac{1}{2}[V_{\mathbb{Y}}(0, T) - V_{\mathbb{Y}}(0, t)], \\
 M_{\mathbb{S}}(t, T) &= \ln \frac{P_{\mathbb{S}}(0, t)}{P_{\mathbb{S}}(0, T)} + y_{\mathbb{S}}(t)C_{\mathbb{S}}(t, T) + \frac{1}{2}[V_{\mathbb{S}}(0, T) - V_{\mathbb{S}}(0, t)].
 \end{aligned}$$

2.4.3 Calibration of Multi-Currency Framework

Based on Brigo and Mercurio (2007, Chapter 3), under the Hull-White short rate model with mean reversion rate a and the short rate volatility coefficient σ , closed-form pricing formula for an interest rate cap with strike K , maturity T and notional N at time t can be

expressed as follows:

$$Cap(t, T, N, K) = N \sum_{i=1}^n [P(t, t_{i-1})\Phi(-h_i + \sigma_p^i) - (1 + K\tau_i)P(t, t_i)\Phi(-h_i)], \quad (2.64)$$

$$\sigma_p^i = \sigma \sqrt{\frac{1 - e^{-2a(t_i - t_{i-1})}}{a}} B(t_{i-1}, t_i), \quad B(t_{i-1}, t_i) = \frac{1}{a} [1 - e^{-a(t_i - t_{i-1})}],$$

$$h_i = \frac{1}{\sigma_p^i} \ln \frac{P(t, t_i)(1 + K\tau_i)}{P(t, t_{i-1})} + \frac{\sigma_p^i}{2},$$

where $P(t, t_i)$ is the zero coupon bond price, $\{t_i\}$, $i = 1, \dots, n$ are the payment dates, $\tau_i = t_i - t_{i-1}$ and Φ is the cumulative standard normal distribution function.

The parameters of the dollar and yen short rate processes are a , $\sigma_{\$}$ and b , $\sigma_{¥}$, we calibrate the two pairs to the implied volatilities of at-the-money (ATM) dollar and yen caps with maturities up to thirty years respectively on 28th April 2014, summarized in Table 2.4.1:

Maturity	ATM Yen Cap Implied Volatility	ATM Dollar Cap Implied Volatility
1y	0.6295	0.5735
2y	0.7385	0.7215
3y	0.7772	0.618
4y	0.8068	0.518
5y	0.752	0.4538
6y	0.6743	0.4047
7y	0.6198	0.3763
8y	0.5585	0.3495
9y	0.514	0.332
10y	0.483	0.3198
12y	-	0.2957
15y	-	0.2703
20y	-	0.2452
25y	-	0.2388
30y	-	0.2343

Table 2.4.1: ATM Yen cap and ATM Dollar cap implied volatility quotes on 28th April 2014. Data Source: Bloomberg

Following the least square calibration procedures taken in Brigo and Mercurio (2007, Chapter 3), we set the range of the mean reversion rates a , b to be in the interval $[0.001, 0.1]$ and

the range of the volatility parameters to be in the interval $(0, 1)$, the values of the parameters are:

$$a = 0.0906, \sigma_{\$} = 0.0116, b = 0.0397, \sigma_{¥} = 0.0061.$$

The calibration of the USDJPY exchange rate dynamics involves pricing options written on the USDJPY exchange rate with maturity T and strike K at time t , whose value is by market standard expressed as:

$$V(t, S(t), r_{\$}(t), r_{¥}(t)) = E_t^{\mathbb{Q}^{\text{¥}}} \left[\frac{B_{¥}(t)}{B_{¥}(T)} \max(S(T) - K, 0)^+ \right], \quad (2.65)$$

with $B_{¥}(t)$ given in equation 2.37. To reduce the complexity of the pricing problem, we move from the yen risk-neutral measure generated by the yen money market account to the yen forward measure where the numeraire is the yen zero coupon bond. Given $S^T(t) = S(t) \frac{P_{\$}(t, T)}{P_{¥}(t, T)}$, by switching from the $\mathbb{Q}^{\text{¥}}$ to the forward FX measure $\mathbb{Q}^{T^{\text{¥}}}$, we have

$$V(t, S^T(t)) = P_{¥}(t, T) E_t^{\mathbb{Q}^{T^{\text{¥}}}} [\max(S^T(T) - K, 0)^+]. \quad (2.66)$$

In order to arrive at a closed-form pricing formula for $V(t, S^T(t))$, we need to determine the dynamics of the forward exchange rate $S^T(t)$. Following Grzelak and Oosterlee (2011), we first apply Ito's Lemma to $S^T(t)$:

$$\begin{aligned} dS^T(t) &= \frac{P_{\$}(t, T)}{P_{¥}(t, T)} dS(t) + \frac{S(t)}{P_{¥}(t, T)} dP_{\$}(t, T) - S(t) \frac{P_{\$}(t, T)}{(P_{¥}(t, T))^2} dP_{¥}(t, T) \\ &+ S(t) \frac{P_{\$}(t, T)}{(P_{¥}(t, T))^3} (dP_{¥}(t, T))^2 + \frac{1}{P_{¥}(t, T)} dS(t) dP_{\$}(t, T) \\ &\frac{P_{\$}(t, T)}{(P_{\$}(t, T))^2} dP_{¥}(t, T) dS(t) - \frac{S(t)}{(P_{¥}(t, T))^2} dP_{¥}(t, T) dP_{\$}(t, T) \end{aligned} \quad (2.67)$$

and plug the risk-neutral dynamics of $S(t)$, $P_{\$}(t, T)$ and $P_{¥}(t, T)$ under $\mathbb{Q}^{\text{¥}}$ into equation

2.67, the forward exchange rate dynamics under $\mathbb{Q}^{\text{¥}}$ will then become:

$$\begin{aligned} \frac{dS^T(t)}{S^T(t)} &= \sigma_{\text{¥}}C_{\text{¥}}(t, T)[\sigma_{\text{¥}}C_{\text{¥}}(t, T) - \rho_{S, \text{¥}}\sigma_S - \rho_{\$, \text{¥}}\sigma_{\$}C_{\$}(t, T)]dt \\ &+ \sigma_S dW_S^{Q^{\text{¥}}}(t) - \sigma_{\text{¥}}C_{\text{¥}}(t, T)dW_{\text{¥}}^{Q^{\text{¥}}}(t) + \sigma_{\$}C_{\$}(t, T)dW_{\$}^{Q^{\text{¥}}}(t). \end{aligned} \quad (2.68)$$

Since the forward exchange rate process $S^T(t)$ is a martingale under $\mathbb{Q}^{T^{\text{¥}}}$, we then switch again from $\mathbb{Q}^{\text{¥}}$ to $\mathbb{Q}^{T^{\text{¥}}}$, which implies that all processes originally under $\mathbb{Q}^{\text{¥}}$ will change their dynamics.

Lemma 2.4.4. *Under the yen T -forward measure $\mathbb{Q}^{T^{\text{¥}}}$, the forward exchange rate dynamics become*

$$\frac{dS^T(t)}{S^T(t)} = \sigma_S dW_S^{T^{\text{¥}}}(t) - \sigma_{\text{¥}}C_{\text{¥}}(t, T)dW_{\text{¥}}^{T^{\text{¥}}}(t) + \sigma_{\$}C_{\$}(t, T)dW_{\$}^{T^{\text{¥}}}(t), \quad (2.69)$$

where

$$\begin{aligned} dW_S^{T^{\text{¥}}}(t) &= dW_S^{Q^{\text{¥}}}(t) - \rho_{S, \text{¥}}\sigma_{\text{¥}}C_{\text{¥}}(t, T)dt, \\ dW_{\text{¥}}^{T^{\text{¥}}}(t) &= dW_{\text{¥}}^{Q^{\text{¥}}}(t) - \sigma_{\text{¥}}C_{\text{¥}}(t, T)dt, \\ dW_{\$}^{T^{\text{¥}}}(t) &= dW_{\$}^{Q^{\text{¥}}}(t) - \rho_{\$, \text{¥}}\sigma_{\text{¥}}C_{\text{¥}}(t, T)dt, \end{aligned} \quad (2.70)$$

and correspondingly the short rate dynamics will become

$$\begin{aligned} r_{\$}(t) &= \theta_{\$}(t) + y_{\$}(t), \quad r_{\$}(0) > 0, \\ r_{\text{¥}}(t) &= \theta_{\text{¥}}(t) + y_{\text{¥}}(t), \quad r_{\text{¥}}(0) > 0, \\ dy_{\$}(t) &= (-ay_{\$}(t) - \sigma_{\$}\sigma_S\rho_{S, \$} + \sigma_{\$}\sigma_{\text{¥}}\rho_{\$, \text{¥}}C_{\text{¥}}(t, T))dt + \sigma_{\$}dW_{\$}^{T^{\text{¥}}}(t), \\ dy_{\text{¥}}(t) &= (-by_{\text{¥}}(t) + \sigma_{\text{¥}}C_{\text{¥}}(t, T))dt + \sigma_{\text{¥}}dW_{\text{¥}}^{T^{\text{¥}}}(t). \end{aligned} \quad (2.71)$$

Proof. For proof see Grzelak and Oosterlee (2011). □

It can be observed in equation 2.69 that through change of measure the forward exchange rate dynamics no longer depends explicitly on the two short rate processes. Denote a random

variable S as the sum of three correlated, normally distributed random variables, $A \sim N(\mu_A, v_A^2)$, $B \sim N(\mu_B, v_B^2)$ and $C \sim N(\mu_C, v_C^2)$, it is easily proved that S remains normal with its mean μ_S equal to $\mu_S = \mu_A + \mu_B + \mu_C$ and the variance v_S^2 equal to

$$v_S^2 = v_A^2 + v_B^2 + v_C^2 + 2\rho_{A,B}v_Av_B + 2\rho_{A,C}v_Av_C + 2\rho_{B,C}v_Bv_C. \quad (2.72)$$

Therefore, the forward exchange rate dynamics can be rearranged further to:

$$\frac{dS^T(t)}{S^T(t)} = \sigma_F^T(t, T)dW_F^{T^\mathbb{Y}}(t), \quad (2.73)$$

where

$$\begin{aligned} \sigma_F^T(t, T) = & [\sigma_S^2 + (\sigma_{\mathbb{Y}}C_{\mathbb{Y}}(t, T))^2 + (\sigma_{\mathbb{S}}C_{\mathbb{S}}(t, T))^2 + 2\rho_{S,\mathbb{Y}}\sigma_{\mathbb{Y}}C_{\mathbb{Y}}(t, T)\sigma_S - 2\rho_{S,\mathbb{S}}\sigma_{\mathbb{S}}C_{\mathbb{S}}(t, T)\sigma_S \\ & - 2\rho_{\mathbb{S},\mathbb{Y}}\sigma_{\mathbb{Y}}\sigma_{\mathbb{S}}C_{\mathbb{Y}}(t, T)C_{\mathbb{S}}(t, T)]^{\frac{1}{2}} \end{aligned} \quad (2.74)$$

and $W_F^{T^\mathbb{Y}}(t)$ is a standard Brownian motion under $\mathbb{Q}^{T^\mathbb{Y}}$. Since the change of measure only involves the change of the drift term of the dynamics, the full correlation matrix is retained such that:

$$\begin{aligned} dW_F^{T^\mathbb{Y}}(t)dW_{\mathbb{Y}}^{T^\mathbb{Y}}(t) &= \rho_{S,\mathbb{Y}}dt, \\ dW_F^{T^\mathbb{Y}}(t)dW_{\mathbb{S}}^{T^\mathbb{S}}(t) &= \rho_{S,\mathbb{S}}dt, \\ dW_{\mathbb{S}}^{T^\mathbb{S}}(t)dW_{\mathbb{Y}}^{T^\mathbb{Y}}(t) &= \rho_{\mathbb{S},\mathbb{Y}}dt. \end{aligned}$$

The integral form solution of $S^T(T)$ can then be easily obtained:

$$S^T(T) = S^T(t) \exp\left(-\frac{1}{2} \int_t^T \sigma_F^T(u, T)^2 du + \int_t^T \sigma_F^T(u, T) dW_F^{T^\mathbb{Y}}(u)\right) \quad (2.75)$$

and the closed-form pricing formula for FX call option can be expressed as:

$$V(t, S^T(t)) = P_{\mathbb{Y}}(t, T)[S^T(t)\Phi(d_1) - K\Phi(d_2)], \quad (2.76)$$

where

$$d_{1,2} = \frac{\log\left(\frac{S^T(t)}{K}\right)}{\Gamma(t, T)\sqrt{T-t}} \pm \frac{1}{2}\Gamma(t, T)\sqrt{T-t},$$

$$\Gamma(t, T)^2 = \frac{1}{T-t} \int_t^T \sigma_F^T(u, T)^2 du. \quad (2.77)$$

Before fitting equation 2.76 to the ATM USDJPY FX call options data observed on 28th April 2014 summarized in Table 2.4.2, it is essential to estimate the correlation parameters $\rho_{S,\text{¥}}$, $\rho_{S,\$}$ and $\rho_{\$, \text{¥}}$. As indicated in Piterbarg (2006), the correlation parameters are typically chosen either by historical estimation or from occasionally observed prices of 'quanto' interest rate derivatives (payoff settled in one currency but linked to rates in another currency). Since the latter is usually illiquid and consequently subject to data gaps, we decide to estimate the correlation matrix based on historical observations of USDJPY exchange rate and interest rates given a specific time horizon. We choose the 5-year time horizon between 28th April 2009 and 28th April 2014 and obtain the estimated values of the correlation parameters² as follows:

$$\begin{pmatrix} 1 & \rho_{S,\$} & \rho_{S,\text{¥}} \\ \rho_{S,\$} & 1 & \rho_{\$, \text{¥}} \\ \rho_{S,\text{¥}} & \rho_{\$, \text{¥}} & 1 \end{pmatrix} = \begin{pmatrix} 1 & -0.33 & -0.56 \\ -0.33 & 1 & 0.51 \\ -0.56 & 0.51 & 1 \end{pmatrix}.$$

Given the calibrated parameters for the short rate dynamics in the previous section and the estimated correlation parameters, the only parameters left to be calibrated is the volatility coefficient σ_S of the exchange rate process. Given the spot USDJPY exchange rate on 28th April 2014 is 102.5, we can then fit the pricing formula of the FX call option in equation 2.76 to the market data and obtain $\sigma_S = 0.066$.

²The correlation parameters are estimated using the standard Pearson approach. The standard errors are computed with formula $SE = \sqrt{\frac{1-\rho^2}{n-2}}$, where n is the number of observations, $n = 1260$. The corresponding standard errors for $\rho_{S,\$}$, $\rho_{S,\text{¥}}$, $\rho_{\$, \text{¥}}$ are hence 0.026614781, 0.023358681, 0.024251924 respectively.

Maturity	ATM USDJPY FX Implied Volatility
0.25y	0.0706
0.5y	0.0785
1y	0.0877
1.5y	0.518
2y	0.0929
3y	0.1059
5y	0.1254
7y	0.1488
10y	0.1685

Table 2.4.2: ATM USDJPY FX call option implied volatility quotes on 28th April 2014. Data Source: Bloomberg

2.4.4 Calibration of Risk-Neutral Default Time Distribution

To calibrate the credit index process Y , we consider credit default swaps (CDSs), which is a contracts written on a reference entity "RN" ensuring protection of its default. Given maturity T , a CDS involves two counterparties "PB" the protection buyer and "PS" the protection seller exchanging periodic cash flows, i.e., in the premium leg "PB" makes constant payment c to "PS" on fixed dates $\{t_k\}_{k=0,\dots,n}$, $\alpha_k = t_k - t_{k-1}$, $t_n = T$ while in the protection leg in case of default of the reference entity "RN" on the underlying bond before T , "PS" will be liable to pay "PB" the unrecovered value of the bond equal to $1 - RR$ at the time of default $\tau_{RN} \in (t_{k-1}, t_k]$, where $RR \in (0, 1)$ is the recovery rate of the underlying bond issued by "RN". Assuming that the CDS contract used for calibration is immune from default risk from both the protection buyer and seller, we consider a simplified CDS valuation formula based on Bielecki and Rutkowski (2002):

$$(1 - RR) \sum_{k=1}^n P(t, t_k) \alpha_k (\bar{G}(t_{k-1}) - \bar{G}(t_k)) = \sum_{k=1}^n P(t, t_k) \alpha_k \bar{G}(t_k) \pi, \quad (2.78)$$

where $P(t, t_k)$ is the zero coupon bond price associated with maturity t_k and $\bar{G}(t_k) = 1 - G(t_k)$, which can be interpreted as the survival probability of the reference entity before t_k . It is important to note that, for convenience, we choose two counterparties based in the same credit market. The treatment of quanto adjustment effects involved in calibrating CDS

contracts written on a foreign counterparty but settled in the domestic currency is out of the scope of this thesis.

From Theorem 2.2.1, we know that \bar{G} can be further expressed in terms of the hazard function of the market implied risk-neutral default probability distribution:

$$\bar{G}(t) = \exp\left(-\int_0^t \gamma(s)ds\right), \quad (2.79)$$

where the piece-wise constant hazard function $\gamma(t)$ of the default time distribution defined as

$$\gamma(t) = \gamma_k, \quad t_k \leq t < t_{k+1} \quad (2.80)$$

can be bootstrapped from G and the volatility function of the credit index process can be expressed as

$$\sigma^2(t) = \frac{\gamma(t)}{\lambda}, \quad t_k \leq t < t_{k+1} \quad (2.81)$$

given a reasonable value of λ , used as a scaling factor for numerical stability purposes in case the short term hazard rates are too high, leading to chopping and unrealistic evolution of the credit index process. In this thesis, we set $\lambda = 1$, which is the benchmark case that the variance of the credit index process is equal to the corresponding hazard rate (instantaneous forward default rate) of the counterparty) at time t . This is reasonable as the hazard rate is a measure of default intensity and should in turn correspond to the strength of the credit index variance. This means that given the market CDS term structure of a certain counterparty, we are able to back out the piece-wise constant values of the hazard function, from which the corresponding piece-wise constant implied volatility function of the credit index process can be obtained. We now consider a numerical example on Nomura International given its market CDS data observed on 28th April 2014 in Table 2.4.3:

The resulting implied hazard function γ and the implied piece-wise constant volatilities of the credit index process Y are illustrated in Figure 2.4.1 and Figure 2.4.2 respectively.

Maturity	Par CDS Spreads
0.5y	0.00246
1y	0.00261
2y	0.00388
3y	0.00539
4y	0.00792
5y	0.00973
7y	0.01213
10y	0.0137

Table 2.4.3: Market CDS term structure of Nomura International on 28th April 2014.

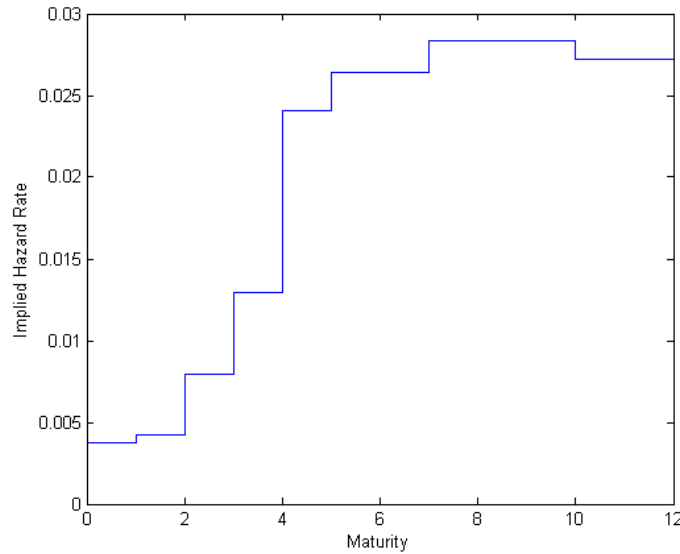


Figure 2.4.1: Implied hazard function calibrated to 8 CDS quotes on Nomura International for maturities ranging from 6 months to 10 years.

2.4.5 Bootstrapping of Survival Curves

In this section, we discuss the bootstrap methods for the survival probability curve of a counterparty. We follow O’Kane (2011), where the interpolation is done on the logarithm of the survival probability, which can be described as exponentially interpolating the survival probability. We define

$$f(t) = -\ln(\bar{G}(t)). \quad (2.82)$$

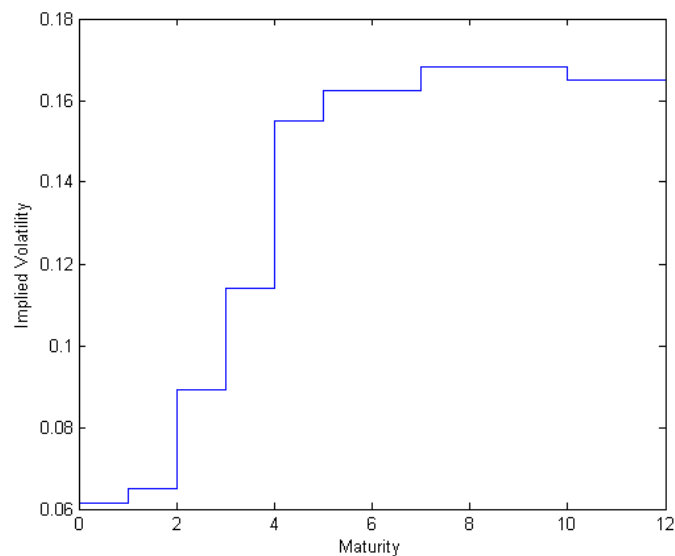


Figure 2.4.2: Implied volatilities of the credit index process calibrated to 8 CDS quotes on Nomura International for maturities ranging from 6 months to 10 years.

Based on equation 2.79, we have

$$f(t) = \int_0^t \gamma(s) ds. \quad (2.83)$$

We therefore can write

$$\gamma(t) = \frac{\partial f(t)}{\partial t}. \quad (2.84)$$

We can therefore write this interpolation scheme for time t^* in terms of $f(t^*)$ by differentiating the standard linear interpolation function of $f(t)$:

$$f(t^*) = \frac{(t_n - t^*)f(t_{n-1}) + (t^* - t_{n-1})f(t_n)}{t_n - t_{n-1}} \quad (2.85)$$

and obtain

$$\gamma(t^*) = \frac{\partial f(t^*)}{\partial t^*} = \frac{f(t_n) - f(t_{n-1})}{t_n - t_{n-1}}. \quad (2.86)$$

Since $\gamma(t^*)$ does not depend on t^* , this interpolation scheme shows that $\gamma(t^*)$ is constant between the interpolation limits, which indicates that linear interpolation of the log of survival probability is equivalent to assuming piece-wise constant forward default rate $\gamma(t)$. There-

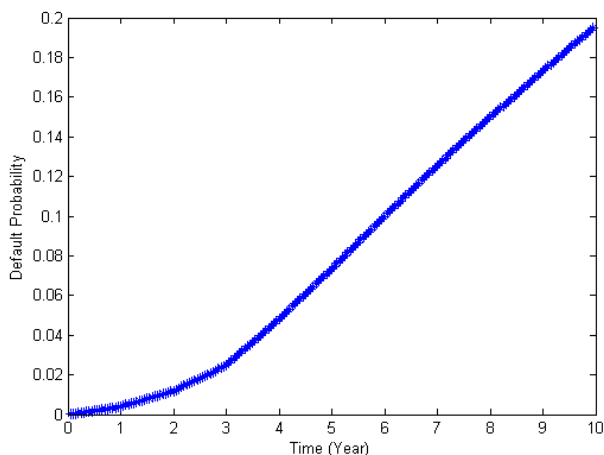


Figure 2.4.3: Interpolated default probability curve generated from CDS quotes of Nomura International on 28th April 2014.

fore, constant continuously compounded forward default rate at time t^* , $t_{n-1} < t^* < t_n$ as

$$\gamma(t^*) = \gamma(t_{n-1}) = \frac{1}{t_n - t_{n-1}} \ln\left(\frac{\bar{G}(t_{n-1})}{\bar{G}(t_n)}\right). \quad (2.87)$$

The formula for the survival probability at time t^* is therefore

$$\bar{G}(t^*) = \bar{G}(t_{n-1}) \exp((t^* - t_{n-1})\gamma(t_{n-1})). \quad (2.88)$$

This ensures no arbitrage between the interpolation points as $\gamma(t) \geq 0$ such that $\bar{G}(t_n) \leq \bar{G}(t_{n-1})$. For more details, please refer to O’Kane (2011). Figure 2.4.3 is the interpolated default probability curve for Nomura International given the CDS quotes on 28th April 2014.

2.5 Numerical Tests

In this section, we perform numerical examples of our joint FX-credit model and quantify the impact of wrong way correlation on the counterparty exposure of FX derivatives through various risk measures. We will continue to use the values of the model parameters having been calibrated to market data on 28th April 2014 in the previous sections. First of all,

we introduce the two FX derivatives we consider in the numerical examples, which are FX forwards and cross currency swaps.

2.5.1 Comparison with Hull and White (2001)

Since our approach is a further development of the inverse first-passage time approach. It would be necessary to compare with a similar approach, for example Hull and White (2001). Under their approach, the credit index process is assumed to be a standard Brownian motion starting from 0, with variance 1 per year. The default barrier is explicitly bootstrapped such that given a discrete set of default times, the first time the credit index process crosses the barrier level yields a distribution equal to the market implied default probability density. As a numerical example, we choose to bootstrap the default barrier of Nomura International given the CDS quotes on 28th April 2014 provided in Table 2.4.3. In order to make the default barrier close to the continuous case, we set 1000 default points with time step 0.05 (years) up to 10 year period, see Figure 2.5.1 the bootstrapped default barrier. The MATLAB running time for bootstrapping the default barrier only is 3140 seconds (≈ 53 min). First of all, the drawback of this approach is accuracy as numerical methods are applied to approximate the continuous integral and solve for the barrier level that renders the probability generated by the model to be equal to the market implied one in the discrete case. And interpolation or extrapolation scheme will have to be used to obtain the intermediate barrier levels in between the discrete default time points, leading to further inaccuracy and even arbitrage opportunities. Furthermore, the default barrier is generated based on the assumption that the credit index process follows a normal distribution, which is not the case in reality and consequently the default barrier generated is not a true reflection of the distance to default and capital structure of the company, leading to bias in counterparty exposure calculations. Third, the more default points you introduce to smoothen the default barrier, the longer it will take to bootstrap the default barrier.

With our approach, a fixed zero barrier is chosen, which avoids the explicit bootstrapping of the default barrier while maintaining an exact calibration to the market implied

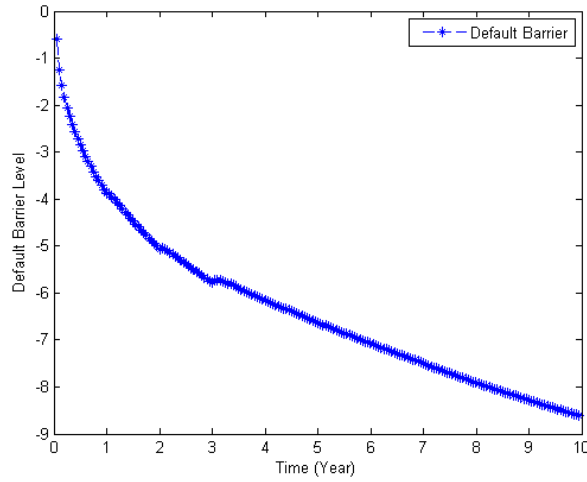


Figure 2.5.1: Implied Default barrier generated from CDS quotes of Nomura International on 28th April 2014, based on Hull and White (2001) approach.

default probability distribution of any form, not limited to normal. In addition, the volatility of the credit index process is calibrated to the piece-wise constant hazard rates of the default time distribution, which is more realistic and flexible and the random starting point offers an extra degree of freedom.

2.5.2 FX Forward

An FX forward contract is an agreement to purchase or sell a set amount of a foreign currency at a specified price K for settlement at a predetermined time T in the future. The strike price K is usually set to be equal to the at-the-money forward exchange rate at inception $S^T(0)$:

$$S^T(0) = S(0) * \frac{1 + T * R_d(0, T)}{1 + T * R_f(0, T)}, \quad (2.89)$$

where $R_d(0, T)$ and $R_f(0, T)$ are the domestic and foreign zero rates for maturity T . Specifically, the yen and dollar zero rates for maturity T in our example. The payoff of the FX forward at maturity T is:

$$V(T) = S(T) - K. \quad (2.90)$$

2.5.3 Cross Currency Swap

A cross currency swap (CCS), also referred to as cross currency interest rate swap, is an agreement between two counterparties, "A" and "B", to exchange interest rate payments denominated in two different currencies periodically. Unlike single currency interest rate swaps, a CCS involves actual exchange of notionals in the two currencies at both inception and expiration. Specifically, for constant notional CCSs the notional to be exchanged at expiry is based on the exchange rate at inception while for Mark-to-Market (MtM) CCSs the notional is reset periodically using the prevailing spot exchange rate.

Since cross currency basis spreads are involved in floating-for-floating cross currency swaps and the treatment of such spreads has become increasingly sophisticated since the 2007-2008 financial crisis where increased liquidity and credit risks caused the spreads to widen significantly and behave in a quite volatile fashion, to simplify the matter, we consider fixed-for-fixed cross currency swap, where periodic fixed rate payments denominated in two different currencies are exchanged. Specifically, given the currency pair USDJPY and the contract maturity T , we assume that party "A" is the yen payer while party "B" is the dollar payer, we denote the USDJPY exchange rate process as $S(t)$ and the quarterly payment dates as $\{T_i\}_{i=0}^n$, with $T_0 = 0$, $T_n = T$ and $\delta_i = T_i - T_{i-1}$, the cash flows of the trade from the point of view of party "A" can be described as follows:

- At $T_0 = 0$, pay dollar notional $N_0^\$$, receive yen notional $N_0^\yen = S(0)N_0^\$$
- At T_i , $i = 1, \dots, n$, receive $N_0^\$ \delta_i K^\$$ and pay $N_0^\yen \delta_i K^\yen$ quarterly, where $K^\$$ and K^\yen are the constant dollar and yen fixed payment rate agreed at T_0 such that the contract is entered into at zero cost
- At $T_n = T$, receive dollar notional $N_0^\$$, pay back the yen notional N_0^\yen

2.5.4 Cross Currency Swap Valuation Formula

Suppose we are at time $t \in (T_{j-1}, T_j]$, $j = 1, \dots, n$, according to Brigo et al. (2013), the mark-to-market value of the fixed-for-fixed cross currency swap $V(t)$ denominated in yen terms from the point of view of the yen payer can be expressed as

$$\begin{aligned}
 V(t) &= E_t^{\mathbb{Q}^\yen} \left[N_0^\$ \sum_{i=j}^n S(T_i) K^\$ \delta_i e^{-\int_t^{T_i} r_\yen(s) ds} - N_0^\yen \sum_{i=j}^n K^\yen \delta_i e^{-\int_t^{T_i} r_\yen(s) ds} \right. \\
 &\quad \left. + (-N_0^\yen + S(T_n) N_0^\$) e^{-\int_t^{T_n} r_\yen(s) ds} \right] \\
 &= N_0^\$ \sum_{i=j}^n E_t^{T_i^\yen} [S(T_i)] K^\$ \delta_i P_\yen(t, T_i) - N_0^\yen \sum_{i=j}^n K^\yen \delta_i P_\yen(t, T_i) \\
 &\quad + (-N_0^\yen + E_t^{T_n^\yen} [S(T_n)] N_0^\$) P_\yen(t, T_n), \tag{2.91}
 \end{aligned}$$

where $E_t^{\mathbb{Q}^\yen}$ and $E_t^{T_i^\yen}$ are conditional expectations taken under \mathbb{Q}^\yen and $\mathbb{Q}^{T_i^\yen}$ respectively. Since the forward USDJPY exchange rate process $S(t, T_i) = S(t) \frac{P_\$(t, T_i)}{P_\yen(t, T_i)}$ is a martingale under $\mathbb{Q}^{T_i^\yen}$, equation 2.91 can be rearranged as

$$\begin{aligned}
 V(t) &= N_0^\$ \sum_{i=j}^n S(t, T_i) K^\$ \delta_i P_\yen(t, T_i) - N_0^\yen \sum_{i=j}^n K^\yen \delta_i P_\yen(t, T_i) \\
 &\quad + (-N_0^\yen + S(t, T_n) N_0^\$) P_\yen(t, T_n). \tag{2.92}
 \end{aligned}$$

Furthermore, define for the dollar leg

$$K_{T_i}^\$ = \begin{cases} \frac{K^\$}{S(0)}, & i = j + 1, \dots, n - 1 \\ K^\$ + \frac{1}{\delta_i}, & i = n \end{cases}$$

then we have

$$\begin{aligned}
 V(t) &= N_0^{\text{¥}} \left[\frac{N_0^{\text{§}}}{N_0^{\text{¥}}} \sum_{i=j}^n S(t, T_i) K^{\text{§}} \delta_i P_{\text{¥}}(t, T_i) - \sum_{i=j}^n K^{\text{¥}} \delta_i P_{\text{¥}}(t, T_i) \right. \\
 &\quad \left. + (-1 + S(t, T_n) \frac{N_0^{\text{§}}}{N_0^{\text{¥}}}) P_{\text{¥}}(t, T_n) \right] \\
 &= N_0^{\text{¥}} \left[\frac{1}{S(0)} \sum_{i=j}^n S(t, T_i) K^{\text{§}} \delta_i P_{\text{¥}}(t, T_i) - \sum_{i=j}^n K^{\text{¥}} \delta_i P_{\text{¥}}(t, T_i) \right. \\
 &\quad \left. + (-1 + \frac{S(t, T_n)}{S(0)}) P_{\text{¥}}(t, T_n) \right] \\
 &= N_0^{\text{¥}} \left[\sum_{i=j}^n S(t, T_i) K_{T_i}^{\text{§}} \delta_i P_{\text{¥}}(t, T_i) - \sum_{i=j}^n K^{\text{¥}} \delta_i P_{\text{¥}}(t, T_i) - P_{\text{¥}}(t, T_n) \right]. \quad (2.93)
 \end{aligned}$$

Finally, define for the yen leg

$$K_{T_i}^{\text{¥}} = \begin{cases} K^{\text{¥}}, & i = j + 1, \dots, n - 1 \\ K^{\text{¥}} + \frac{1}{\delta_i}, & i = n \end{cases}$$

and we have

$$\begin{aligned}
 V(t) &= N_0^{\text{¥}} \left[\sum_{i=j}^n S(t, T_i) K_{T_i}^{\text{§}} \delta_i P_{\text{¥}}(t, T_i) - \sum_{i=j}^n K_{T_i}^{\text{¥}} \delta_i P_{\text{¥}}(t, T_i) \right] \\
 &= N_0^{\text{¥}} \left[\sum_{i=j}^n S(t) K_{T_i}^{\text{§}} \delta_i P_{\text{¥}}(t, T_i) - \sum_{i=j}^n K_{T_i}^{\text{¥}} \delta_i P_{\text{¥}}(t, T_i) \right]. \quad (2.94)
 \end{aligned}$$

As can be seen in equation 2.94, $V(t)$ is driven by the USDJPY exchange rate process and the two interest rate processes driving the values of the dollar and yen ZCBs.

2.5.5 Case Study I

In this case study, we consider a 5-year FX forward contract traded on 28th April 2014 between a US financial institution assumed to be default-free, taking a long position in the FX forward and Nomura Securities assumed to be defaultable, taking a short position in the FX forward. Since the FX forward can only be settled at maturity, the default can only occur at time $\tau_0^Y = 5Y$ and we are able to estimate the counterparty exposure from the

perspective of the US financial institution through Monte-Carlo simulations. We consider a set of exogenously specified correlation scenarios ($\rho_{S,Y} = -0.5, -0.3, 0, +0.3, +0.5$) between the credit index process and the exchange rate process and illustrate the impact of varying correlations on PFEs and EPEs.

We depict the histograms of the Monte Carlo approximations of the contract value conditional on default at time $\tau_0^Y = 5Y$ for each correlation scenario. In Figure 2.5.2(a)-2.5.2(b), it can be observed that in the case of negative exchange rate-credit correlations (wrong way risk), $\rho_{S,Y} = -0.5, -0.3$ where as the credit quality of Nomura Securities deteriorates the counterparty exposure increases, the probability distribution of the counterparty exposure tends to have fatter right tail and correspondingly the US financial institution is expected to have larger expected positive exposure compared to that of the zero correlation case in Figure 2.5.4, where the credit quality of Nomura Securities is independent of the exchange rate process. As $\rho_{S,Y}$ gradually increases to positive levels (right way risk), $\rho_{S,Y} = 0.3, 0.5$ as shown in Figure 2.5.3(a)-2.5.3(b) where as the credit quality of Nomura Securities deteriorates the counterparty exposure diminishes, the probability distribution of the counterparty exposure begins to move towards the negative territory and there is an increasing likelihood that the US financial institution will have negative counterparty exposure to Nomura International. Hence, it can be observed that the expected positive exposure will decrease as exchange rate-credit correlation increases from zero to positive levels.

Next, we compute the PFEs of the cross currency swap contract from the perspective of the US financial institution at confidence interval α equal to 97.5% and 2.5% respectively across the same set of exchange rate-credit correlation scenarios. Along with the EPEs, we observe in Figure 2.5.5 that the three set of quantities are all decreasing as the exchange rate-credit correlation increases, which is in line with intuition.

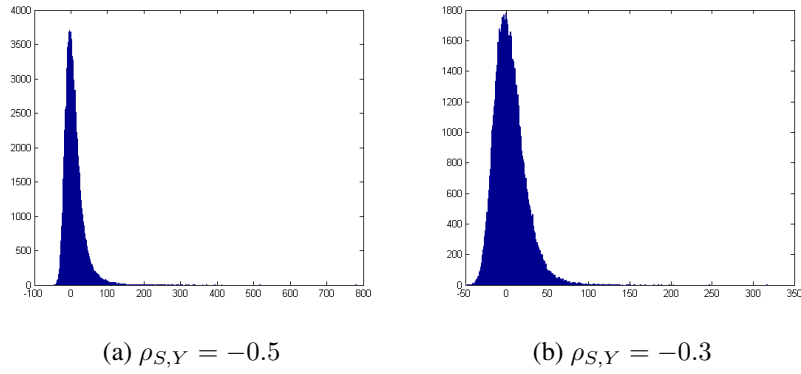


Figure 2.5.2: Histograms of simulated exposure of 5-year USDJPY FX forward contract with strike $K = 95$ at $T = 5Y$ when $\rho_{S,Y} = -0.5$ and $\rho_{S,Y} = -0.3$.

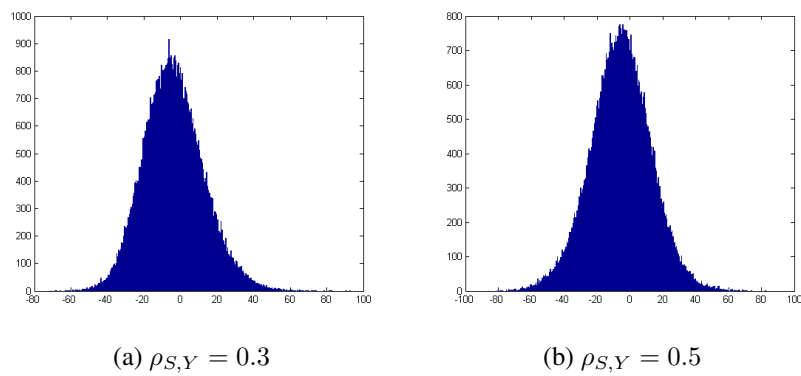


Figure 2.5.3: Histograms of simulated exposure of 5-year USDJPY FX forward contract with strike $K = 95$ at $T = 5Y$ when $\rho_{S,Y} = 0.3, 0.5$.

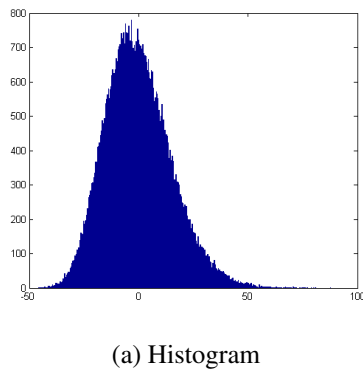


Figure 2.5.4: Histograms of simulated exposure of 5-year USDJPY FX forward contract with strike $K = 95$ at $T = 5Y$ when $\rho_{S,Y} = 0$.

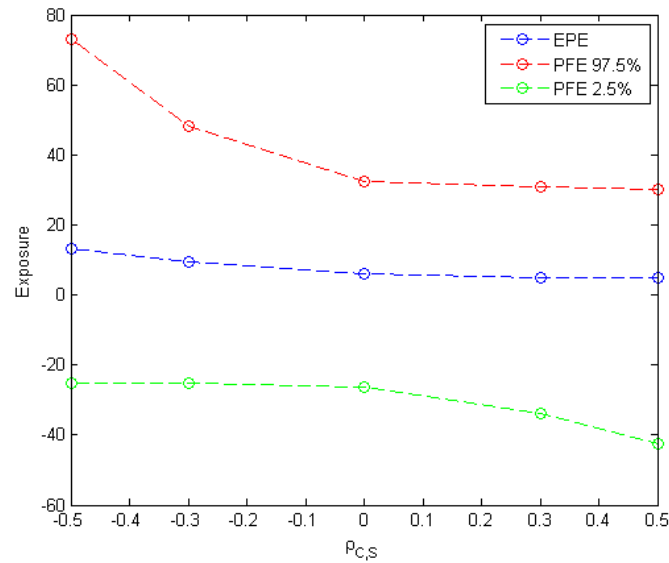


Figure 2.5.5: EPEs and PFEs of the 5-year USDJPY FX forward contract across correlation scenarios ($\rho_{S,Y} = -0.5, -0.3, 0, +0.3, +0.5$).

2.5.6 Case Study II

The second case study involves a hypothetical 5-year fixed-for-fixed USDJPY cross currency swap with unit notional traded between the same counterparties on the same date as in the first case study. The fixed swap rates for the dollar and yen leg are set to be $K^{\$} = 1.5\%$ and $K^{\text{¥}} = 1.38\%$ respectively. Here, given the same set of exchange rate-credit correlation scenarios ($\rho_{S,Y} = -0.5, -0.3, 0, +0.3, +0.5$), we compute the EPEs and PFEs with $\alpha = 97.5\%, 2.5\%$ of the contract value on a quarterly basis throughout the life of the contract, assuming that default occurs on one of the payment dates.

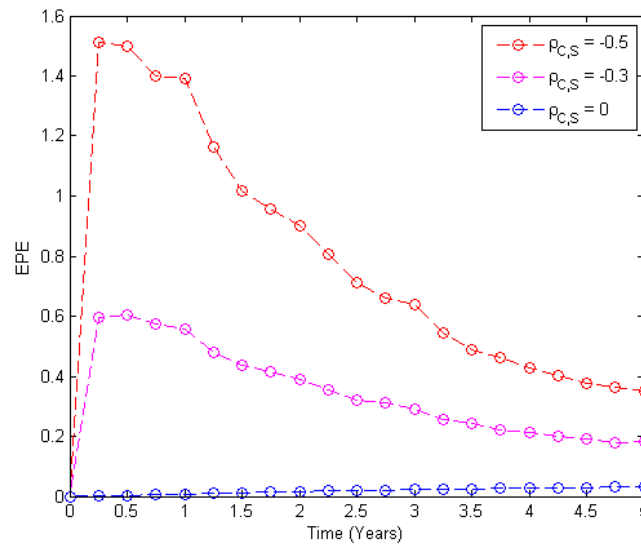
First of all, as shown in Figure 2.5.6(a), in the cases of negative exchange rate-credit correlations, $\rho_{S,Y} = -0.5, -0.3$ (wrong way risk) illustrated in the top two lines, the EPEs upon default are higher compared to that of the corresponding zero and positive correlation scenarios across time. Furthermore, if the counterparty defaults early during the life of the contract (e.g. $\tau^Y = 0.25$), it can be observed that for $\rho_{S,Y} = -0.5, -0.3$ respectively EPE goes up dramatically higher compared to the cases where the counterparty defaults at a later time during the life of the contract. The reason for this is that an early default time would

mean the credit quality of the counterparty deteriorates to default status more rapidly within a very short period of time, resulting in downward leaps of greater magnitudes for the credit index process and the negative dependence relationship between the credit index process and the exchange rate process indicates that the exchange rate will rise significantly, driving the EPE up. The opposite phenomenon can be observed in the case of positive correlations, $\rho_{S,Y} = 0.3, 0.5$ where early default leads to considerably lower EPEs compared to default occurring at a later payment date. Finally, unlike interest rate swaps where there is no actual exchange of notional, cross currency swap contracts do involve notional exchanges at both the inception and maturity with the latter contributing predominantly to the counterparty exposure. Therefore, if default occurs at the maturity of the contract, the US financial institution is expected to have non-zero EPE to Nomura Securities. Similar observations can be found for PFEs with 97.5% confidence interval as shown in Figure 2.5.7.

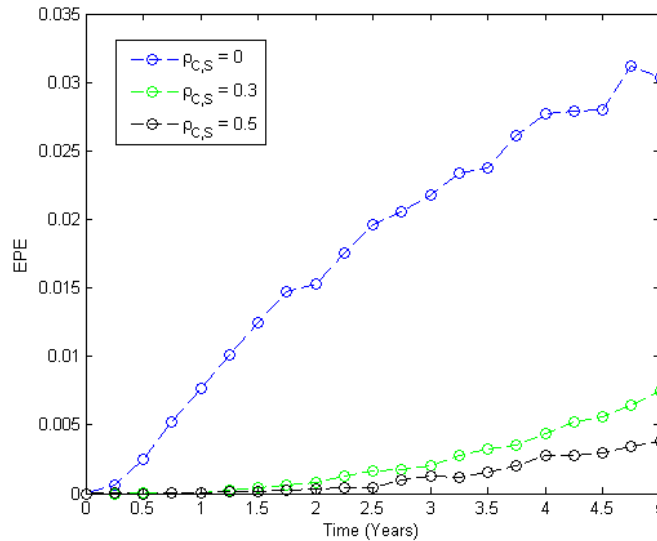
Regarding the PFEs with 2.5% confidence interval, since they represent the left tail region of the probability distribution of the simulated counterparty exposures, it can be observed in Figure 2.5.8 that the PFEs are lower than that of their counterparts in Figure 2.5.7 and the case where $\rho_{S,Y} = 0.5$, illustrated in the bottom line of Figure 2.5.8, provides the US financial institution with the lowest PFEs 2.5% throughout the life of the contract.

2.6 Conclusions

In this chapter, we have developed a joint model for the exchange rate and counterparty default risk, which enables us to capture unilateral wrong way/right way risk of cross currency swap trades given an exogenously specified set of exchange rate-credit correlation scenarios. We take the first step by establishing a multi-currency framework for cross currency swap valuation based on FX-Hull-White hybrid model with correlated one-factor short interest rate processes. We assume constant parameters for the short rate and exchange rate dynamics and calibrate them to ATM interest rate caps and vanilla FX options data observed in the market on the same specific date correspondingly. The correlation between the short



(a) Wrong Way Expected Positive Exposure

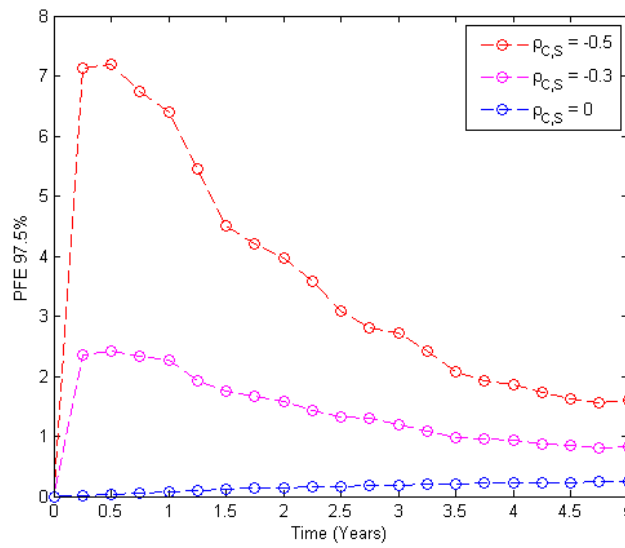


(b) Right Way Expected Positive Exposure

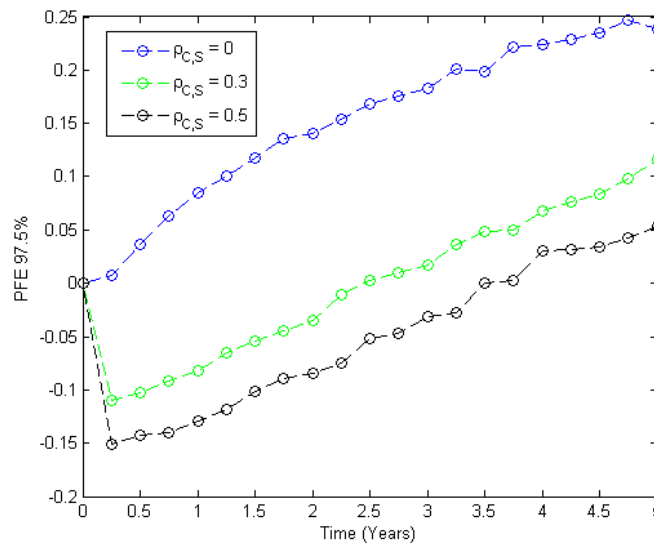
Figure 2.5.6: EPEs of the 5-year USDJPY fixed-for-fixed cross currency swap computed on a quarterly basis across exchange rate-credit correlation scenarios.

rate processes and their correlations with the exchange rate are obtained by historical estimation.

Secondly, we follow Davis & Pistorius (2010) to model the default time of counterparty as the first passage time of a credit index process crossing the zero barrier. With



(a) Wrong Way Potential Future Exposure 97.5%



(b) Right Way Potential Future Exposure 97.5%

Figure 2.5.7: PFEs 97.5% of the 5-year USDJPY fixed-for-fixed cross currency swap computed on a quarterly basis across exchange rate-credit correlation scenarios.

the appropriate specification of the initial distribution of the random starting point, time-dependent drift and volatility component, the default time distribution of the counterparty generated by the model is consistent with one implied from the market CDS term structure of the counterparty. It is shown that the law of the credit index process conditional on default occurring at τ^Y can be identified in terms of a time-changed three-dimensional Bessel

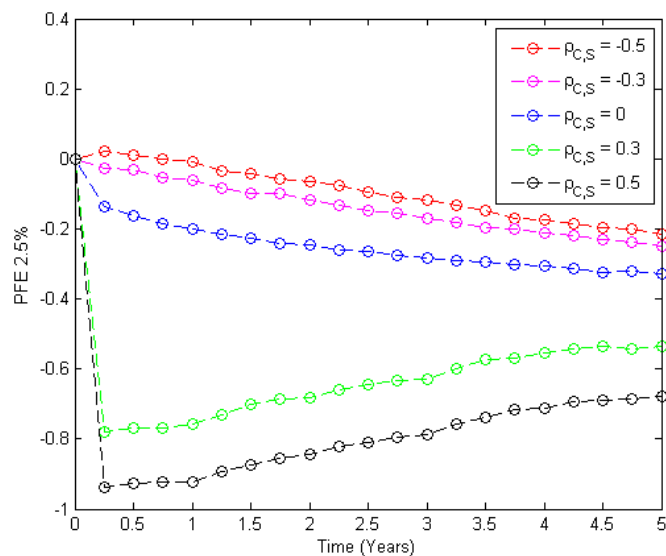


Figure 2.5.8: PFEs 2.5% of the 5-year USDJPY fixed-for-fixed cross currency swap computed on a quarterly basis across exchange rate-credit correlation scenarios.

bridge with the same starting point as Y . The exchange rate process conditional on default can be expressed directly in terms of the time-changed three-dimensional Bessel bridge.

Finally, we conduct case studies on two hypothetical cross currency swap contracts traded between a US financial institution assumed to be default-free and Nomura International assumed to be defaultable. Monte Carlo simulation is applied to compute EPEs and PFEs of the contract for various exchange rate-credit correlation scenarios to quantify the impact of wrong way/right way risk on the counterparty exposure.

It can be illustrated in the numerical examples that negative asset-credit correlation can have a significant impact on the counterparty exposure profiles compared with the case where such correlation is taken the value zero. The simultaneous occurrence of currency devaluation and counterparty credit quality deterioration is properly captured as shown in the EPE/PFE profiles. Furthermore, our comparison with Hull and White (2001) shows that our model is more efficient as no numerical identification of the default barrier is required and more accurate since the default probabilities generated are calibrated exactly to the market implied ones.

Chapter 3

Bilateral Counterparty Risk

Modelling of Cross Currency Swaps

3.1 Chapter Overview

Soon after the financial crisis, given the high profile defaults of Bear Stearns, Lehman Brothers and write-downs associated with insurance purchased from monoline insurance companies, there has been an increasing trend of considering the bilateral nature when quantifying counterparty risk. A clear advantage of doing so is that it will dampen the effect of credit spread increases by offsetting the MTM losses arising from increases in required reserves held against some proportion of expected and unexpected losses taking into account hedges. This will in turn require financial institutions to attach economic value to its own defaults and cause a derivatives portfolio with counterparty risk to be more valuable than the equivalent risk-free positions. For example, Citigroup, in its press release on its first-quarter revenues, reported a positive MTM due to its worsened credit quality: "Revenues also included... a net \$2.5 billion positive CVA on derivative positions, excluding monolines, mainly due to the widening of Citi's CDS spreads." Gregory (2009) discusses the bilateral pricing of counterparty risk and presents an approach that accounts for default of both

parties. He argues that the unilateral treatment of counterparty risk neglects the fact that an institution may default before its counterparty, in which case the counterparty default would become irrelevant. In addition, the institution actually gains following its own default as it will pay its counterparty only a fraction of the contract value. Interestingly, a simplified formula for bilateral risk that is often used in the industry, which, instead of considering the full bilateral CVA framework as in the previous articles, is based on subtracting the unilateral CVAs from the point of view of the party who is doing the calculation. The reason why the simplified formula is appealing is that it allows one to compute a bilateral CVA adjustment by resorting to unilateral ones. This way one needs not implement a bilateral CVA system, but only needs to combine the output of a unilateral CVA one. The problem with this approach is that it ignores the fact that upon first to default of either party, closeout proceedings are started and the transaction is closed. Consequently, it involves inconsistent scenarios in the two terms. With the simplified formula, DVA payout term may still be considered even in a scenario where the counterparty defaults first and the transaction will be closed with a solvent investor. Brigo et al. (2011a) compare the correct one and the one neglecting the first to default check and closeout in detail and find that a sizeable difference between the two formulas are obtained even assuming no credit spread volatility or wrong way risk in the CVA model. The bilateral issue is further studied by the work of Brigo and Capponi (2010), which restrict the analysis to CDSs as the underlying portfolio. Motivated by Brigo and Chourdakis (2009) who partially address the issue of modelling credit spread volatility and wrong way risk but only deal with unilateral and asymmetric counterparty risk, the authors rectify the issue by considering bilateral nature of counterparty risk. Based on the possibility of bilateral defaults, they derive a symmetric mathematical expression for bilateral CVA, where both counterparty can agree on its value.

In this chapter, we generalize the unilateral counterparty default framework proposed in Chapter 1 to the bilateral version to capture the impact of the following three correlations embedded in a foreign exchange setting. Similar to Brigo and Capponi (2010), we extend the unilateral FX-credit dependency between the exchange rate and the counterparty quality to capture the following correlations:

- Dependence between default of the counterparty and default of the investor
- Dependence between the underlying asset value and the credit quality of the counterparty
- Dependence between the underlying asset value and the credit quality of the investor

The three dependence structures are explicitly incorporated onto the credit index processes of the two counterparties and the exchange rate dynamics such that the range of asset-credit and default correlations that can be captured are enriched. Furthermore, This is one of the main contributions of the chapter as opposed to the existing reduced-form approaches where the bilateral asset-credit dependencies are usually captured through a Copula function and based on the choice of the function the range of correlation that can be captured is often limited (e.g. Gaussian Copula).

We model the credit quality of the investor and counterparty as credit index processes in the form of two linear time-inhomogeneous Brownian motions and their times of default as the first-passage times the credit index processes down-cross zero respectively. Given the explicit solution of the IFPT problem derived in Davis and Pistorius (2010), it can be easily shown that our model yields an exact calibration to the CDS quotes for the investor and counterparty. To model the default correlation between the investor and counterparty, one would usually attempt to identify the bivariate joint default time distribution. However, results for the first-passage time problem of correlated Brownian motions are scarce and fragmentary and many require computationally intensive numerical schemes to approximate the joint density function (see, for example, Metzler (2010); Sacerdote et al. (2016)). We propose a comparatively simple approach by imposing the default correlation onto the Brownian motions driving the two credit index processes and express them as a linear transformation of a vector of two independent Brownian motions through Cholesky decomposition. Specifically, to model first-to-default of either the investor or the counterparty at a particular time $s > 0$ in the future, we simulate the credit index process of the assumed first-to-default party in terms of its corresponding three-dimensional time-changed Bessel bridge hitting zero for the first time. We then show that it can be used to retrieve the cor-

responding path of the credit index process of the other party which may have or have not defaulted prior to time s via their correlated driving Brownian motions and we only consider cases where the other party has not defaulted at time s . In this setting, dependence between the two credit index processes and the asset value dynamics can be incorporated by introducing correlations between their driving Brownian motions and it can be shown that the asset value dynamics at time s can be effectively expressed directly in terms of the credit index process of the first-to-default party. A major contribution of this framework is that there is no need finding the joint default probability distribution function of the two credit index processes. With the traditional structural approaches, this often involves sophisticated PDE systems and heavy numerical methods to derive joint default distribution and bilateral counterparty exposure and CVA formulas. A joint asset-credit model is then built under a foreign exchange setting to quantify the impact of the previously mentioned three correlations on the modified expected positive/negative exposure (EPE^{mod}/ENE^{mod}) from the point of view of the investor and the counterparty. Numerical examples shows that both counterparty risk measures are sensitive to default correlation and FX-credit dependency structures. Therefore, our approach provides a tractable and flexible way of capturing the impact of wrong way/right way risk and default correlations in exposure and CVA calculations for FX derivatives.

3.2 Bilateral Joint Asset-Credit Modelling via Bessel bridges

Let us model the credit quality of the investor and the counterparty as credit index processes Y_I and Y_C defined as follows:

$$Y_I(t) = A_I + \int_0^t \nu_I \sigma_I^2(s) ds + \int_0^t \sigma_I(s) dB_I(s), \quad Y_I(0) = A_I, \quad t \in (0, T], \quad (3.1)$$

$$Y_C(t) = A_C + \int_0^t \nu_C \sigma_C^2(s) ds + \int_0^t \sigma_C(s) dB_C(s), \quad Y_C(0) = A_C, \quad t \in (0, T], \quad (3.2)$$

where $A_I \sim F_{\lambda_I}^{\nu_I}$ and $A_C \sim F_{\lambda_C}^{\nu_C}$ are independent of B_I and B_C respectively and the two credit index processes are correlated via their driving Brownian motions $[B_I, B_C]_t =$

$\rho_{I,C}t$, $t > 0$. Through Cholesky decomposition, B_I and B_C can be expressed in terms of a linear transform of a vector of independent Brownian motions:

$$B_I(t) = \rho_{I,C}B_C(t) + \sqrt{1 - \rho_{I,C}^2}B_*(t), \quad (3.3)$$

where B_* is a Brownian motion independent of B_C . Since

$$dY_I(t) = \nu_I\sigma_I^2(t)dt + \sigma_I(t)dB_I(t), \quad Y_I(0) = A_I, \quad t \in (0, T], \quad (3.4)$$

$$dY_C(t) = \nu_C\sigma_C^2(t)dt + \sigma_C(t)dB_C(t), \quad Y_C(0) = A_C, \quad t \in (0, T], \quad (3.5)$$

and

$$dB_I(t) = \frac{1}{\sigma_I(t)}dY_I(t) - \nu_I\sigma_I(t)dt, \quad (3.6)$$

$$dB_C(t) = \frac{1}{\sigma_C(t)}dY_C(t) - \nu_C\sigma_C(t)dt. \quad (3.7)$$

By integrating both sides of the above two equations, B_I and B_C can be expressed in terms of Y_I and Y_C respectively as

$$B_I(t) = \int_0^t \frac{1}{\sigma_I(s)}dY_I(s) - \nu_I \int_0^t \sigma_I(s)ds, \quad (3.8)$$

$$B_C(t) = \int_0^t \frac{1}{\sigma_C(s)}dY_C(s) - \nu_C \int_0^t \sigma_C(s)ds. \quad (3.9)$$

Suppose that the counterparty defaults at time $\tau_C = s$, $s \in (t, T]$, by which time the investor may or may not have defaulted, given the conditional law of the credit index process on default identified in the previous section, Y_C conditional on $\tau_C = s$ is in law equal to that of the three-dimensional Bessel bridge satisfying the SDE:

$$dY_C(t) = \left(\frac{1}{Y_C(t)} - \frac{Y_C(t)}{\int_t^s \sigma_C^2(u)du} \right) \sigma_C^2(t)dt + \sigma_C(t)dB_C(t), \quad t \in (0, s), \quad Y_C(0) = A_C \quad (3.10)$$

and simulated as

$$Y_C(t) = \sqrt{\left[\frac{A_C(I_C(s) - I_C(t))}{I_C(s)} + Z_1^2(I_C(t))\right]^2 + Z_2^2(I_C(t)) + Z_3^2(I_C(t))}, \quad (3.11)$$

where Z_i , $i = 1, 2, 3$, are independent $0 \rightarrow 0$ Brownian bridges defined in 2.32 and $I_C(t) = \int_0^t \sigma_C(u) du$.

For each simulated path of Y_C , we can obtain the corresponding path of B_C through equation 2.58 and then by independently simulating the path of B_* we can generate the path of the Brownian motion driving the investor's credit index up to time s via equation 3.3:

$$\begin{aligned} B_I(t) &= \rho_{I,C} B_C(t) + \sqrt{1 - \rho_{I,C}^2} B_*(t) \\ &= \rho_{I,C} \left[\int_0^t \frac{1}{\sigma_C(s)} dY_C(s) - \nu_C \int_0^t \sigma_C(s) ds \right] + \sqrt{1 - \rho_{I,C}^2} B_*(t), \end{aligned} \quad (3.12)$$

and then based on equation 3.1 we can retrieve the path of Y_I , which may have not or have crossed zero at time s , see Figure 3.2.1 for the sample paths of credit index processes of the investor and the counterparty. When we calculate the counterparty exposure from the investor point of view, we only pick the cases where Y_I has not crossed zero at time s . Similarly, suppose that the investor defaults at time $\tau_I = s$, $s \in (t, T]$, we can also retrieve the path of the credit index process of the counterparty from that of the investor. Again we will pick the cases where Y_C has not crossed zero at time s to calculate the investor's default exposure from the counterparty point of view.

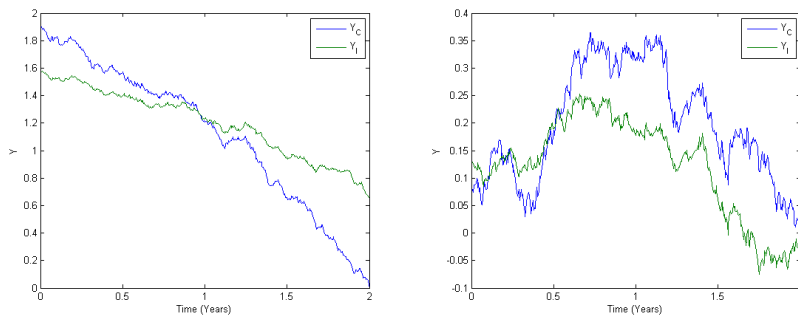


Figure 3.2.1: Sample paths of investor and counterparty credit index processes, conditional on counterparty default at time $2Y$.

Hence, instead of identifying the joint distribution density function of Y_I and Y_C through computationally intensive numerical methods and jointly simulating their paths, the model is constructed such that the path of one party's credit index process conditional on default at a particular time can be simulated, based on which the corresponding path of the other party's credit index process can be extracted through their correlated driving Brownian motions.

We now show how to characterize the conditional law of the asset price dynamics on first-to-default and embed the asset-credit dependencies associated with both the investor and the counterparty. Let us follow the asset value dynamics specified in equation 2.33. Now that the d -dimensional Brownian motion driving the asset price is correlated with B_I and B_C respectively, with $[B_I, W_i] = \rho_{I,i}t$ and $[B_C, W_i] = \rho_{C,i}t$, $t > 0$. The corresponding row-vector correlation are denoted by $\rho_I = (\rho_{I,1}, \dots, \rho_{I,d})$ and $\rho_C = (\rho_{C,1}, \dots, \rho_{C,d})$. If we denote B_x , $x = I, C$, as the Brownian motion driving the credit index process Y_x of the first-to-default party that defaults at a particular time $\tau_x = s$, $s \in (t, T]$, and the associated asset-credit correlation as $\rho_x = (\rho_{x,1}, \dots, \rho_{x,d})$, then W can be expressed in terms of $d + 2$ independent Brownian motions $B_x, B_*, B_1, \dots, B_d$ by

$$W_i(t) = \rho_{x,i}B_x(t) + \rho_i^*B_*(t) + \sum_{k=1}^d Q^{ik}B_k(t), \quad i = 1, \dots, d, \quad (3.13)$$

where $\rho_i^* = \frac{\rho_{y,i} - \rho_{I,C}\rho_{x,i}}{\sqrt{1 - \rho_{I,C}^2}}$, $\rho_{y,i}$ is the asset-credit correlation associated with the non-default party and $Q = (Q^{ik})_{i,k=1}^d$ is the Cholesky decomposition of the matrix $\Sigma - \rho_x\rho_x' - \rho_*\rho_*'$, $\rho_* = (\rho_1^*, \dots, \rho_d^*)$. The asset price dynamics can now be expressed in terms of the credit index process of the first-to-default party Y_x and the independent Brownian motions B_*, B_1, \dots, B_d as:

$$\begin{aligned} \frac{dS_i(t)}{S_i(t)} &= [\mu_i(t) - \nu_x\sigma_x(t)\rho_{x,i}]dt + \frac{1}{\sigma_x(t)} \sum_{j=1}^d v_{ij}(t)\rho_{x,j}dY_x(t) + \sum_{j=1}^d v_{ij}(t)\rho_j^*dB_*(t) + \sum_{j,k=1}^d v_{ij}(t)Q^{jk}dB_k(t), \\ S(0) &= s(0). \end{aligned} \quad (3.14)$$

where the asset-credit correlation associated with the investor and the counterparty is em-

bedded through the credit index process of the first-to-default party Y_x and the independent Brownian motion B_* defined as part of the linear transform in equation 3.3.

3.3 Application to Foreign Exchange Setting

In this section, we will apply our bilateral IFPT model with Bessel bridges to the foreign exchange setting established in Chapter 1. We integrate our bilateral default model into the multi-currency framework and establish a joint FX-credit bilateral default model.

3.3.1 Calibration of Risk-Neutral Default Time Distribution

First of all, we model the credit quality of the investor and the counterparty as two credit index processes Y_I and Y_C as in section 3.2. In order to specify the volatility functions $\sigma_I(t)$ and $\sigma_C(t)$, $t \geq 0$ such that the default time distribution of the investor and the counterparty is consistent with the market, we need to obtain the market implied risk-neutral default probability distributions and back-out the implied hazard rate functions, to which $\sigma_I(t)$ and $\sigma_C(t)$ are taken proportional as in equation 2.8.

In this paper, we consider Daiwa Securities and Nomura Securities as the investor and the counterparty respectively and obtain their market CDS quotes observed on 28th April 2014, given in Table 3.3.1. Both recovery rates are set to be $RR = 35\%$. The implied piece-wise constant hazard functions $\gamma_I(t)$ and $\gamma_C(t)$, $t \geq 0$ are displayed in Figure 3.3.1a and 3.3.2a respectively. As an example, we also set $\lambda_I = 1$ and $\lambda_C = 1$, the corresponding implied volatility functions $\sigma_I(t)$ and $\sigma_C(t)$, $t \geq 0$ are displayed in Figure 3.3.1b and 3.3.2b.

3.3. APPLICATION TO FOREIGN EXCHANGE SETTING

Maturity	Daiwa Securities CDS Par Spreads	Nomura Securities CDS par Spreads
0.5y	0.0017	0.00246
1y	0.00234	0.00261
2y	0.00334	0.00388
3y	0.0046	0.00539
4y	0.0057	0.00792
5y	0.00705	0.00973
7y	0.00978	0.01213
10y	0.01183	0.0137

Table 3.3.1: Market CDS term structures of Daiwa Securities and Nomura Securities on 28th April 2014. Data Source: Bloomberg

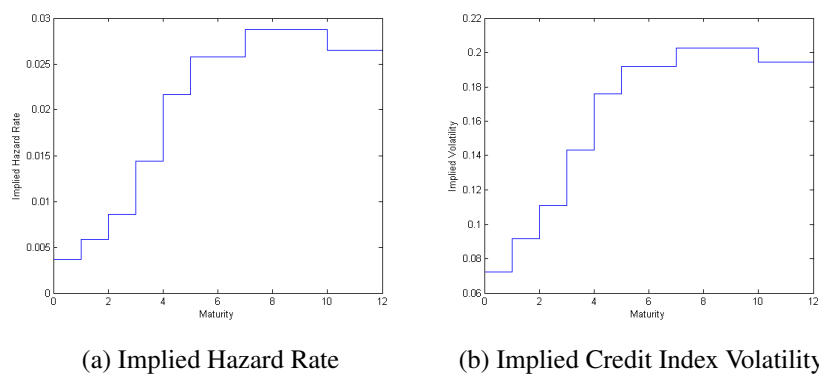


Figure 3.3.1: Implied hazard rate and credit index volatility term structure from par CDS spreads of Daiwa Securities observed on 28th April 2014.

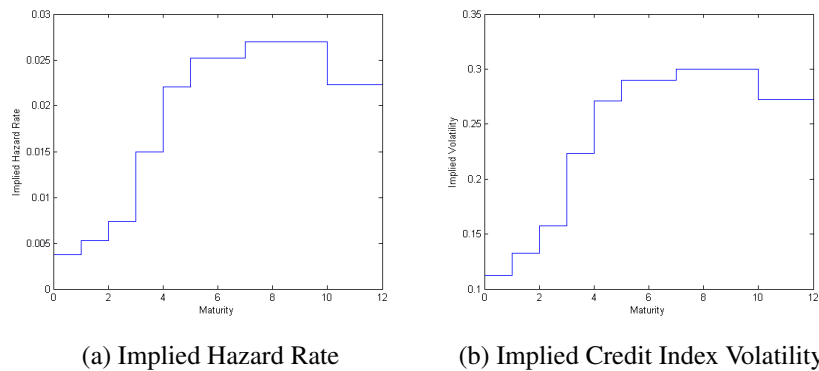


Figure 3.3.2: Implied hazard rate and credit index volatility term structure from par CDS spreads of Nomura Securities observed on 28th April 2014.

3.3.2 Exchange Rate Dynamics Conditional on First-to-Default

For simplicity, we assume that the credit index processes Y_I and Y_C are correlated with the exchange rate process and independent of the two interest rate processes though additional correlation structure can be introduced if necessary. As in section 3.2, we denote the credit index processes of the first-to-default and non-default parties as Y_x , $x = I, C$, Y_y , $y = I, C$, $x \neq y$ and the respective asset-credit correlation as $\rho_{x,S}$, $\rho_{y,S} \in (-1, 1)$. We also assume that the driving Brownian motions W_I and W_C are both defined under the yen risk-neutral measure \mathbb{Q}^\yen such that the default probabilities of the dollar counterparty implied from the yen risk-neutral measure are consistent with those from the dollar risk-neutral measure.

Based on equation 3.12 and 3.14, we can express the Brownian motions driving Y_x , Y_y , S , $r_\$, r_\yen$ as

$$W_x^{\mathbb{Q}^\yen}(t) = \int_0^t \frac{1}{\sigma_x(s)} dY_x(s) - \nu_x \int_0^t \sigma_x(s) ds, \quad x = I, C, \quad (3.15)$$

$$W_y^{\mathbb{Q}^\yen}(t) = \rho_{I,C} W_x^{\mathbb{Q}^\yen}(t) + \sqrt{1 - \rho_{I,C}^2} W_*^{\mathbb{Q}^\yen}(t), \quad y = I, C, \quad x \neq y, \quad (3.16)$$

$$W_S^{\mathbb{Q}^\yen}(t) = \rho_{x,S} W_x^{\mathbb{Q}^\yen}(t) + \rho_1 W_*^{\mathbb{Q}^\yen}(t) + \sqrt{1 - \rho_{x,S}^2 - \rho_1^2} W_1^{\mathbb{Q}^\yen}(t), \quad (3.17)$$

$$W_\yen^{\mathbb{Q}^\yen}(t) = \rho_2 W_1^{\mathbb{Q}^\yen}(t) + \sqrt{1 - \rho_2^2} W_2^{\mathbb{Q}^\yen}(t), \quad (3.18)$$

$$W_\$^{\mathbb{Q}^\yen}(t) = \rho_3 W_1^{\mathbb{Q}^\yen}(t) + \rho_4 W_2^{\mathbb{Q}^\yen}(t) + \rho_5 W_3^{\mathbb{Q}^\yen}(t), \quad (3.19)$$

where $W_*^{\mathbb{Q}^\yen}$, $W_1^{\mathbb{Q}^\yen}$, $W_2^{\mathbb{Q}^\yen}$, $W_3^{\mathbb{Q}^\yen}$, $W_4^{\mathbb{Q}^\yen}$ are independent Brownian motions under \mathbb{Q}^\yen and

$$\begin{aligned} \rho_1 &= \frac{\rho_{y,S} - \rho_{I,C} \rho_{x,S}}{\sqrt{1 - \rho_{I,C}^2}}, \quad \rho_2 = \frac{\rho_{S,d}}{\sqrt{1 - \rho_{x,S}^2 - \rho_1^2}}, \quad \rho_3 = \frac{\rho_{S,f}}{\sqrt{1 - \rho_{x,S}^2 - \rho_1^2}}, \\ \rho_4 &= \frac{\rho_{d,f}(1 - \rho_1^2 - \rho_{x,S}^2) - \rho_{S,d} \rho_{S,f}}{\sqrt{(1 - \rho_1^2 - \rho_{x,S}^2 - \rho_{S,d}^2)(1 - \rho_1^2 - \rho_{x,S}^2)}}, \quad \rho_5 = \sqrt{1 - \rho_3^2 - \rho_4^2}. \end{aligned}$$

The full correlation matrix of Brownian motions $W_x^{\mathbb{Q}^\yen}$, $W_y^{\mathbb{Q}^\yen}$, $W_S^{\mathbb{Q}^\yen}$, $W_\yen^{\mathbb{Q}^\yen}$, $W_\$^{\mathbb{Q}^\yen}$ is now

$$H = \begin{pmatrix} 1 & \rho_{S,\$} & \rho_{S,\yen} & \rho_{S,Y_x} & \rho_{S,Y_y} \\ \rho_{S,\$} & 1 & \rho_{\$, \yen} & 0 & 0 \\ \rho_{S,\yen} & \rho_{\$, \yen} & 1 & 0 & 0 \\ \rho_{S,Y_x} & 0 & 0 & 1 & \rho_{I,C} \\ \rho_{S,Y_y} & 0 & 0 & \rho_{I,C} & 1 \end{pmatrix},$$

where constraints on $\rho_{S,\$}$, $\rho_{S,\yen}$, $\rho_{\$, \yen}$ are imposed in the previous chapter, additional constraints should also be imposed on ρ_{S,Y_x} , ρ_{S,Y_y} , $\rho_{I,C}$ to ensure positive semi-definiteness. Specifically, given

$$-\sqrt{\frac{\beta}{\alpha}} \leq \rho_{S,Y_x} \leq \sqrt{\frac{\beta}{\alpha}}, \quad (3.20)$$

$$-1 < \rho_{I,C} < 1, \quad (3.21)$$

we have

$$\rho_{I,C}\rho_{S,Y_x} - \sqrt{(\rho_{I,C}^2 - 1)(\rho_{S,Y_x}^2 - \frac{\beta}{\alpha})} \leq \rho_{S,Y_y} \leq \rho_{I,C}\rho_{S,Y_x} + \sqrt{(\rho_{I,C}^2 - 1)(\rho_{S,Y_x}^2 - \frac{\beta}{\alpha})}, \quad (3.22)$$

or given

$$-\sqrt{\frac{\beta}{\alpha}} \leq \rho_{S,Y_x} \leq \sqrt{\frac{\beta}{\alpha}}, \quad (3.23)$$

$$-\sqrt{\frac{\beta}{\alpha}} \leq \rho_{S,Y_y} \leq \sqrt{\frac{\beta}{\alpha}}, \quad (3.24)$$

we have

$$\frac{\alpha\rho_{S,Y_x}\rho_{S,Y_y} - \sqrt{(\alpha\rho_{S,Y_x}^2 - \beta)(\alpha\rho_{S,Y_y}^2 - \beta)}}{\beta} \leq \rho_{I,C} \leq \frac{\alpha\rho_{S,Y_x}\rho_{S,Y_y} + \sqrt{(\alpha\rho_{S,Y_x}^2 - \beta)(\alpha\rho_{S,Y_y}^2 - \beta)}}{\beta}, \quad (3.25)$$

where $\alpha = 1 - \rho_{\$, \yen}^2$ and $\beta = 1 - \rho_{S,\$}^2 - \rho_{S,\yen}^2 - \rho_{\$, \yen}^2 + 2\rho_{\$, \yen}\rho_{S,\$}\rho_{S,\yen}$.

Assume we are at time t , conditional on default at time $\tau = s > t$, the integral form of

the exchange rate process can be expressed as

$$S(s) = S(t) \exp\left\{\int_t^s [r_{\mathbb{Y}}(u) - r_{\mathbb{S}}(u)]du + \sigma_S [W_S^{\mathbb{Q}^{\mathbb{Y}}}(s) - W_S^{\mathbb{Q}^{\mathbb{Y}}}(t)]\right\}. \quad (3.26)$$

Referring to Brigo and Mercurio (2007), we have

$$\int_t^s r_{\mathbb{Y}}(u)du = \ln \frac{1}{P_{\mathbb{Y}}(t, s)} + y_{\mathbb{Y}}(t)C_{\mathbb{Y}}(t, s) + \frac{1}{2}V_{\mathbb{Y}}(t, s) + \sigma_{\mathbb{Y}} \int_t^s C_{\mathbb{Y}}(u, s)dW_{\mathbb{Y}}^{\mathbb{Q}^{\mathbb{Y}}}(u), \quad (3.27)$$

$$\begin{aligned} \int_t^s r_{\mathbb{S}}(u)du &= \ln \frac{1}{P_{\mathbb{S}}(t, s)} + y_{\mathbb{S}}(t)C_{\mathbb{S}}(t, s) + \frac{1}{2}V_{\mathbb{S}}(t, s) - \int_t^s \sigma_{\mathbb{S}}\sigma_S\rho_{\mathbb{S},\mathbb{Y}}C_{\mathbb{S}}(u, s)du \\ &\quad + \sigma_{\mathbb{S}} \int_t^s C_{\mathbb{S}}(u, s)dW_{\mathbb{S}}^{\mathbb{Q}^{\mathbb{Y}}}(u), \end{aligned}$$

where

$$\begin{aligned} V_{\mathbb{Y}}(t, s) &= \frac{\sigma_{\mathbb{Y}}^2}{b^2} \left[s - t + \frac{2}{b} e^{-b(s-t)} - \frac{1}{2b} e^{-2b(s-t)} - \frac{3}{2b} \right], \\ V_{\mathbb{S}}(t, s) &= \frac{\sigma_{\mathbb{S}}^2}{a^2} \left[s - t + \frac{2}{a} e^{-a(s-t)} - \frac{1}{2a} e^{-2a(s-t)} - \frac{3}{2a} \right]. \end{aligned}$$

Given further that

$$W_x^{\mathbb{Q}^{\mathbb{Y}}}(s) = \int_t^s \frac{1}{\sigma_x(u)} dY_x(u) - \nu_x \int_t^s \sigma_x(u)du, \quad Y_x(s) = 0, \quad Y_x(t) = A_x \sim F_{\lambda_x}^{\nu_x}, \quad (3.28)$$

the Brownian motion driving the exchange rate process under measure $\mathbb{Q}^{\mathbb{Y}}$ conditional on default can be further expressed directly in terms of the credit index process of the default party:

$$W_S^{\mathbb{Q}^{\mathbb{Y}}}(s) = \int_t^s \frac{\rho_{x,S}}{\sigma_x(u)} dY_x(u) - \nu_x \rho_{x,S} \int_t^s \sigma_x(u)du + \rho_1 W_*^{\mathbb{Q}^{\mathbb{Y}}}(s) + \sqrt{1 - \rho_{x,S}^2 - \rho_1^2} W_1^{\mathbb{Q}^{\mathbb{Y}}}(s), \quad (3.29)$$

we can then express the exchange rate process as

$$\begin{aligned}
 S(s) = S(t) \exp\{ & M_{\mathbb{Y}}(t, s) - M_{\mathbb{S}}(t, s) - \frac{1}{2}\sigma_S^2(s-t) + \int_t^s [\sigma_{\mathbb{S}}\sigma_S\rho_{S,\mathbb{S}}C_{\mathbb{S}}(u, s) - \nu_x\sigma_S\rho_{x,S}\sigma_x(u)]du \\
 & + \rho_1 W_*^{\mathbb{Q}^{\mathbb{Y}}}(s-t) + \sigma_S\sqrt{1-\rho_{x,S}^2-\rho_1^2}W_1^{\mathbb{Q}^{\mathbb{Y}}}(s-t) + \sigma_{\mathbb{Y}}\int_t^s C_{\mathbb{Y}}(u, s)dW_{\mathbb{Y}}^{\mathbb{Q}^{\mathbb{Y}}}(u) - \sigma_{\mathbb{S}}\int_t^s C_{\mathbb{S}}(u, s)dW_{\mathbb{S}}^{\mathbb{Q}^{\mathbb{Y}}}(u) \\
 & + \int_t^s \frac{\sigma_S\rho_{x,S}}{\sigma_x(u)}dY_x(u)\}. \tag{3.30}
 \end{aligned}$$

Substitute equations 3.18-3.19 into equation 3.30, we have

$$\begin{aligned}
 S(s) = S(t) \exp\{ & M_{\mathbb{Y}}(t, s) - M_{\mathbb{S}}(t, s) - \frac{1}{2}\sigma_S^2(s-t) + \int_t^s [\sigma_{\mathbb{S}}\sigma_S\rho_{S,\mathbb{S}}C_{\mathbb{S}}(u, s) - \nu_x\sigma_S\rho_{x,S}\sigma_x(u)]du \\
 & + \rho_1 W_*^{\mathbb{Q}^{\mathbb{Y}}}(s-t) + \sigma^S\sqrt{1-\rho_{S,Y}^2-\rho_1^2}W_1^{\mathbb{Q}^{\mathbb{Y}}}(s-t) + \sigma_{\mathbb{Y}}\int_t^s C_{\mathbb{Y}}(u, s)d[\rho_2 W_1^{\mathbb{Q}^{\mathbb{Y}}}(u) + \sqrt{1-\rho_2^2}W_2^{\mathbb{Q}^{\mathbb{Y}}}(u)] \\
 & - \sigma_{\mathbb{S}}\int_t^s C_{\mathbb{S}}(u, s)d[\rho_3 W_1^{\mathbb{Q}^{\mathbb{Y}}}(u) + \rho_4 W_2^{\mathbb{Q}^{\mathbb{Y}}}(u) + \rho_5 W_3^{\mathbb{Q}^{\mathbb{Y}}}(u)] + \int_t^s \frac{\sigma_S\rho_{x,S}}{\sigma_x(u)}dY_x(u)\} \\
 = S(t) \exp\{ & M_{\mathbb{Y}}(t, s) - M_{\mathbb{S}}(t, s) - \frac{1}{2}\sigma_S^2(s-t) + \int_t^s [\sigma_{\mathbb{S}}\sigma_S\rho_{S,\mathbb{S}}C_{\mathbb{S}}(t, s) - \nu_x\sigma_S\rho_{x,S}\sigma_x(u)]du \\
 & + \int_t^s [\sigma_S\sqrt{1-\rho_{x,S}^2-\rho_1^2} + \rho_2\sigma_{\mathbb{Y}}C_{\mathbb{Y}}(u, s) - \rho_3\sigma_{\mathbb{S}}C_{\mathbb{S}}(u, s)]dW_1^{\mathbb{Q}^{\mathbb{Y}}}(u) + \int_t^s [\sqrt{1-\rho_2^2}\sigma_{\mathbb{Y}}C_{\mathbb{Y}}(u, s) - \rho_4\sigma_{\mathbb{S}}C_{\mathbb{S}}(u, s) \\
 & - \int_t^s \rho_5\sigma_{\mathbb{S}}C_{\mathbb{S}}(u, s)dW_3^{\mathbb{Q}^{\mathbb{Y}}}(u) + \rho_1 W_*^{\mathbb{Q}^{\mathbb{Y}}}(s-t) + \int_t^s \frac{\sigma_S\rho_{x,S}}{\sigma_x(u)}dY_x(u)\}, \tag{3.31}
 \end{aligned}$$

where

$$\begin{aligned}
 M_{\mathbb{Y}}(t, s) &= \ln \frac{1}{P_{\mathbb{Y}}(t, s)} + y_{\mathbb{Y}}(t)C_{\mathbb{Y}}(t, s) + \frac{1}{2}V_{\mathbb{Y}}(t, s), \\
 M_{\mathbb{S}}(t, T) &= \ln \frac{1}{P_{\mathbb{S}}(t, s)} + y_{\mathbb{S}}(t)C_{\mathbb{S}}(t, s) + \frac{1}{2}V_{\mathbb{S}}(t, s).
 \end{aligned}$$

3.4 Numerical Results

In this section, we conduct numerical case studies of our bilateral joint FX-Credit default model with applications to the calculation of the modified EPEs and ENEs of cross currency swaps. Specifically, we consider Daiwa Securities as the investor and Nomura Securities as the counterparty entering into a hypothetical fixed-for-fixed USDJPY cross currency swap of unit notional on 28th April 2014, with the former being the yen payer and the latter being

the dollar payer. Note that we continue to use the model parameters calibrated to market data in previous sections and the EPEs and ENEs are calculated from the point of view of the investor (Daiwa Securities).

3.4.1 Case Study I

First of all, we study how bilateral counterparty default differs from the unilateral default in terms of the expected positive exposure conditional on first-to-default of the counterparty at a particular time in the future ($\tau_C = Y2.5$ for example). Assume the default correlation between the investor and counterparty $\rho_{I,C} = 0.3$ and the correlation between the investor and the exchange rate $\rho_{I,S} = 0$, given a set of scenarios of the correlation between the counterparty credit quality and the exchange rate $\rho_{C,S} = -0.5, -0.3, 0, 0.3, 0.5$, we observe in Figure 3.4.1 a similar pattern as in the case of unilateral counterparty default that both the unilateral adjusted and bilateral EPEs defined in equation 1.8 and 1.10 are higher for high negative levels of $\rho_{C,S}$ (wrong way risk) and lower for high positive levels of $\rho_{C,S}$ (right way risk). Furthermore, we observe that the unilateral adjusted EPE is lower than the corresponding EPE in the case of unilateral counterparty default. This is due to the fact that possible default of the investor decreases the joint probability of first-to-default of the counterparty and the underlying cross currency swap having positive value upon default. As it is also shown in Figure 3.4.1, the bilateral EPE is further lower than the corresponding unilateral adjusted EPE since the increasing joint probability of first-to-default of the investor and the underlying cross currency swap having negative value drives up the unilateral adjusted ENE component defined in equation 1.9 of the bilateral EPE. Therefore, we can conclude that by considering the investor's own default the EPE to the counterparty is reduced compared to that of the unilateral counterparty default case.

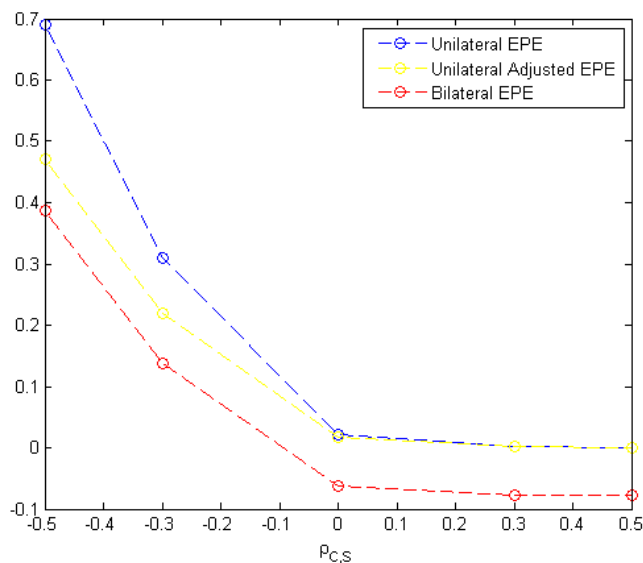


Figure 3.4.1: EPE profile of a 5-year fixed-for-fixed USDJPY cross currency swap from the point of view of Daiwa Securities conditional on first-to-default of Nomura Securities at $t = 2.5$ (years). Trade date: 28th April 2014, yen payer: Daiwa Securities, dollar payer: Nomura Securities, $K_{¥} = 1.38\%$, $K_{\$} = 1.5\%$, $S(0) = 102.5$, $N_0^¥ = 1$, $\rho_{I,C} = 0.3$, $\rho_{I,S} = 0$, $\rho_{C,S} = \{-0.5, -0.3, 0, 0.3, 0.5\}$. Table 3.4.1 is the corresponding summary of the correlation scenarios, numerical results and the standard errors of EPE simulations.

$\rho_{C,S}$	Unilateral EPE ($\pm \frac{1}{2}$ Confidence Interval)	Standard Error
-0.5	0.69 (± 0.007)	0.004
-0.3	0.31 (± 0.002)	0.001
0	0.022 (± 0.0003)	0.0001
0.3	0.0018 ($\pm 9E-5$)	5E-5
0.5	0.0008 ($\pm 6E-5$)	3E-5
$(\rho_{I,C}, \rho_{C,S}, \rho_{I,S})$	Unilateral Adjusted EPE ($\pm \frac{1}{2}$ Confidence Interval)	Standard Error
(0.3, -0.5, 0)	0.47 (± 0.04)	0.002
(0.3, -0.3, 0)	0.22 (± 0.002)	0.0009
(0.3, 0, 0)	0.018 (± 0.0002)	0.0002
(0.3, 0.3, 0)	0.0017 ($\pm 9E-5$)	5E-5
(0.3, 0.5, 0)	0.0007 ($\pm 6E-5$)	3E-5

Table 3.4.1: Summary of the correlation scenarios, numerical results and the standard error of unilateral and unilateral adjusted EPE simulations.

3.4.2 Case Study II

For a fixed level of $\rho_{C,S}$ as $\rho_{I,C}$ rises the unilateral adjusted EPE begins to decrease. This is because a higher default correlation indicates a lower joint probability of first-to-default of

counterparty and the underlying cross currency swap having positive value upon default and hence the investor's EPE to the counterparty should be correspondingly lower. Such pattern can be illustrated in Figure 3.4.2 and it can also be observed that the effect of increasing default correlation is particularly strong for high negative levels of $\rho_{C,S}$ but less so for high positive levels of $\rho_{C,S}$. This is because high positive levels of $\rho_{C,S}$ has already kept the joint probability of first-to-default of counterparty and the underlying cross currency swap having positive value very low that a rise in default correlation alone will have a limited impact on the unilateral adjusted EPE. These patterns can be further illustrated in the histograms of the exposures upon first-to-default of the counterparty for a range of correlation scenarios presented in Figure A.0.1-A.0.5.

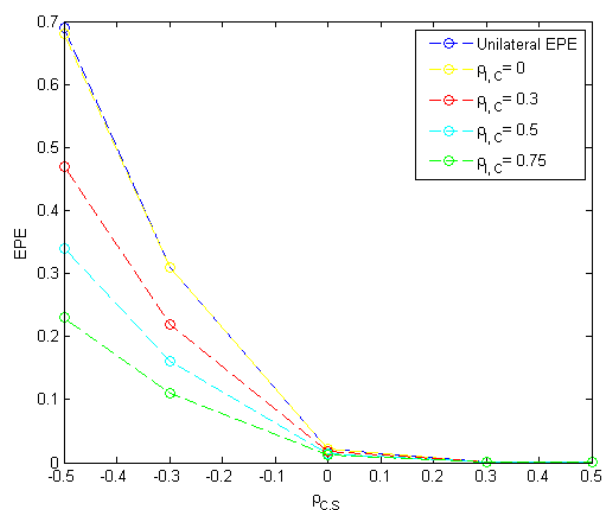


Figure 3.4.2: Unilateral adjusted EPE profile of a 5-year fixed-for-fixed USDJPY cross currency swap from the point of view of Daiwa Securities conditional on first-to-default of Nomura Securities at $t = 2.5$ (years). Trade date: 28th April 2014, yen payer: Daiwa Securities, dollar payer: Nomura Securities, $K_{\text{¥}} = 1.38\%$, $K_{\text{\$}} = 1.5\%$, $S(0) = 102.5$, $N_0^{\text{¥}} = 1$, $\rho_{I,S} = 0$, $\rho_{C,S} = \{-0.5, -0.3, 0, 0.3, 0.5\}$, $\rho_{I,C} = \{0, 0.3, 0.5, 0.75\}$. Table 3.4.2 is the corresponding summary of the correlation scenarios, numerical results and the standard errors of EPE simulations.

With respect to unilateral adjusted ENE, we observe in Figure 3.4.3 that for a fixed level of $\rho_{C,S}$ an increase in the default correlation leads to a decrease in unilateral adjusted ENE since from the point of view of the investor the counterparty is becoming more likely to default, which results in a lower joint probability of first-to-default of investor and the un-

3.4. NUMERICAL RESULTS

$\rho_{C,S}$	Unilateral EPE ($\pm\frac{1}{2}$ Confidence Interval)	Standard Error
-0.5	0.69 (± 0.007)	0.004
-0.3	0.31 (± 0.002)	0.001
0	0.022 (± 0.0003)	0.0001
0.3	0.0018 ($\pm 9E-5$)	5E-5
0.5	0.0008 ($\pm 6E-5$)	3E-5
$(\rho_{I,C}, \rho_{C,S}, \rho_{I,S})$	Unilateral Adjusted EPE ($\pm\frac{1}{2}$ Confidence Interval)	Standard Error
(0, -0.5, 0)	0.68 (± 0.006)	0.003
(0, -0.3, 0)	0.31 (± 0.002)	0.001
(0, 0, 0)	0.021 (± 0.0003)	0.0002
(0, 0.3, 0)	0.0017 ($\pm 9E-5$)	4E-05
(0, 0.5, 0)	0.0007 ($\pm 6E-5$)	3E-05
(0.3, -0.5, 0)	0.47 (± 0.04)	0.002
(0.3, -0.3, 0)	0.22 (± 0.002)	0.0009
(0.3, 0, 0)	0.018 (± 0.0002)	0.0002
(0.3, 0.3, 0)	0.0017 ($\pm 9E-5$)	5E-5
(0.3, 0.5, 0)	0.0007 ($\pm 6E-5$)	3E-5
(0.5, -0.5, 0)	0.34 (± 0.003)	0.0016
(0.5, -0.3, 0)	0.16 (± 0.0015)	0.0007
(0.5, 0, 0)	0.015 (± 0.0002)	0.0001
(0.5, 0.3, 0)	0.0017 ($\pm 9E-5$)	5E-05
(0.5, 0.5, 0)	0.0007 ($\pm 6E-5$)	3E-05
(0.75, -0.5, 0)	0.23 (± 0.002)	0.0012
(0.75, -0.3, 0)	0.11 (± 0.001)	0.0006
(0.75, 0, 0)	0.012 (± 0.0002)	0.0001
(0.75, 0.3, 0)	0.0016 ($\pm 9E-5$)	4E-05
(0.75, 0.5, 0)	0.0007 ($\pm 5E-5$)	3E-05

Table 3.4.2: Summary of the correlation scenarios, numerical results and the standard errors of unilateral and unilateral adjusted EPE simulations.

derlying cross currency swap having negative value upon default. Furthermore, it is shown that the unilateral adjusted ENE is higher when the counterparty credit quality is more negatively correlated with the exchange rate and lower when they are more positively correlated. This is because a negative correlation between the survival counterparty and the exchange rate increases the joint probability of first-to-default of the investor and the underlying cross currency having negative value upon default. The corresponding histograms of the exposures conditional on first-to-default of the investor are presented in Figure A.0.6-A.0.10.

In Figure 3.4.4 we observe that for a fixed level of $\rho_{I,C}$ the bilateral EPE is higher for high negative levels of $\rho_{C,S}$ as wrong way risk dominates, leading to a higher weighting of

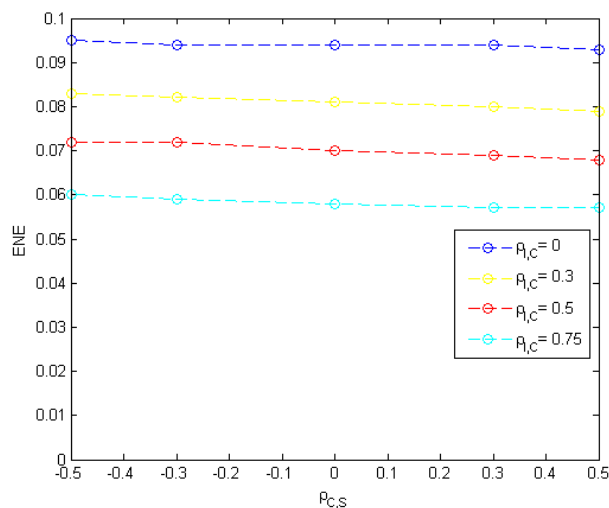


Figure 3.4.3: Unilateral adjusted ENE profile of a 5-year fixed-for-fixed USDJPY cross currency swap from the point of view of Daiwa Securities conditional on first-to-default of Nomura Securities at $t = 2.5$ (years). Trade date: 28th April 2014, yen payer: Daiwa Securities, dollar payer: Nomura Securities, $K_{\text{¥}} = 1.38\%$, $K_{\text{\$}} = 1.5\%$, $S(0) = 102.5$, $N_0^{\text{¥}} = 1$, $\rho_{I,S} = 0$, $\rho_{C,S} = \{-0.5, -0.3, 0, 0.3, 0.5\}$, $\rho_{I,C} = \{0, 0.3, 0.5, 0.75\}$. Table 3.4.3 is the corresponding summary of the correlation scenarios, numerical results and the standard errors of ENE simulations.

the unilateral adjusted EPE component and lower for high positive levels of $\rho_{C,S}$ as right way risk dominates, leading to a lower weighting of the unilateral adjusted EPE component and the bilateral EPE even changing sign. In addition, for a more negative level of $\rho_{C,S}$ and a positive bilateral EPE, rising default correlation leads to a decreasing bilateral EPE while for a more positive level of $\rho_{C,S}$ and a negative bilateral EPE, rising default correlation leads to an increasing bilateral EPE. Specifically, when $\rho_{C,S}$ is negative, dominant wrong way risk yields a higher weighting for the unilateral adjusted EPE component, which is more sensitive to rising default correlation as described previously and decreases more sharply than the corresponding unilateral adjusted ENE component, while for positive levels of $\rho_{C,S}$, right way risk yields a more dominant unilateral adjusted ENE component, which is more sensitive to rising default correlation and decreases more sharply than the corresponding unilateral adjusted EPE component. From an intuitive perspective, when the investor is more likely to have a net positive exposure towards the counterparty, the counterparty is understood to be more likely to default first. A rising default correlation increases

3.4. NUMERICAL RESULTS

$(\rho_{I,C}, \rho_{C,S}, \rho_{I,S})$	Unilateral Adjusted ENE ($\pm \frac{1}{2}$ Confidence Interval)	Standard Error
(0, -0.5, 0)	0.095 (± 0.0006)	0.0003
(0, -0.3, 0)	0.094 (± 0.0006)	0.0003
(0, 0, 0)	0.094 (± 0.0006)	0.0003
(0, 0.3, 0)	0.094 (± 0.0006)	0.0003
(0, 0.5, 0)	0.093 (± 0.0006)	0.0003
(0.3, -0.5, 0)	0.083 (± 0.0006)	0.0003
(0.3, -0.3, 0)	0.082 (± 0.0006)	0.0003
(0.3, 0, 0)	0.081 (± 0.0005)	0.0003
(0.3, 0.3, 0)	0.08 (± 0.0005)	0.0003
(0.3, 0.5, 0)	0.079 (± 0.0005)	0.0003
(0.5, -0.5, 0)	0.072 (± 0.0005)	0.0003
(0.5, -0.3, 0)	0.072 (± 0.0005)	0.0003
(0.5, 0, 0)	0.07 (± 0.0005)	0.0003
(0.5, 0.3, 0)	0.069 (± 0.0005)	0.0003
(0.5, 0.5, 0)	0.068 (± 0.0005)	0.0003
(0.75, -0.5, 0)	0.06 (± 0.0005)	0.0003
(0.75, -0.3, 0)	0.059 (± 0.0005)	0.0003
(0.75, 0, 0)	0.058 (± 0.0005)	0.0003
(0.75, 0.3, 0)	0.057 (± 0.0005)	0.0003
(0.75, 0.5, 0)	0.057 (± 0.0005)	0.0003

Table 3.4.3: Summary of the correlation scenarios, numerical results and the standard errors of unilateral adjusted ENE simulations.

the probability of the first-to-default of the investor and hence the gain from the investor's own default reduces the exposure upon default of the counterparty. On the other hand, when investor is more likely to have a net negative exposure towards the counterparty upon first-to-default of the counterparty, which can be seen as a gain for the investor as it is more likely to default. A rising default correlation increases the possibility of the first-to-default of the counterparty and hence raises the investor's exposure to the counterparty.

3.4.3 Case Study III

In this case study, we analyze the impact of the correlation between the investor and the exchange rate and the default correlation on the unilateral adjusted EPE, ENE and bilateral EPE. Here, we assume $\rho_{C,S} = 0$ and consider different scenarios of the correlation between the investor and the exchange rate and the default correlation, $\rho_{I,S} = -0.5, -0.3, 0, 0.3,$

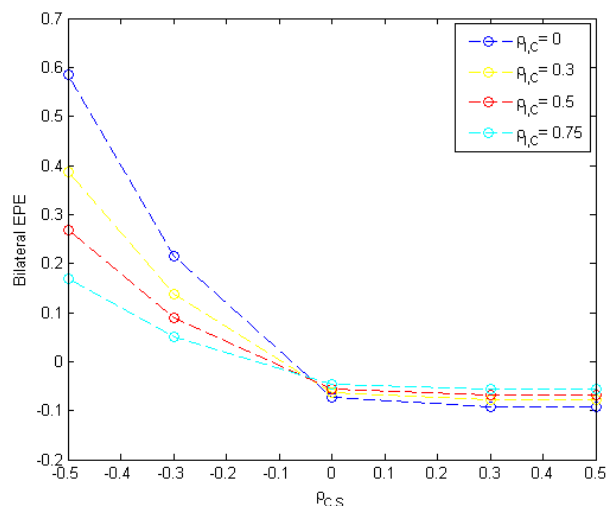


Figure 3.4.4: Bilateral EPE of a 5-year fixed-for-fixed USDJPY cross currency swap at $t = 2.5$ (years) observed on 28th April 2014. $K_{\text{¥}} = 1.38\%$, $K_{\text{₹}} = 1.5\%$, $S(0) = 102.5$, $N_0^{\text{¥}} = 1$, $\rho_{I,S} = 0$, $\rho_{C,S} = \{-0.5, -0.3, 0, 0.3, 0.5\}$, $\rho_{I,C} = \{0, 0.3, 0.5, 0.75\}$.

0.5, $\rho_{I,C} = 0, 0.3, 0.5, 0.75$. First, as shown in Figure 3.4.5, for any fixed level of $\rho_{I,S}$ the unilateral adjusted EPE decreases with rising default correlation as the joint probability of the first-to-default of the investor and the underlying cross currency swap having positive value upon default decreases. We also observe that for a fixed level of $\rho_{I,C}$ the unilateral adjusted EPE increases with $\rho_{I,S}$ since a higher positive correlation between the investor and the exchange rate leads to a higher joint probability of counterparty default and the underlying cross currency swap having positive value upon default, and vice versa for high negative levels of $\rho_{I,S}$. The histograms of the exposures conditional on first-to-default of the counterparty are presented in Figure A.0.11-A.0.15.

Regarding the unilateral adjusted ENE, we observe in Figure 3.4.7 that for a given level of $\rho_{I,C}$, the unilateral adjusted ENE is lower for high negative levels of $\rho_{I,S}$ in which case the default of the investor leads to the underlying cross currency swap having more positive value upon default. Similarly, it is higher for high positive levels of $\rho_{I,S}$ in which case the default of the investor drives the underlying cross currency swap to have more negative value upon default. Furthermore, for a fixed level of $\rho_{I,S}$, an increase in the default correlation leads to correspondingly lower unilateral adjusted ENE due to increasing likelihood of

3.4. NUMERICAL RESULTS

$(\rho_{I,C}, \rho_{C,S}, \rho_{I,S})$	Unilateral Adjusted EPE ($\pm \frac{1}{2}$ Confidence Interval)	Standard Error
(0, 0, -0.5)	0.02 (± 0.0003)	0.0002
(0, 0, -0.3)	0.021 (± 0.0003)	0.0002
(0, 0, 0)	0.021 (± 0.0003)	0.0002
(0, 0, 0.3)	0.021 (± 0.0003)	0.0002
(0, 0, 0.5)	0.021 (± 0.0003)	0.0002
(0.3, 0, -0.5)	0.017 (± 0.0003)	0.0001
(0.3, 0, -0.3)	0.017 (± 0.0003)	0.0001
(0.3, 0, 0)	0.018 (± 0.0003)	0.0002
(0.3, 0, 0.3)	0.018 (± 0.0003)	0.0002
(0.3, 0, 0.5)	0.019 (± 0.0003)	0.0002
(0.5, 0, -0.5)	0.015 (± 0.0003)	0.0001
(0.5, 0, -0.3)	0.015 (± 0.0003)	0.0001
(0.5, 0, 0)	0.015 (± 0.0003)	0.0001
(0.5, 0, 0.3)	0.016 (± 0.0003)	0.0001
(0.5, 0, 0.5)	0.016 (± 0.0003)	0.0001
(0.75, 0, -0.5)	0.012 (± 0.0002)	0.0001
(0.75, 0, -0.3)	0.012 (± 0.0002)	0.0001
(0.75, 0, 0)	0.013 (± 0.0002)	0.0001
(0.75, 0, 0.3)	0.013 (± 0.0002)	0.0001
(0.75, 0, 0.5)	0.014 (± 0.0002)	0.0001

Table 3.4.4: Summary of the correlation scenarios, numerical results and the standard errors of unilateral adjusted EPE simulations.

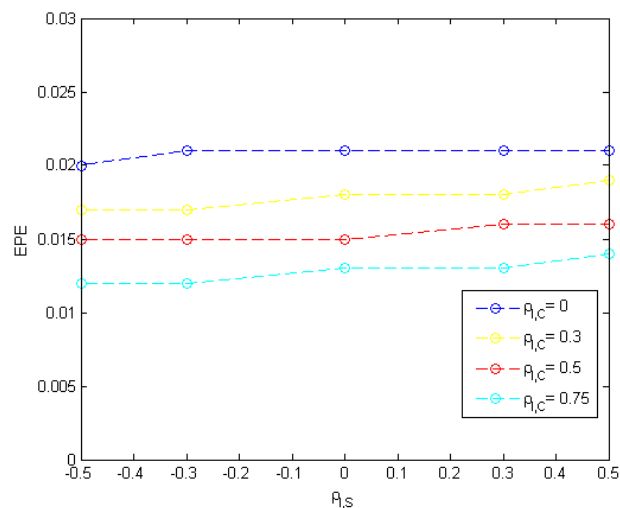


Figure 3.4.5: Unilateral adjusted EPE profile of a 5-year fixed-for-fixed USDJPY cross currency swap from the point of view of Daiwa Securities conditional on first-to-default of Nomura Securities at $t = 2.5$ (years). Trade date: 28th April 2014, yen payer: Daiwa Securities, dollar payer: Nomura Securities, $K_{\text{¥}} = 1.38\%$, $K_{\text{\$}} = 1.5\%$, $S(0) = 102.5$, $N_0^{\text{¥}} = 1$, $\rho_{C,S} = 0$, $\rho_{I,S} = \{-0.5, -0.3, 0, 0.3, 0.5\}$, $\rho_{I,C} = \{0, 0.3, 0.5, 0.75\}$. Table 3.4.4 is the corresponding summary of the correlation scenarios, numerical results and the standard errors of EPE simulations.

counterparty default and it can be seen that this effect is more pronounced for high positive levels of $\rho_{I,S}$ when the joint probability of first-to-default of the investor and the underlying cross currency swap having negative value is kept very low and is less sensitive to rising default correlation. Similarly to case study II, it can also be observed that the unilateral adjusted ENE is lower than the corresponding unilateral ENE. The histograms of the exposures conditional on first-to-default of the investor are presented in Figure A.0.16-A.0.20.

Finally, as shown in Figure 3.4.7, for a given level of $\rho_{I,C}$, the bilateral EPE is higher when the investor and the exchange rate are more negatively correlated and lower when they are more positively correlated. This is because for high negative levels of $\rho_{I,S}$ tends to lead to a more positive value of the cross currency swap and hence a lower weighting of the unilateral adjusted ENE component?as $\rho_{I,S}$ becomes more positive, first-to-default of the investor tends to lead to a more negative value of the cross currency swap and hence a higher weighting for the unilateral adjusted ENE component. Similar to case study II, we also observe that for a more negative level of $\rho_{I,S}$ and a positive bilateral EPE to the counterparty,

3.4. NUMERICAL RESULTS

$\rho_{I,S}$	Unilateral ENE ($\pm \frac{1}{2}$ Confidence Interval)	Standard Error
-0.5	0.008 (± 0.0002)	0.0001
-0.3	0.016 (± 0.0003)	0.0001
0	0.095 (± 0.0005)	0.0003
0.3	0.3 (± 0.001)	0.0005
0.5	0.41 (± 0.001)	0.0006
$(\rho_{I,C}, \rho_{C,S}, \rho_{I,S})$	Unilateral Adjusted ENE ($\pm \frac{1}{2}$ Confidence Interval)	Standard Error
(0, 0, -0.5)	0.008 (± 0.0001)	9E-5
(0, 0, -0.3)	0.016 (± 0.0002)	0.0001
(0, 0, 0)	0.093 (± 0.0005)	0.0002
(0, 0, 0.3)	0.3 (± 0.001)	0.0005
(0, 0, 0.5)	0.4 (± 0.001)	0.0006
(0.3, 0, -0.5)	0.008 (± 0.0002)	1E-4
(0.3, 0, -0.3)	0.016 (± 0.0003)	0.0001
(0.3, 0, 0)	0.081 (± 0.0005)	0.0002
(0.3, 0, 0.3)	0.24 (± 0.001)	0.0005
(0.3, 0, 0.5)	0.33 (± 0.001)	0.0007
(0.5, 0, -0.5)	0.008 (± 0.0002)	0.0001
(0.5, 0, -0.3)	0.0015 (± 0.0003)	0.0001
(0.5, 0, 0)	0.07 (± 0.0005)	0.0003
(0.5, 0, 0.3)	0.2 (± 0.001)	0.0005
(0.5, 0, 0.5)	0.27 (± 0.001)	0.0007
(0.75, 0, -0.5)	0.008 (± 0.0002)	0.0001
(0.75, 0, -0.3)	0.014 (± 0.0003)	0.0001
(0.75, 0, 0)	0.059 (± 0.0005)	0.0003
(0.75, 0, 0.3)	0.15 (± 0.001)	0.0005
(0.75, 0, 0.5)	0.21 (± 0.001)	0.0007

Table 3.4.5: Summary of the correlation scenarios, numerical results and the standard errors of unilateral and unilateral adjusted ENE simulations.

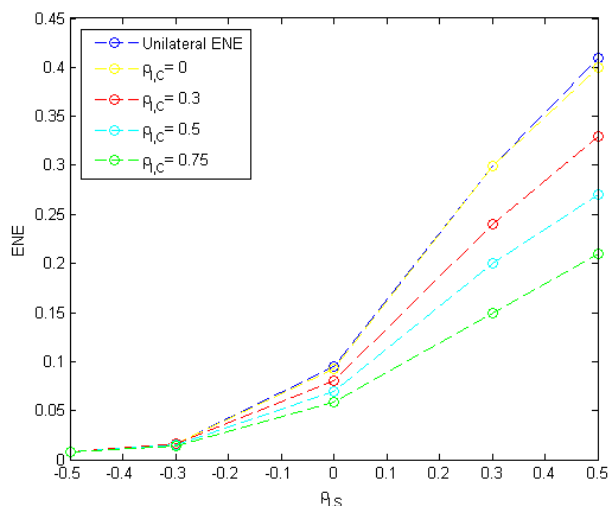


Figure 3.4.6: Unilateral adjusted ENE profile of a 5-year fixed-for-fixed USDJPY cross currency swap from the point of view of Daiwa Securities conditional on first-to-default of Daiwa Securities at $t = 2.5$ (years). Trade date: 28th April 2014, yen payer: Daiwa Securities, dollar payer: Nomura Securities, $K_{\text{¥}} = 1.38\%$, $K_{\text{\$}} = 1.5\%$, $S(0) = 102.5$, $N_0^{\text{¥}} = 1$, $\rho_{I,S} = 0$, $\rho_{C,S} = \{-0.5, -0.3, 0, 0.3, 0.5\}$, $\rho_{I,C} = \{0, 0.3, 0.5, 0.75\}$. Table 3.4.5 is the corresponding summary of the correlation scenarios, numerical results and the standard errors of ENE simulations.

as the default correlation rises the bilateral EPE decreases while for a more positive level of $\rho_{I,S}$ and a negative bilateral EPE to the counterparty, rising default correlation leads to a higher bilateral EPE. This is because when $\rho_{I,S}$ becomes more negative, the unilateral adjusted EPE component is more sensitive to rising default correlation and decreases more sharply than the corresponding unilateral adjusted ENE component, while for more positive levels of $\rho_{I,S}$, the unilateral adjusted ENE is more sensitive to rising default correlation and decreases more sharply than the corresponding unilateral adjusted EPE component. Intuitively, if the investor tends to have a net positive exposure to the counterparty, the counterparty is more likely to default and rising default correlation increases the probability of the first-to-default the investor and therefore reduces the exposure to the counterparty upon its default. On the other hand, if the investor tends to have a net negative exposure to the counterparty, the investor is more likely to default and rising default correlation increases the probability of counterparty default and hence increases the investor's exposure to the counterparty.

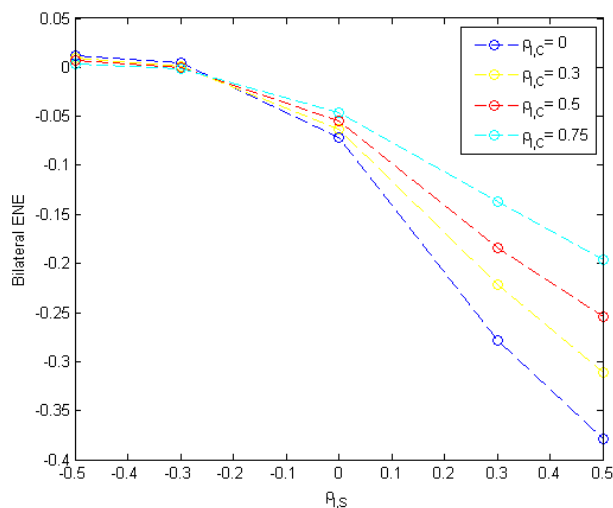


Figure 3.4.7: Bilateral EPE of a 5-year fixed-for-fixed USDJPY cross currency swap at $t = 2.5$ (years) observed on 28th April 2014. $K_{\text{¥}} = 1.38\%$, $K_{\text{₹}} = 1.5\%$, $S(0) = 102.5$, $N_0^{\text{¥}} = 1$, $\rho_{C,S} = 0$, $\rho_{I,S} = \{-0.5, -0.3, 0, 0.3, 0.5\}$, $\rho_{I,C} = \{0, 0.3, 0.5, 0.75\}$.

3.4.4 Conclusion

We extend the unilateral joint FX-credit default model to incorporate bilateral counterparty default. To achieve this, we impose the default correlation on the driving Brownian motions of the two credit index processes and express them in terms of independent Brownian motions through Cholesky decomposition. Conditional on the default of the counterparty (investor) at a particular time t in the future, we simulate the path of its credit index process conditional on hitting zero at t via Bessel bridges and back out the path of the credit index process of the investor (counterparty) through their correlated driving Brownian motions. The first-to-default of the counterparty (investor) will then be modelled by picking the cases where the credit index process of the investor (counterparty) has not hit zero prior to time t . Hence, instead of identifying the joint probability distribution of the two-dimensional Bessel bridges through computationally extensive numerical schemes, we are able to obtain the paths of the two credit index processes by simply simulating the credit index process of the default counterparty.

Next, we integrate the bilateral default setting into a multi-currency framework with correlated interest rates. The exchange rate is modelled as a lognormal geometric Brownian

motion with constant volatility while the interest rate processes are modelled as Hull-White dynamics. We then show that the exchange rate process conditional on default happening at time t can be expressed directly in terms of the credit index process of the default counterparty and independent Brownian motions such that the correlation between the exchange rate and the investor (counterparty) can be explicitly incorporated.

Finally, we apply our bilateral joint FX-credit model to a hypothetical fixed-for-fixed USDJPY cross currency swap entered into by Daiwa Securities and Nomura Securities and quantify the impact of the correlation between the exchange rate and the investor (counterparty) and the default correlation between the investor and the counterparty through exposure metrics such as modified EPEs and ENEs through numerical case studies.

It can be shown in the numerical examples that in the bilateral setting, the possibility of default of both counterparty tends to offset the expected positive exposure towards either counterparty compared with the exposure profiles in the unilateral case. This is very important in CVA calculations as the bilateral nature of default will influence the amount CVA and DVA to be charged. Furthermore, the impact of asset-credit correlation is significant to both counterparties and the flexibility offered by our model in terms of the way the correlations are embedded and the efficiency in the joint simulation of credit index processes provides a powerful tool for counterparty risk management.

Chapter 4

Bermudan Swaption CVA and Wrong Way Risk

4.1 Chapter Overview

Based on Basel (1988) and Basel (2005) regimes, the regulatory landscape has gone a step further through Basel (2010) to call for the need of enhanced sensitivity of credit risk measurement. Specifically, capital requirements have been directly associated with more advanced counterparty risk metrics such as Credit Value Adjustment (CVA) used to compensate for the loss due to counterparty default and Debt Value Adjustment (DVA) intended as the additional benefit of one's own default, and more recently the potential volatility of the value at risk (VaR) of CVA in conjunction with stress testing under extreme market scenarios. The introduction of CVA and DVA requires corporates engaging in derivatives transactions for hedging purposes to undertake proper hedge accounting for counterparty risk in the valuation of over-the-counter (OTC) derivatives (see IASB, 2011, for example). According to Basel Committee on Banking Supervision, roughly two-thirds of credit counterparty losses during the financial crisis were due to credit value adjustment losses and only one-third were due to actual defaults, which highlights the necessity of having a uniform

evaluation methodology for CVA and DVA and how to allocate them to individual hedges. Given that the notional of outstanding over-the-counter (OTC) derivatives has over the last two decades grown exponentially, mainly due to the increase in OTC interest rate derivatives, any rates trading desk entering an OTC deal will face the risk that the counterparty at a future date may default and cannot fulfil its payment obligations. Therefore the bank needs to estimate the total risk it is facing with respect to a particular counterparty and to keep a capital buffer i.e., the capital requirement, to cover for losses due to a default. Figure 4.1.1 illustrates the Bank for International Settlements (BIS) semi-annual market survey of outstanding OTC derivatives from June 1998 through December 2013. As of December 2013, the total amount of outstanding notional in OTC derivatives was 710.2 trillion USD, with 584.4 trillion USD in interest rate derivatives.

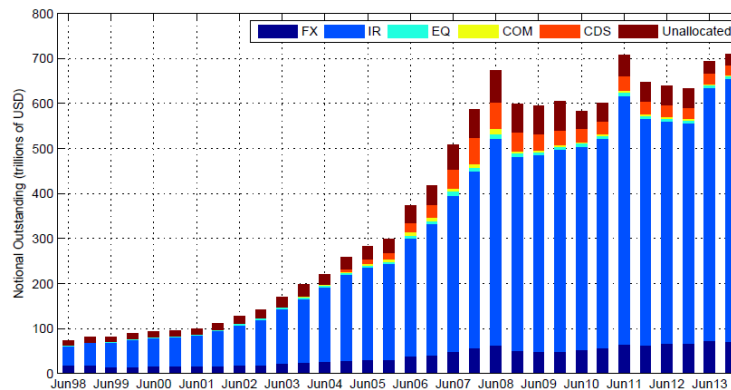


Figure 4.1.1: The notional amounts (in trillions of US dollars) outstanding of OTC derivatives by risk category from BIS semi-annual survey, June 1998 through December 2013.

In this chapter, we aim to provide a solid framework for the CVA calculation of Bermudan swaptions. To achieve this, there are two main issues that we need to consider. First, estimating CVA charges requires an underlying model to compute simulated counterparty exposures at default dates and therefore makes it a model dependent quantity. Before the financial crisis, it was standard market practice to price and hedge interest rate derivatives for a given currency under a single-curve framework, usually established by bootstrapping a single yield curve from liquidly traded vanilla interest rate instruments of various maturities and the corresponding forward rates, discount factors and numeraires were all generated



Figure 4.1.2: 3-month Libor-OIS spread since June 2008

from this single curve. Unfortunately, the pre-crisis approach has become obsolete and is no longer consistent with the current market conditions in several aspects. First and foremost, it does not capture the widening basis swap spreads that are now much larger than those of the pre-crisis period, see Figure 4.1.2 for example. This is mainly attributed to the credit or liquidity driven, non-negligible divergence between similar rates with the same maturity that used to chase each other closely (e.g. 3-month OIS rate vs 3-month deposit rate), swap rates based on different payment frequencies of the underlying floating legs and rates based on different underlying tenors (e.g. 1-month Libor vs 3-month Libor) which reflects higher liquidity risk suffered by financial institutions and the corresponding preference for receiving payments with higher frequency, see Figure 4.1.3 for example. Second, the post-crisis interest rate markets have been segmented into sub areas corresponding to instruments with distinct underlying rate tenors, characterized, in principle, by different dynamics (e.g. short rate processes) and the classic no-arbitrage condition is no longer satisfied. Finally, a unique discounting curve is needed where two identical future cash flows of different origins must have the same present value. Earlier developments such as Tuckman and Porfirio (2003) and Boenkost and Schmidt (2005) had already pointed to the weakness of the single curve framework even before the crisis but without providing a theoretically sound alternative.

As pioneer attempts, Henrard (2007, 2010) splits risk-free discounting from Libor rate

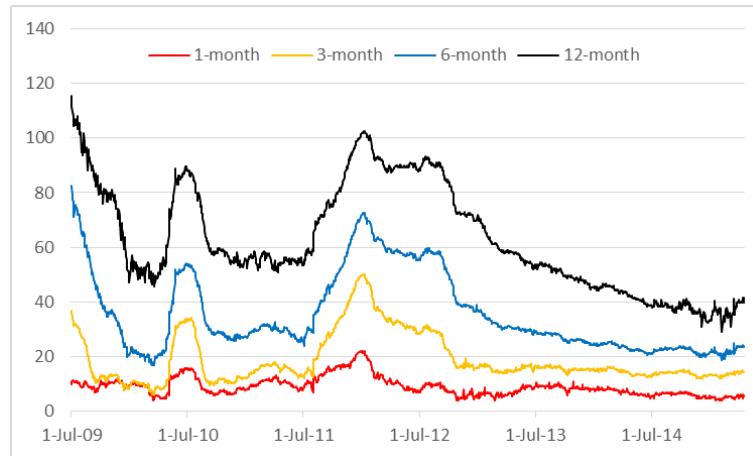


Figure 4.1.3: Libor rates of tenor 1M, 3M, 6M, 12M since the crisis

fixing and assumes constant or deterministic basis spreads, but he fails to consider each forward rate as a single asset without investigating the complex dynamics involved by liquidity and credit risks in a practical way. Morini (2009) is to our knowledge the first paper to address this problem and develop a theoretical foundation that motivates the divergence of rates outlined above. To this end, he introduces a stochastic default probability to account for counterparty risk and, assuming no liquidity risk and that the risk in the forward rate agreements (FRAs) exceeds that in the Libor rates, obtains patterns similar to the market observations. Bianchetti (2010) as a further development proposes the first sound multi-curve framework to price single currency interest rate derivatives.

Recent literatures have gone beyond the simplistic constant or deterministic spread hypothesis. In particular, Kenyon (2010) models both the discounting curve and the forward curves with short rate dynamics but, beyond the fact that the short rate is ill-defined for the forward curves, his approach is arbitrage-free only for zero basis spread. Mercurio (2009) uses a full Libor market model on both curves, of which full parameterization of the volatility functions is required. Alternatively, Mercurio (2010) takes a different approach by jointly modelling the basis spread explicitly with a stochastic volatility function and the discounting curve with Libor market model. A similar approach is also considered by Mercurio and Xie (2012) who model the discounting curve with Hull-White model and the additive forward basis spread as a function of the forward OIS rate and a stochastic basis

factor. Semi-analytical pricing formulas for European swaptions are derived in their work. This approach is not only computationally tractable but is also able to ensure a positive basis spread as seen in the market.

Henrard (2013) follows a similar path by modelling the stochastic basis spread explicitly but develops a multiplicative spread model and use it to price short-term interest rate (STIR) futures and their options. Fujii et al. (2011) model the stochastic basis spread with HJM framework but no examples of dynamics or corresponding explicit pricing formulas for calibration instruments are obtained. A hybrid method is studied by Moreni and Pallavicini (2014) who model the discounting curve with a HJM framework and the forward curve via Libor market like approach. The spread is modelled implicitly as the difference of the two curves. Given the parsimonious nature of their model, the spread is modelled implicitly by the same stochastic process than the rate level and thus not fully stochastic. Crépey et al. (2012, 2015) are the latest contributions to go along the path of using HJM type multi-curve framework driven by Lévy process and the latter apply it to the CVA and other funding cost calculations of interest rate derivatives through reduced form methodologies. Other developments have also been done in various directions, these include Chibane and Sheldon (2009), Ametrano and Bianchetti (2009), Andersen and Piterbarg (2010) and Pallavicini and Tarengi (2010) just to mention a few. However, literature concerning Bermudan swaptions under multi-curve framework have been scarce. Given that a valid interest rate modelling framework in line with market practice is a key building block in CVA calculations, one of the main objectives of this chapter is to establish such a framework for Bermudan swaption valuation.

Furthermore, although there are an extensive literature regarding CVA methodologies, which notably include Canabarro and Duffie (2003), Picoult (2005), Pykhtin and Zhu (2006), Gregory (2010) and Brigo et al. (2013), few focus on Bermudan swaptions and traditional approaches rarely take into account the embedded correlation between the evolution of counterparty credit quality and the market risk factors driving the underlying exposure of the contract. For example, Karlsson et al. (2014) apply the stochastic bundling grid ap-

proach to compute Bermudan swaption CVA but they assume default to be independent of both the portfolio value and the numeraires. Empirical evidences from the Asia financial crisis in the late 1990s and the recent US subprime mortgage crisis suggest that these correlations affect the derivative price and the subsequent hedging strategy significantly.

According to the International Swap and Derivatives Association (ISDA), when the exposure to a counterparty is adversely correlated with the credit quality of that counterparty (also known as wrong way risk, WWR) and these two effects tend to happen together, then that co-dependence will generally increase the CVA on the contract and it will make the CVA larger than when the effects were independent. Hence, an increasing amount of work has been done to model asset-credit correlation in CVA calculations, which can usually be divided into the following categories: i) Modelling of stochastic intensity of default and its correlation with driving market risk factors, notable literatures include Rosen and Saunders (2012) who model wrong way risk with an ordered-scenario copula model allowing for the performance of multiple CVA calculations for sensitivities, stress testing and value-at-risk (VaR), Ghamami and Goldberg (2014) who consider reduced-form CVA models that include Hull-White formulations, El Hajjaji and Subbotin (2015) whose model is based on a doubly stochastic default process with the default intensities proxied by credit spreads, Boenkost and Schmidt (2015) who aim for a "correlation adjustment" to account for wrong way risk by introducing the correlation between the interest rate curve and hazard rate changes as a main input in the CVA formula without additional simulations needed, Carr and Ghamami (2015) who develop path-independent probabilistic valuation formulas that have closed-form solution or can lead to computationally efficient pricing schemes by imposing restrictions on the dynamics of the risk-free rate and the stochastic intensities of the counterparties' default times. The main advantage of the reduced form method is that the default probabilities generated by the model are consistent with the ones implied from market CDS spread quotes, but it lacks economic rationale and the dependency structures are limited; ii) Structural approaches with correlations between asset and counterparty credit quality dynamics. In this context, the correlation between asset and the counterparty firm value dynamics is easy to incorporate, offering an economic interpretation behind default.

However, the default probabilities generated from traditional first-passage time models are not consistent with market implied ones. Relevant contributions include Redon (2006) who gives an analytical method based on the Merton type model by correlating the Brownian motions used to model mark-to-market and default, Lipton and Sepp (2009) who propose a jump diffusion approach, Lipton and Savescu (2012, 2013) who employs the Eigen function expansion technique combined with finite element method and obtain a semi-analytical expression for CVA and DVA, and Ballotta and Fusai (2014) who model the asset price and firm value dynamics with normal inverse Gaussian processes; iii) Modelling dependence between default times and exposures at different observation dates using Copula models, like Pykhtin and Rosen (2010), Boukhobza and Maetz (2012), Pykhtin (2012), Cherubini (2013), Böcker and Brunnbauer (2014) and Lee and Capriotti (2015); iv) Adjusting default probability functions in the independence-based CVA formula as in Hull and White (2012); v) Introducing jump diffusions at time of default to model gap risk or default risk in emerging currencies or other risk factors such as Pykhtin and Sokol (2012) and ?; iv) Using alternative methods including scenario weighting, for example, Finger (2000), Turlakov (2013) and Glasserman and Yang (2015), modelling simultaneous defaults as in ? and introducing jumps at default to quantify the impact of wrong way correlation like Li and Mercurio (2015). Since analytical pricing formulas for Bermudan swaptions are not available and Monte-Carlo simulation is usually required, also we are going to work under the multi-curve framework, correctly correlating counterparty credit quality with various interest rate dynamics, thus establishing a computationally efficient joint asset-credit model is another key objective of our work.

In this chapter, we follow similarly as Mercurio (2009, 2010) and Mercurio and Xie (2012) to model stochastic additive basis spreads explicitly along with the OIS discounting curve and express the corresponding (forward) Libor fixing in terms of the sum of the two. In market practice (see Pallavicini and Tarengi (2010) for example), the OIS curve and the forward Libor curves are constructed as the following: 1) for the short end of the curve (i.e. tenors up to 48m), to achieve smoothness we use OIS swap rate quotes as the levels at the corresponding nodes of the curve and interpolate/extrapolate it using cubic spline method;

2) for the mid-to-long end of the curve (i.e. tenors greater than or equal to 5Y), we calibrate the curve to fixed-for-floating, floating-for-floating interest rate swaps by using the 3-month Libor curve as the base curve. Taking market quotes of the Libor swap rates and intra-currency basis swap spreads as inputs, the forward Libor index curves and the OIS curve are solved simultaneously using appropriate root-finding algorithms. To model the OIS curve, we choose the Hull-White short rate dynamics for the discounting curve of a given currency. With respect to the basis spread, we make a simplified assumption that the spread evolution is independent of the discounting curve and model the forward basis spread with a given tenor for various maturities in terms of a one-factor lognormal process with zero drift. The multi-curve model can be easily calibrated to interest rate caps through modifications of the cap pricing formulas developed in Mercurio (2010). Once this is done, we apply the standard Longstaff-Schwartz algorithm under our multi-curve framework to obtain the optimal exercise boundary of Bermudan swaption. Then, to account for wrong way risk, we follow Davis and Pistorius (2010) to model the default time of a certain financial entity as the first time a time-changed Brownian motion (credit index process) down crosses zero and the conditional law upon default of the credit index process is equal to that of the corresponding three-dimensional Bessel bridge. Given that the basis spreads are a reflection of credit and liquidity risk and that a widening of the spreads is a manifestation of credit and liquidity squeeze in the systemic macro economic environment, we correlate the credit index process with the driving Brownian motion of the basis spreads instead of that of the OIS curve and jointly simulate them conditional on default at certain dates given the value of the asset-credit correlation. Finally, Monte Carlo simulation is used to compute expected positive exposures (EPE) at default dates and subsequently the CVAs. The main contribution of this chapter is that it is the first paper to study CVA calculation of Bermudan swaption under the multi-curve framework with wrong way/right way risk embedded. Furthermore, conditional on default at a certain time in the future, the default probabilities generated by the model can be calibrated exactly to the market implied ones from CDSs and the credit index process can be easily simulated via Bessel bridges, which can in turn be correlated easily with the Libor-OIS spread dynamics such that the impact of rising Libor-OIS spread

and falling counterparty credit quality can be quantified by CVAs against a range of asset-credit correlation scenarios. The rest of the chapter is organized as follows. In section 2, we introduce the definitions of EPE and CVA. In section 3, we establish the multi-curve interest rate modelling framework with stochastic basis spreads. In section 4, we revisit the standard Longstaff-Schwartz algorithm in the valuation of American style options. In section 5, we construct the joint asset-credit default model via Bessel bridges. In section 6, we conduct numerical studies on Bermudan swaptions and illustrate the impact of wrong way risk on their CVA and EPEs. We conclude in section 7.

4.2 Credit Value Adjustment

CVA is the market value of counterparty credit risk, i.e., the difference between the risk-free contract value and the value taking into account the counterparty's default probability. Denoting the recovery rate of the counterparty as R_C , we expect to be compensated from the contract should the counterparty default, if the time horizon of the contract is T , then following Cesari et al. (2009), the CVA at time 0 is defined as:

$$CVA_{0,T} = (1 - R_C) \int_0^T E^{\mathbb{Q}}[D(0, u)E(u)|\tau_C = u]dPD(u). \quad (4.2.1)$$

Since we take into account the correlation between counterparty default and the underlying asset value, numerical methods will be required for accurate calculation of CVA. However, for convenience, we would like to introduce the simplified approximation of CVA defined as below:

$$\begin{aligned} CVA_{0,T} &\approx (1 - R_C) \int_0^T E^{\mathbb{Q}}\left[\frac{1}{P(0, u)}D(0, u)E(u)\right]P(0, u)dPD(u), \\ &\approx (1 - R_C) \int_0^T P(0, u)EPE_u dPD(u), \end{aligned} \quad (4.2.2)$$

where $EPE_u = E^{\mathbb{Q}}[\frac{1}{P(0,u)}D(0,u)E(u)]$,

or

$$\begin{aligned} CVA_{0,T} &\approx (1 - R_C) \int_0^T E^{\mathbb{Q}}[D(0,u)E(u)]dPD(u), \\ &\approx (1 - R_C) \int_0^T EPE_u^D dPD(u), \end{aligned} \quad (4.2.3)$$

where $EPE_u^D = E^{\mathbb{Q}}[D(0,u)E(u)]$, $PD(t)$ is the risk-neutral default probability of the counterparty before time t usually defined as:

$$PD(t) = 1 - \exp\{-\int_0^t \gamma(u)du\}, \quad (4.2.4)$$

and $\gamma(t)$ is the hazard rate function or the instantaneous credit spread. Such default distribution of the counterparty is bootstrapped from its corresponding market CDS quotes. For discrete time grid $0 = T_0 < T_1 < \dots < T_n = T$ of the observation dates equation 4.2.3 can be further approximated in the discrete time space as:

$$CVA_{0,T} \approx (1 - R_C) \sum_{i=0}^{n-1} P(0, T_i) EPE_{T_i} (PD(T_{i+1}) - PD(T_i)), \quad (4.2.5)$$

or

$$CVA_{0,T} \approx (1 - R_C) \sum_{i=0}^{n-1} EPE_{T_i}^D (PD(T_{i+1}) - PD(T_i)). \quad (4.2.6)$$

Hence, CVA can be seen as a weighted average of EPEs at different observation dates with the weights given by the default probabilities.

4.3 Multi-Curve Framework with Stochastic Basis Spreads

In this section, we establish the multi-curve interest rate framework with stochastic basis spreads.

4.3.1 Assumptions and Notations

Based on Mercurio (2010), we assume a single currency multi-curve framework where distinct discount and forward curves indexed by different tenors ($x = 1m, 3m, 6m, \dots$) are constructed. To comply with the credit support annex (CSA) agreement, we assume the discount curve to be the OIS zero-coupon curve as the credit risk embedded in an overnight loan can be deemed to be negligible, and the discount factor at time t for maturity T to be $D^{OIS}(t, T)$. The OIS zero-coupon bond price can be then defined as $P_D(t, T) = E_t^{\mathbb{Q}}[D^{OIS}(t, T)]$.

Given a tenor x and a discrete time grid $0 = T_0 < T_1 < \dots < T_n = T$, with $x = T_i - T_{i-1}$, $i = 1, \dots, n$, the OIS forward rate can be defined as:

$$F_D^x(t, T_{i-1}, T_i) = \frac{1}{\tau_i^x} \left[\frac{P_D(t, T_{i-1})}{P_D(t, T_i)} - 1 \right], \quad (4.3.1)$$

where τ_i^x is the year fraction for $(T_{i-1}, T_i]$. The pricing measures are associated with those of the OIS curve. Denote \mathbb{Q}_D^T the T -forward measure with the associated numeraire being the OIS zero-coupon bond $P_D(t, T)$, the forward Libor rate for time interval $[T_{i-1}, T_i]$ is defined as:

$$L(t, T_{i-1}, T_i) = E_D^{T_i}[L^x(T_{i-1}, T_i) | \mathcal{F}_t], \quad (4.3.2)$$

where $L^x(T_{i-1}, T_i)$ is the spot Libor rate fixed at T_{i-1} for the maturity T_i . $L^x(t, T_{i-1}, T_i)$ is the fixed rate to be exchanged for the spot Libor rate $L^x(T_{i-1}, T_i)$ so that the forward rate agreement (FRA) is entered at zero cost.

Following Mercurio (2010) and Mercurio and Xie (2012), we model the basis swap spreads explicitly and express the forward Libor rate in terms of the forward OIS rate and the basis swap spreads:

$$L^x(t, T_{i-1}, T_i) = S^x(t, T_{i-1}, T_i) + F^x(t, T_{i-1}, T_i). \quad (4.3.3)$$

This choice is more realistic as the Libor curves are usually built as a spread over the OIS

curve and therefore it is reasonable to model $S^x(t, T_{i-1}, T_i)$ as positive stochastic processes, preserving the positive sign of the basis spreads which is typically observed in the market.

4.3.2 Model Dynamics

We now assume suitable dynamics for $F^x(t, T_{i-1}, T_i)$ and $S^x(t, T_{i-1}, T_i)$ under the corresponding OIS T_i -forward measure $\mathbb{Q}_D^{T_i}$, $i = 1, \dots, n$.

The OIS curve is assumed to follow the Hull-White short rate dynamics (see Mercurio and Xie (2012)) as follows:

$$\begin{aligned} r(t) &= \theta(t) + y(t), \\ dy(t) &= -\kappa y(t)dt + \sigma dW^{\mathbb{Q}}(t), \quad y(0) = 0, \end{aligned} \quad (4.3.4)$$

where $\theta(t)$ is a deterministic function defined as:

$$\theta(t) = -\frac{\partial}{\partial T} \log P_D(0, t) + \frac{\sigma^2}{2\kappa^2} (1 - e^{-\kappa t})^2, \quad (4.3.5)$$

such that the model is consistent with the initial OIS rate term structure, κ is the constant mean reversion rate, σ is the constant implied volatility and $W^{\mathbb{Q}}$ is a standard Brownian motion under measure \mathbb{Q} . The OIS discount factor at time t for maturity T can then be defined as:

$$D^{OIS}(t, T) = \exp\left\{-\int_t^T r(u)du\right\}, \quad (4.3.6)$$

where

$$\int_t^T r(u)du = y(t)B(t, T) + \ln \frac{P_D(0, t)}{P_D(0, T)} + \frac{1}{2}[M(0, T) - M(0, t)] + \sigma \int_t^T B(u, T)dW^{\mathbb{Q}}(u), \quad (4.3.7)$$

$$B(t, T) = \frac{1}{\kappa}[1 - e^{-\kappa(T-t)}], \quad (4.3.8)$$

$$M(t, T) = \frac{\sigma^2}{\kappa^2}\left[T - t + \frac{2}{\kappa}e^{-\kappa(T-t)} - \frac{1}{2\kappa}e^{-2\kappa(T-t)} - \frac{3}{2\kappa}\right], \quad (4.3.9)$$

and the OIS zero-coupon bond price is defined as:

$$P_D(t, T) = E^{\mathbb{Q}}[\exp - \int_t^T r(u) du | \mathcal{F}_t]. \quad (4.3.10)$$

Also, the closed-form solution is known to be:

$$P_D(t, T) = \exp\{A(t, T) - B(t, T)y(t)\}, \quad (4.3.11)$$

where

$$A(t, T) = \log \frac{P_D(0, T)}{P_D(0, t)} + \frac{\sigma^2}{2\kappa^3} \left[-\frac{3}{2} + 2e^{-\kappa(T-t)} - \frac{1}{2}e^{-2\kappa(T-t)} + 2(e^{-\kappa t} - e^{-\kappa T}) - \frac{1}{2}(e^{-2\kappa t} - e^{-2\kappa T}) \right].$$

It is important to note that such specification of the OIS rate is consistent with the initial term structure of the OIS curve. At time $t = 0$, $A(0, T) = \log P_D(0, T)$, the zero-coupon bond prices are simply equal to the market implied zero-coupon bond prices at time zero. However, the mean reversion rate parameter can be alternatively estimated in the real probability measure using historical data, while the volatility parameter still needs to be calibrated to interest rate caps. For $S^x(t, T_{i-1}, T_i)$, we follow Mercurio and Xie (2012)'s example and assume a one-factor lognormal stochastic process with zero-drift as follows:

$$dS^x(t, T_{i-1}, T_i) = \eta_x S^x(t, T_{i-1}, T_i) dZ_x^{\mathbb{Q}}(t), \quad (4.3.12)$$

where η_x is the constant spread volatility for all maturities T_i , $i = 1, \dots, n$ given tenor x and $Z_x^{\mathbb{Q}}$ is a standard Brownian motion under measure \mathbb{Q} independent of $W^{\mathbb{Q}}$. In Mercurio (2010), the stochastic basis spreads are assumed to have a stochastic volatility function for more accurate calibration to market data and pricing of interest rate derivatives. Furthermore, given tenor x the forward basis spreads for various maturities are driven by their own Brownian motions and are correlated with the forward OIS rate. Since the main objective of this chapter is CVA calculation with specific focus on wrong way risk, we tend to choose relatively simple dynamics for the forward OIS rate and the basis spreads so that wrong way risk can be easily incorporated. Therefore, we assume parallel movement of forward basis

swap spreads across various maturities and a constant volatility parameter for a given tenor x .

4.3.3 Caplet Pricing

For the calibration of our multi-curve framework, we choose interest rate caps as calibration instruments.

Consider a caplet written on the x -tenor Libor rate $L^x(T_{i-1}, T_i)$ at strike rate K and notional N , which pays out at time T_i :

$$V_i^{Cplt}(T_i) = Nx[L^x(T_{i-1}, T_i) - K]. \quad (4.3.13)$$

Under our multi-curve framework, the caplet price at time $t \leq T_i$ is given by:

$$V_i^{Cplt}(t) = NxP_D(t, T_i)E^{\mathbb{Q}_D^{T_i}}\{[L^x(T_{i-1}, T_i) - K]^+|\mathcal{F}_t\}. \quad (4.3.14)$$

With application of tower property of conditional expectations, we have:

$$\begin{aligned} V_i^{Cplt}(t) &= NxP_D(t, T_i)E^{\mathbb{Q}_D^{T_i}}\{[F^x(T_{i-1}, T_{i-1}, T_i) + S^x(T_{i-1}, T_{i-1}, T_i) - K]^+|\mathcal{F}_t\} \\ &= NxP_D(t, T_i)E^{\mathbb{Q}_D^{T_i}}\{[F^x(T_{i-1}, T_{i-1}, T_i) - (K - S^x(T_{i-1}, T_{i-1}, T_i))]^+|\mathcal{F}_t\} \\ &= NxP_D(t, T_i)E^{\mathbb{Q}_D^{T_i}}\{E^{\mathbb{Q}_D^{T_i}}\{[F^x(T_{i-1}, T_{i-1}, T_i) - (K - u)]^+|S^x(T_{i-1}, T_{i-1}, T_i) = u\}|\mathcal{F}_t\}. \end{aligned} \quad (4.3.15)$$

Following similarly as in Mercurio (2010), the inner and outer conditional expectations are calculated thanks to the independence between the OIS forward rate $F^x(T_{i-1}, T_{i-1}, T_i)$ and the forward basis swap spread $S^x(T_{i-1}, T_{i-1}, T_i)$:

$$V_i^{Cplt}(t) = NxP_D(t, T_i) \int_{-\infty}^{+\infty} E^{\mathbb{Q}_D^{T_i}}\{[F^x(T_{i-1}, T_{i-1}, T_i) - (K - u)]^+|\mathcal{F}_t\} f_{S^x(T_{i-1})}(u) du, \quad (4.3.16)$$

where $f_{S^x(T_{i-1})}$ is the density function of the basis swap spread at time t $S^x(T_{i-1}, T_{i-1}, T_i)$. Since the support of $f_{F^x(T_{i-1})}$, the density function of the forward OIS rate $F^x(T_{i-1}, T_{i-1}, T_i)$ at time t , is the positive half-line, the above equation can be further derived as:

$$\begin{aligned}
 V^{Cplt}(t) &= NxP_D(t, T_i) \left[\int_{-\infty}^K E^{\mathbb{Q}_D^{T_i}} \{ [F^x(T_{i-1}, T_{i-1}, T_i) - (K - u)] | \mathcal{F}_t \} f_{S^x(T_{i-1})}(u) du \right. \\
 &\quad \left. + \int_K^{+\infty} [F^x(t, T_{i-1}, T_i) - (K - u)] f_{S^x(T_{i-1})}(u) du \right] \\
 &= N \int_0^K \mathbf{Cplt}(t, K - u; T_{i-1}, T_i) f_{S^x(T_{i-1})}(u) du \\
 &\quad + xP_D(t, T_i) (F^x(t, T_{i-1}, T_i) - K) Q_{S^x(T_{i-1})}(t, K) \\
 &\quad + xP_D(t, T_i) \int_K^\infty u f_{S^x(T_{i-1})}(u) du, \tag{4.3.17}
 \end{aligned}$$

where the last integral

$$\int_K^\infty u f_{S^x(T_{i-1})}(u) du = S^x(t, T_{i-1}, T_i) \Phi \left(\frac{\ln \frac{S^x(t, T_{i-1}, T_i)}{K} + \frac{1}{2} \eta_x^2 (T_{i-1} - t)}{\eta_x \sqrt{T_{i-1} - t}} \right), \tag{4.3.18}$$

and

$$\begin{aligned}
 \mathbf{Cplt}(t, K; T_{i-1}, T_i) &= xP_D(t, T_i) [F^x(t, T_{i-1}, T_i) \Phi(d_1) - K \Phi(d_2)], \\
 d_1 &= \frac{\ln \frac{F^x(t, T_{i-1}, T_i)}{K} + \frac{1}{2} \sigma^2 (T_{i-1} - t)}{\sigma \sqrt{T_{i-1} - t}}, \\
 d_2 &= d_1 - \sigma \sqrt{T_{i-1} - t}, \\
 Q_{S^x(T_{i-1})}(t, K) &= \Phi \left(\frac{\ln \frac{S^x(t, T_{i-1}, T_i)}{K} - \frac{1}{2} \eta_x^2 (T_{i-1} - t)}{\eta_x \sqrt{T_{i-1} - t}} \right), \\
 f_{S^x(T_{i-1})}(u) &= \exp \left\{ -\frac{1}{2} \frac{(\ln \frac{u}{S^x(t, T_{i-1}, T_i)} + \frac{1}{2} \eta_x^2 (T_{i-1} - t))^2}{\eta_x^2 (T_{i-1} - t)} \right\},
 \end{aligned}$$

with Φ the cumulative standard normal distribution function. In equation 4.3.17, the first integral can be calculated via numerical integration as an approximation of the definite integral. Specifically, we use Gauss-Legendre quadrature (see Abramowitz and Stegun (1964) for more details).

An interest rate cap is composed of a series of interest rate caplets at strike K and

notional N , therefore the price of an interest rate cap at time t is subsequently equal to the sum of the underlying caplet prices:

$$V^{Cap}(t) = \sum_{i=1}^n V_i^{Cplt}(t). \quad (4.3.19)$$

4.3.4 A Example of Calibration to Market Data

We now give an example on calibrating our multi-curve framework to interest rate caps across various maturities in the US market as of 28th April 2014. The calibrated parameters are:

$$\kappa = 0.088, \sigma = 0.0114, \eta_x = 0.1642. \quad (4.3.20)$$

Table 4.3.1 summarizes the strikes and implied volatilities of at-the-money (ATM) dollar caps with maturities up to thirty years.

Maturity	ATM Strike	ATM Implied Volatility
1y	0.27%	0.5735
2y	0.57%	0.7215
3y	1.05%	0.618
4y	1.51%	0.518
5y	1.87%	0.4538
6y	2.16%	0.4047
7y	2.38%	0.3763
8y	2.56%	0.3495
9y	2.71%	0.332
10y	2.83%	0.3198
12y	3.02%	0.2958
15y	3.21%	0.2703
20y	3.37%	0.2452
25y	3.43%	0.2387
30y	3.46%	0.2342

Table 4.3.1: ATM Dollar cap implied volatility quotes on 28th April 2014. Data Source: Bloomberg

4.4 Pricing Bermudan Swaption with Least Square Method

In this section, we revisit the classical Longstaff-Schwartz Algorithm used to price Bermudan-type options. First of all, we introduce the definition of Bermudan swaptions.

4.4.1 Bermudan Swaption

Given a discrete time grid $0 = T_0 < T_1 < \dots < T_n = T$, $x = T_i - T_{i-1}$, $i = 0, \dots, n$, a payer swaption maturing at time T_k , $k \geq 1$, gives the holder the right to enter an vanilla interest rate swap (IRS) at time T_k with the first reset date being T_k and payment dates being T_{k+1}, \dots, T_n at the fixed rate K and notional N . Under our pre-specified multi-curve framework, the value of a payer swap at time $t \leq T_k$ is given by:

$$\begin{aligned}
 V(t) &= E^{\mathbb{Q}}[Nx \sum_{i=k}^{n-1} \exp\{-\int_t^{T_{i+1}} r(u)du\} [L^x(T_i, T_{i+1}) - K] | \mathcal{F}_t] \\
 &= Nx \sum_{i=k}^{n-1} E^{\mathbb{Q}}[\exp\{-\int_t^{T_{i+1}} r(u)du\} [L^x(T_i, T_{i+1}) - K] | \mathcal{F}_t] \quad (4.4.1) \\
 &= Nx \sum_{i=k}^{n-1} P_D(t, T_{i+1}) E^{\mathbb{Q}_D^{T_{i+1}}} [L^x(T_i, T_{i+1}) - K | \mathcal{F}_t] \\
 &= Nx \sum_{i=k}^{n-1} P_D(t, T_{i+1}) [L^x(t, T_i, T_{i+1}) - K] \\
 &= Nx \sum_{i=k}^{n-1} P_D(t, T_{i+1}) [F^x(t, T_i, T_{i+1}) + S^x(t, T_i, T_{i+1}) - K], \quad (4.4.2)
 \end{aligned}$$

given equation 4.3.1 and the closed-form solution of the forward basis spreads $S^x(t, T_i, T_{i+1})$, we have

$$\begin{aligned}
 V(t) &= N[P_D(t, T_k) - P_D(t, T_n)] + Nx \sum_{i=k}^{n-1} P_D(t, T_{i+1}) [S^x(0, T_i, T_{i+1}) \exp\{-\frac{1}{2}\eta_x^2 t + \eta_x Z_x^{\mathbb{Q}}(t)\} - K] \\
 &= N[P_D(t, T_k) - P_D(t, T_n)] + N \exp\{-\frac{1}{2}\eta_x^2 t + \eta_x Z_x^{\mathbb{Q}}(t)\} x \sum_{i=k}^{n-1} P_D(t, T_{i+1}) S^x(0, T_i, T_{i+1}) \\
 &\quad - NKx \sum_{i=k}^{n-1} P_D(t, T_{i+1}). \quad (4.4.3)
 \end{aligned}$$

The corresponding values of the forward swap rate $S_{k,n}^x(t)$ and annuity $A_{k,n}^x(t)$ at time t are given by:

$$S_{k,n}^x(t) = \frac{P_D(t, T_k) - P_D(t, T_n) + \exp\{-\frac{1}{2}\eta_x^2 t + \eta_x Z_x^{\mathbb{Q}}(t)\} x^{\sum_{i=k}^{n-1} P_D(t, T_{i+1})} S^x(0, T_i, T_{i+1})}{x^{\sum_{i=k}^{n-1} P_D(t, T_{i+1})}}, \quad (4.4.4)$$

$$A_{k,n}^x(t) = x^{\sum_{i=k}^{n-1} P_D(t, T_{i+1})}. \quad (4.4.5)$$

Based on Brigo and Mercurio (2007), Bermudan swaptions are defined as follows:

Definition 4.4.1. (Bermudan Swaption) A (payer) Bermudan swaption is a swaption characterized by three dates $T_k < T_h < T_n$, giving the holder the right to enter an IRS at any time T_l in-between T_k and T_h , with the first reset date T_h and the last payment date T_n at the fixed rate K . Thus the start and length of the option depend on the instant T_l when the option is exercised.

Given the lock-out period, i.e., a no-exercise period up to time T_k , a payer Bermudan swaption with fixed coupon K and notional N , exercised at time T_l corresponds to the value:

$$U(T_l) = N A_{l,n}^x(T_l) [S_{l,n}^x(T_l) - K]. \quad (4.4.6)$$

The present value at time 0 of the Bermudan swaption is the supremum taken over all discrete stopping times τ of all conditional expected discounted payoffs:

$$V(0) = \sup_{\tau} E^{\mathbb{Q}}[\exp\{-\int_0^{\tau} r(u)du\} U(\tau) | \mathcal{F}_{\tau}]. \quad (4.4.7)$$

The value at arbitrary exercise date $T_i \geq T_l$ is the maximum of the conditional continuation value $H(T_i)$ and the intrinsic value of the Bermudan swaption $U(T_i)$:

$$V(T_i) = \max(H(T_i), U(T_i)), \quad (4.4.8)$$

where $H(T_n) = 0$. The continuation value $H(T_i)$ is the conditional expected option value

at time T_{i+1} :

$$H(T_i) = E^{\mathbb{Q}}[\exp\{-\int_{T_i}^{T_{i+1}} r(u)du\}V(T_{i+1})|\mathcal{F}_{T_i}]. \quad (4.4.9)$$

Remark. *In this thesis, the Bermudan swaptions we consider are assumed to be of cash-settled type. Hence the investor will only have counterparty exposure upon exercising the contract and there will be no further exposure going forward and the counterparty risk is of unilateral nature. The standard market practice of pricing cash-settled Bermudan swaptions may vary depending on the market they are traded. Specifically, in the Euro market the annuity is actually defined in terms of the swap rate $S_{i,n}^x(T_i)$:*

$$A_{l,n}^x(T_i) = x \sum_{i=l}^{n-1} \frac{1}{(1 + S_{i,n}^x(T_i))^{T_{i+1}-T_i}}, \quad (4.4.10)$$

in order to simplify the determination of cash settlement. However, such discounting is not used in the US market where the traditional payoff as in equation 4.4.6 is preserved. For simplicity and to avoid confusion, we assume that the difference in the prices obtained from the two discounting methods is minimal enough to ignore and treat Bermudan swaptions as the ones in the US market. For more details, see Brigo and Mercurio (2007).

4.4.2 Least Squares Method

As seen above, the valuation of Bermudan swaptions is an optimal exercise problem solved by backward induction, starting from the last exercise date T_{n-1} , recursively repeating equation 4.4.8 and 4.4.9 until time 0. The most common method to solve such optimal exercise method is the least squares method initially introduced by Carriere (1996) and is a simulation based method used to approximate the continuation value $H(T_i)$ through parametric functions. One of the notable works of this method is by Longstaff and Schwartz (2001), where the parametric functions are approximated using least square regression such that the estimated continuation value $\tilde{H}(T_i)$ is given by:

$$\tilde{H}(T_i) = \sum_{d=0}^R \theta_{i,d} \phi_d(X_i), \quad (4.4.11)$$

where $\theta_{i,d}$, $d = 0, \dots, R$ is a set of parameters for the set of basis functions ϕ_d , $d = 0, \dots, R$ and X_i is the explanatory variable driving the holding value at time T_i . The objective of the method is to choose parameters $\theta_{i,d}$ at each exercise date so that the linear combination of the basis functions best approximates $H(T_i)$.

Applying this approach involves choosing a suitable parametric family of basis functions, as mentioned in Glasserman et al. (2004). For our purposes, we believe it is sufficient to choose the ones that are complete and linearly independent and hence we follow Longstaff and Schwartz (2001) to choose weighted Laguerre polynomials defined as:

$$\begin{aligned}\phi_0(x) &= e^{-\frac{x}{2}}, \\ \phi_1(x) &= e^{-\frac{x}{2}}(1-x), \\ \phi_2(x) &= e^{-\frac{x}{2}}\left(1-2x+\frac{x^2}{x}\right), \\ \phi_d(x) &= e^{-\frac{x}{2}}\frac{e^x}{d!}\frac{\partial^d}{\partial x^d}(x^d e^{-x}),\end{aligned}$$

where d is the degree of dimension. The problem now reduces to minimizing the expected squared error with respect to the parameters $\theta_{i,d}$:

$$\epsilon = E[(H(T_i) - \sum_{d=0}^R \theta_{i,d} \phi_d(X_i))^2]. \quad (4.4.12)$$

It is important to note that for CVA calculation we do not set restrictions on the paths based on whether the Bermudan swaption is ITM or not. In addition, to avoid oversight bias, we generated a second set of paths for X_i and the basis functions approximated from the first set of paths will be used for obtaining the exercise boundary.

By differentiating the right hand side of equation 4.4.12 with respect to $\theta_{i,d}$ and set the result equal to zero, we have:

$$E[E[H(T_i)\phi_d(X_i)]] = \sum_{d=0}^R E[\phi_d(X_i)\phi_s(X_i)]. \quad (4.4.13)$$

Now we define matrix formulation

$$(\mathbf{M}_{\phi\phi})_{d,s} = E[\phi_d(X_i)\phi_s(X_i)], \quad (4.4.14)$$

where $\mathbf{M}_{\phi\phi}$ is a non-singular $R \times R$ matrix with $(d+1)s$ entry and

$$(\mathbf{M}_{V\phi})_d = E[E[H(T_i)\phi_d(X_i)]] = E[H(T_i)\phi_d(X_i)], \quad (4.4.15)$$

where $\mathbf{M}_{V\phi}$ is a R -vector with $(d+1)$ th entry. θ_i is then given by:

$$\theta_i = \mathbf{M}_{\phi\phi}^{-1}\mathbf{M}_{V\phi}. \quad (4.4.16)$$

To obtain the value of elements of θ_i , Monte Carlo simulation is applied, $\mathbf{M}_{\phi\phi}$ and $\mathbf{M}_{V\phi}$ can be estimated as follows:

$$(\tilde{\mathbf{M}}_{\phi\phi})_{d+1,s} = \frac{1}{b}\sum_{j=1}^b\phi_d(X_{i,j})\phi_s(X_{i,j}), \quad (4.4.17)$$

$$(\tilde{\mathbf{M}}_{V\phi})_{d+1} = \frac{1}{b}\sum_{q=1}^b\phi_d(X_{i,q})H(X_{i,q}, T_i), \quad (4.4.18)$$

where b is the number of simulated paths for X_i . Then at each downstream node, a second set of paths for X_i is generated, which we denote as \tilde{X}_i , the continuation value $H(T_i)$ can be estimated:

$$H(T_i) \approx \theta_i^\top \phi(\tilde{X}_i), \quad (4.4.19)$$

where $\phi(\tilde{X}_i) = (\phi_0(\tilde{X}_i), \dots, \phi_R(\tilde{X}_i))^\top$.

Based on Chapter 8 of Glasserman et al. (2004), the regression-based algorithm can be summarized as follows:

- Generate b paths of n time steps.
- Simulate b independent paths $\{X_{1,j}, \dots, X_{n,j}\}$, $j = 1, \dots, b$.
- Set $V_j(T_n) = U_j(T_n)$ as the terminal conditional for path j .

- Work backwards: for $i = n - 1, \dots, 1$,
 - given the simulated value of $X_{i,j}, j = 1, \dots, b$, calculate the estimates of $(\tilde{\mathbf{M}}_{\phi\phi})_{(d+1)s}$ and $(\tilde{\mathbf{M}}_{V\phi})_{d+1}$;
 - invert to find $\theta_{i,j} = \tilde{\mathbf{M}}_{\phi\phi}^{-1} \tilde{\mathbf{M}}_{V\phi}$.
- Simulate a second set of $\{X_{1,j}, \dots, X_{n,j}\}, j = 1, \dots, b$, and denote it as $\{\tilde{X}_{1,j}, \dots, \tilde{X}_{n,j}\}, j = 1, \dots, b$.
- Set $V_j(T_i) = \tilde{U}_j(T_i), j = 1, \dots, b, i = 1, \dots, n$, where $\tilde{U}_j(T_i)$ is generated via $\tilde{X}_{i,j}$.
- Work backwards, for $i = n - 1, \dots, 1$,
 - Calculate the estimated continuation value $\tilde{H}_j(T_i) = \theta_i^T \phi(\tilde{X}_{i,j}), j = 1, \dots, b$;
 - Set

$$\tilde{V}_j(T_i) = \max(\tilde{U}_j(T_i), \tilde{H}_j(T_i)), j = 1, \dots, b,$$
 if $\tilde{U}_j(T_i) > \tilde{H}_j(T_i), \tilde{V}_j(T_i) = \tilde{U}_j(T_i)$, otherwise $\tilde{V}_j(T_i) = \tilde{V}_j(T_{i+1}) * DF(\Delta t)$,
 $DF(\Delta t)$ is the discount factor for time period Δt ;
- Until time T_0 , we have an optimal exercise boundary along all the simulated paths of $X_{i,j}, i = 1, \dots, n$. Set $\tilde{V}(T_0) = (\tilde{V}_1(T_1) + \dots + \tilde{V}_b(T_1)) * DF(\Delta t)/b$.

In this context, the interest rate is assumed to be constant and therefore the discount factor for all maturities is also constant. However, as we will see in our case, we assume stochastic interest rates and hence simulation of the paths of the discount factors will be conducted. Another important issue in implementing the Longstaff-Schwartz algorithm is to choose the suitable explanatory variables X and the dimension of the parametric functions R . This is essential in avoiding overfitting with an overly rich set of parametric functions and getting a closer estimate of the exercise boundary as mentioned in Piterbarg (2003). Simple parametric families not only make the algorithm more robust but also reduce the number of paths required to achieve convergence. Furthermore, in choosing suitable explanatory variable(s), given equation 4.4.6, we observe that the swap rate $S_{l,n}^x(T_l)$ and the annuity $A_{l,n}^x(T_l)$ are

the dominant factors in driving the exercise/continuation value of the Bermudan swaption at arbitrary exercise date T_l . In equation 4.4.4, we can also observe that the formula of the swap rate $S_{l,n}^x(T_l)$ incorporates information of the OIS zero-coupon bonds, the overall level of the stochastic basis spreads and the annuity and therefore we believe that the swap rate alone is influential enough to act as the explanatory variable along with the parametric families we defined earlier.

4.5 Joint Interest Rate-Credit Model via Bessel Bridges

In this section, we establish the joint interest rate-credit model to incorporate wrong way/right way risk into the multi-curve valuation framework for Bermudan swaptions.

4.5.1 Counterparty Risk Modelling via Bessel Bridges

In order to integrate the default model into the multi-curve framework, we need to identify the joint distribution of the multi-curve dynamics and the credit index process upon default.

For the credit index process $Y(t)$, given that it is a time-changed Brownian motion $\{X(I(t)), t > 0\}$ defined in equation 2.3, it has been shown in Davis and Pistorius (2010) that conditional on counterparty default at time $\tau_C^Y = s > 0$, Y is in law equal to that of a three-dimensional Bessel bridge process from $A \rightarrow 0$ conditional on $\tau_0^X = I(s)$ such that $Y(t)$ solves the following SDE:

$$dY(t) = \left(\frac{1}{Y(t)} - \frac{Y(t)}{\int_t^s \sigma^2(u) du} \right) \sigma^2(t) dt + \sigma(t) dB(t), \quad t \in (0, s), \quad Y(0) = A, \quad (4.5.1)$$

where $A \sim F_\lambda^\nu$ is independent of B . Paths of Y conditional on default at $\tau_C^Y = s > 0$ can be simulated in terms of the three-dimensional Bessel bridge by replacing $s \rightarrow I(s)$, $t \rightarrow I(t)$, $dt \rightarrow \sigma^2(t) dt$ and exploiting the relation between the three-dimensional Bessel

bridge and a Brownian bridge:

$$Y(t) = \sqrt{\left(\frac{A(s-t)}{s} + Z_1(t)\right)^2 + Z_2^2(t) + Z_3^2(t)}, \quad (4.5.2)$$

where Z_i , $i = 1, 2, 3$, are independent $0 \rightarrow 0$ Brownian bridges:

$$dZ_i(t) = -\frac{Z_i(t)}{s-t}dt + dB_i(t) \quad (4.5.3)$$

where B_i are independent Brownian motions.

Since the Libor rate is decomposed into the OIS rate and the basis swap spread in our multi-curve framework, it is essential that we determine whether we should impose wrong way risk onto the OIS rate or the basis swap spreads. Based on Sengupta and Tam (2008) and Thornton (2009), the OIS rate is a measure of the market expectation of the overnight federal funds rate and there is little default risk embedded in the OIS market since overnight index swaps do not involve exchange of principals as payments are exchanged only at the maturity when one party pays the net rate obligation (i.e. the difference between the term OIS rate and the geometric average of the overnight federal funds rate over the term of the contract) to the other. However, on the other hand, the Libor-OIS spread is assumed to be a measure of the health of financial institutions because it reflects what financial institutions believe is the risk of default associated with lending to others and remains a barometer of the fear of financial institution insolvency. Between August 2007 and December 2008, empirical evidence shows that there was a sharp rise in the Libor-OIS spreads of various tenors (e.g. 1-month, 3-month, 6-month) compared with pre-crisis levels, especially following the announcement of bankruptcy of Bear Stearns and Lehman Brothers, highlighting the distress in the banking industry and money markets. Therefore, we believe that the Libor-OIS spread is more sensitive to the deterioration of counterparty credit quality and wrong way risk should be incorporated into the joint evolution of the Libor-OIS spread and the counterparty credit quality. Given the dynamics of the stochastic forward Libor-OIS spread defined in equation 4.3.12, the driving Brownian motion $Z_x^{\mathbb{Q}}(t)$ can be expressed directly in terms

of the credit index process $Y(t)$ and an independent Brownian motion $B'(t)$:

$$B(t) = \int_0^t \frac{1}{\sigma(u)} dY(u) - \nu \int_0^t \sigma(u) du, \quad (4.5.4)$$

$$\begin{aligned} Z_x^{\mathbb{Q}}(t) &= \rho_{C,S} B(t) + \sqrt{1 - \rho_{C,S}^2} B'(t), \\ &= \rho_{C,S} \left(\int_0^t \frac{1}{\sigma(u)} dY(u) - \nu \int_0^t \sigma(u) du \right) + \sqrt{1 - \rho_{C,S}^2} B'(t), \end{aligned} \quad (4.5.5)$$

where $\rho_{C,S}$ is the correlation between $Y(t)$ and $S_x(t, T_{i-1}, T_i)$. Hence, the integral form of the forward basis spread conditional on default at $\tau_C^Y = s > 0$ can be expressed as:

$$\begin{aligned} S_x(t, T_{i-1}, T_i) &= S_x(0, T_{i-1}, T_i) \exp \left\{ -\frac{1}{2} \eta_x^2 + \eta_x \rho_{C,S} \frac{1}{\sigma(u)} dY(u) - \eta_x \rho_{C,S} \nu \int_0^t \sigma(u) du + \right. \\ &\quad \left. + \eta_x \sqrt{1 - \rho_{C,S}^2} B'(t) \right\}. \end{aligned} \quad (4.5.6)$$

4.6 Numerical Results

In this section, we study numerical examples to show the model performance and illustrate how wrong way/right way risk impacts EPEs and CVAs of Bermudan swaptions.

4.6.1 Setup

Under our multi-curve framework, the short rate and basis spread dynamics are calibrated to the interest rate cap quotes in the US market on 28th April 2014 and the model parameters are summarized in section 4.3.4. We assume the counterparty entering into the Bermudan swaption transaction to be Citigroup and the unilateral counterparty default model is calibrated to the CDS quotes of Citigroup for maturities up to 10 years in the US market on 28th April 2014 (see Table 4.6.1). The calibrated piece-wise constant implied hazard rate $\gamma(t)$ and the corresponding credit index volatility $\sigma(t)$ are plotted against maturities in Figure 4.6.1a and Figure 4.6.1b respectively.

4.6. NUMERICAL RESULTS

For the Least-Square regression used to obtain the optimal exercise boundary of the Bermudan swaption, we use weighted Laguerre polynomials of degree $d = 1$ for 100000 simulations as the regression results for degree $d = 2$ or above are less stable and the number of simulations will increase with the degree of the polynomials.

For Bermudan swaptions, we consider cash settled types with 5-year maturity 1-year lockout period and 10-year maturity 5-year lockout period respectively. We set the notional to be \$100000 and the strike rate to be $K = 0.01\%$. The number of Monte-Carlo simulations we run is 100000. The date for EPE and CVA calculations is on 28th April 2014. We vary the correlation between the counterparty credit quality and the Libor-OIS basis spreads, $\rho_{C,S} = \{-0.5, -0.4, -0.2, 0, 0.2, 0.4, 0.5\}$ and see how it impacts EPEs and CVAs.

Maturity (years)	Citigroup CDS Par Spreads
0.5y	0.0024
1y	0.0031
2y	0.0043
3y	0.0060
4y	0.0080
5y	0.0097
7y	0.012
10y	0.014

Table 4.6.1: Market CDS term structures of Citigroup on 28th April 2014. Data Source: Bloomberg

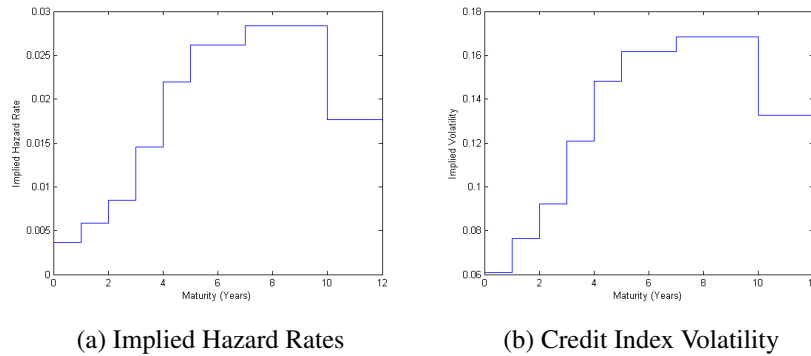


Figure 4.6.1: Implied hazard rate and credit index volatility term structures from par CDS spreads of Citigroup observed on 28th April 2014.

4.6.2 EPE and PFE

Figures 4.6.3-4.6.5 illustrate the EPE profiles of cash-settled Bermudan swaptions with 5-year maturity 1-year lockout, 10-year maturity 1-year lockout and 10-year maturity 5-year lockout. At most fixed time t , the EPE is higher when $\rho_{C,S}$ is more negative and lower as $\rho_{C,S}$ becomes more positive. This is because when the counterparty credit quality deteriorates, negative correlation between the counterparty credit quality and basis spread will cause the basis spreads across maturities to go up and increase the value of the underlying swap, leading to higher counterparty exposure, while a positive correlation between the counterparty credit quality and the basis spread will cause the basis spreads across maturities to fall and decrease the value of the underlying swap, leading to lower counterparty exposure. However, towards the periods where the 3M forward Libor-OIS spread implied from interest rate instruments is very low, see Figure 4.6.2, such effect is less evident. This

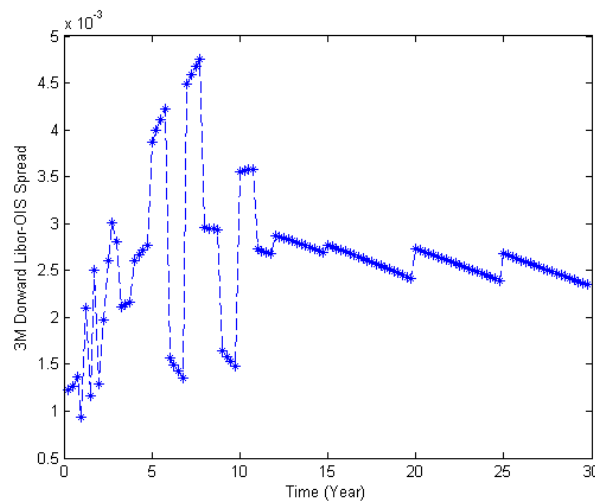


Figure 4.6.2: The 3M USD forward Libor-OIS spread on 28th April 2014. Data Source: Bloomberg

is because the forward Libor-OIS spread is too low and consequently the variability and evolution of the OIS rate tends to outweigh the effect of the forward Libor-OIS spreads. For each fixed $\rho_{C,S}$, the EPEs tend to decrease through time since the earlier the counterparty defaults the longer the maturity of the underlying swap is should the holder exercise the Bermudan swaption given that the swap is in the money, and the higher the value of swap's

4.6. NUMERICAL RESULTS

outstanding payments, leading to higher counterparty exposure. The later the counterparty defaults, the shorter the maturity of the underlying swap and hence the fewer the outstanding payments leading to lower counterparty exposure. Similar patterns can be observed for the potential future exposure profiles of the three Bermudan swaptions considered, see Figure 4.6.6-4.6.8.

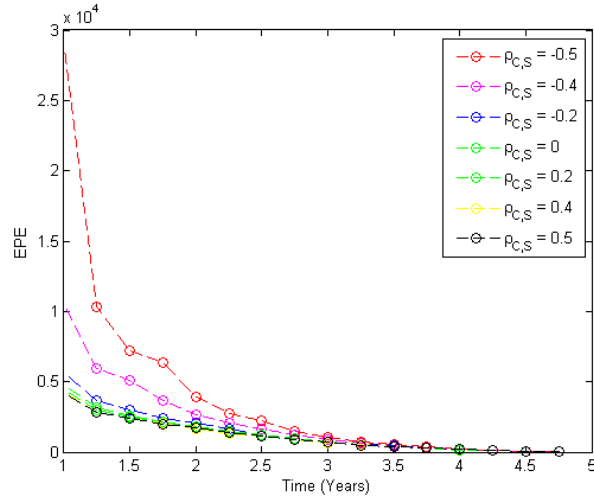


Figure 4.6.3: The EPE of a cash-settled Bermudan swaption with 5-year maturity and 1-year lockout period on 28th April 2014. $K = 1\%$, $N = \$100000$, $\rho_{C,S} = \{-0.5, -0.4, -0.2, 0, 0.2, 0.4, 0.5\}$.

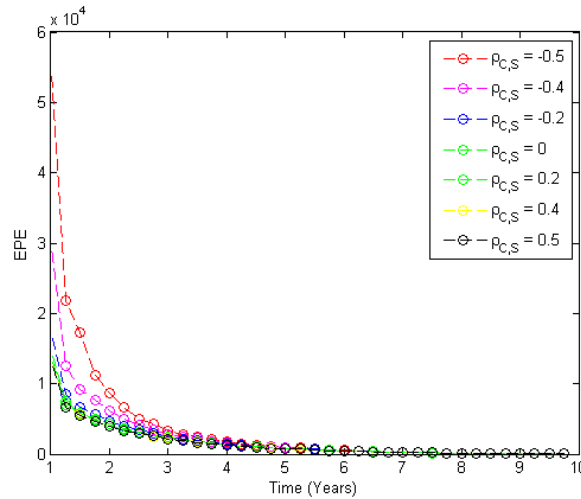


Figure 4.6.4: The EPE of a cash-settled Bermudan swaption with 10-year maturity and 1-year lockout period on 28th April 2014. $K = 1\%$, $N = \$100000$, $\rho_{C,S} = \{-0.5, -0.4, -0.2, 0, 0.2, 0.4, 0.5\}$.

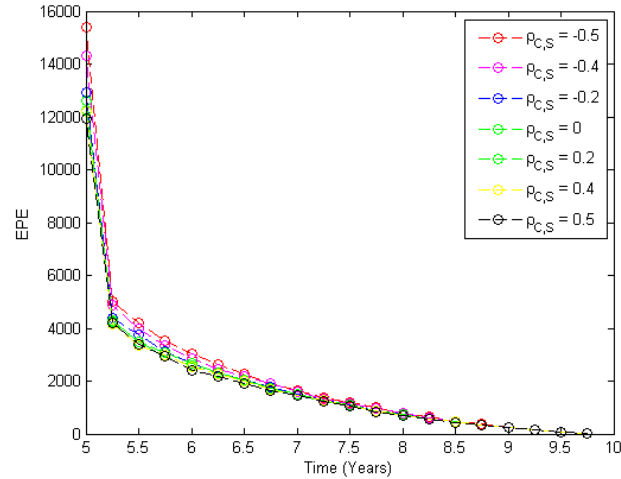


Figure 4.6.5: The EPE of a cash-settled Bermudan swaption with 10-year maturity and 5-year lockout period on 28th April 2014. $K = 1\%$, $N = \$100000$, $\rho_{C,S} = \{-0.5, -0.4, -0.2, 0, 0.2, 0.4, 0.5\}$.

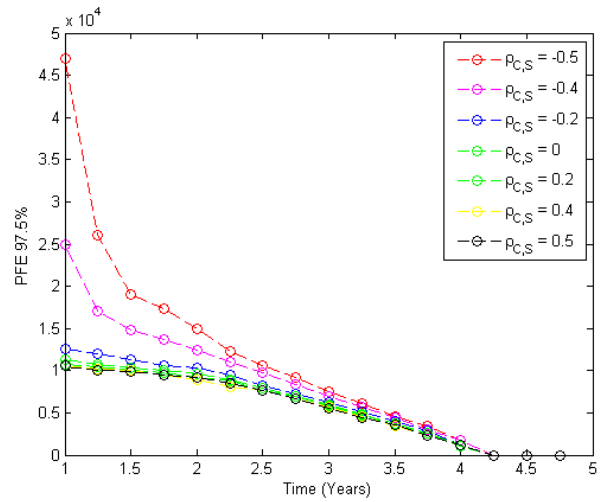


Figure 4.6.6: The 97.5% PFE of a cash-settled Bermudan swaption with 5-year maturity and 1-year lockout period on 28th April 2014. $K = 1\%$, $N = \$100000$, $\rho_{C,S} = \{-0.5, -0.4, -0.2, 0, 0.2, 0.4, 0.5\}$.

4.6.3 CVA

Figures 4.6.9-4.6.11 illustrate the CVAs for the three Bermudan swaption trades we consider. It is shown that if $\rho_{C,S}$ is more negative where wrong way risk dominates, the CVA charge will be higher since the deterioration of the counterparty credit quality leads to higher counterparty exposure upon default and hence a higher CVA will be charged on the counter-

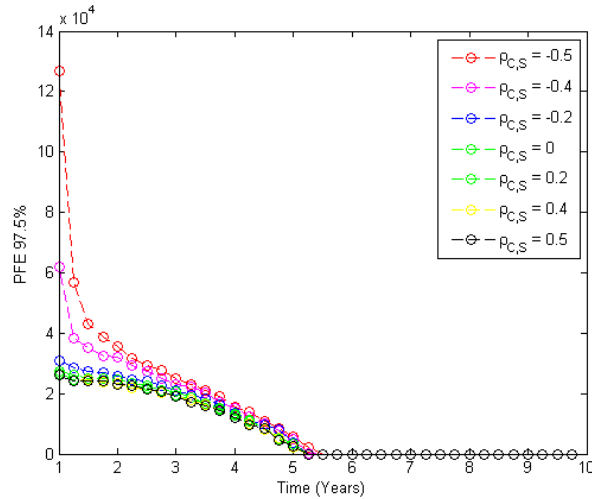


Figure 4.6.7: The 97.5% PFE of a cash-settled Bermudan swaption with 10-year maturity and 1-year lockout period on 28th April 2014. $K = 1\%$, $N = \$100000$, $\rho_{C,S} = \{-0.5, -0.4, -0.2, 0, 0.2, 0.4, 0.5\}$.

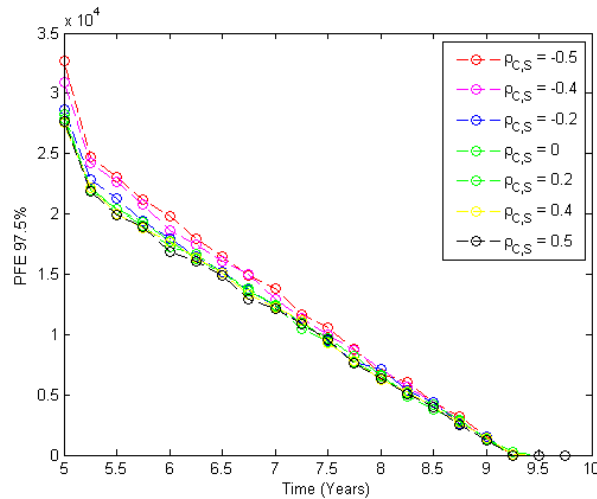


Figure 4.6.8: The 97.5% PFE of a cash-settled Bermudan swaption with 10-year maturity and 5-year lockout period on 28th April 2014. $K = 1\%$, $N = \$100000$, $\rho_{C,S} = \{-0.5, -0.4, -0.2, 0, 0.2, 0.4, 0.5\}$.

party. Conversely, the CVA will decrease as $\rho_{C,S}$ becomes more positive where right way risk dominates and reduces the counterparty exposure upon default, hence a lower CVA will be charged on the counterparty. Furthermore, for each fixed $\rho_{C,S}$, we observe that the CVA charged for the 5-year Bermudan swaption is lower than the one charged for the 10-year Bermudan swaption since the latter has more outstanding payments and hence higher counterparty exposure. Furthermore, given the same maturity, the shorter the lock-out period,

the higher the corresponding CVA charged on the counterparty given a correlation scenario. This is because the more exercise dates the Bermudan swaption has, the more likely the investor will be exposed to counterparty risk, the joint probability that the Bermudan swaption ending in the money and counterparty defaults increases, leading to higher CVA, and this is especially evident when the wrong way correlation is negative since wrong way correlation also increases the likelihood of counterparty default.

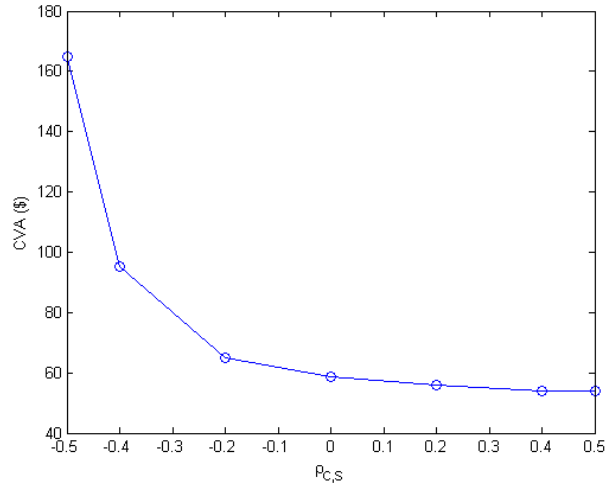


Figure 4.6.9: The CVA of a cash-settled Bermudan swaption with 5-year maturity and 1-year lockout period on 28th April 2014. $K = 1\%$, $N = \$100000$, $\rho_{C,S} = \{-0.5, -0.4, -0.2, 0, 0.2, 0.4, 0.5\}$.

4.7 Conclusion

In this chapter, we establish an efficient and dynamic model to calculate cash-settled Bermudan swaption CVA taking into consideration the impact of wrong way/right way risk. First of all, in the wake of the financial crisis, the traditional single curve framework used in most of the literature concerning Bermudan swaptions has become obsolete and therefore we construct a multi-curve interest rate framework for the valuation of Bermudan swaptions, explicitly modelling the OIS curve (discounting curve) and the basis swap spreads. The OIS rate is assumed to follow one-factor Hull-White dynamics while the stochastic forward basis spread for a given tenor is modelled as a driftless one-factor lognormal process

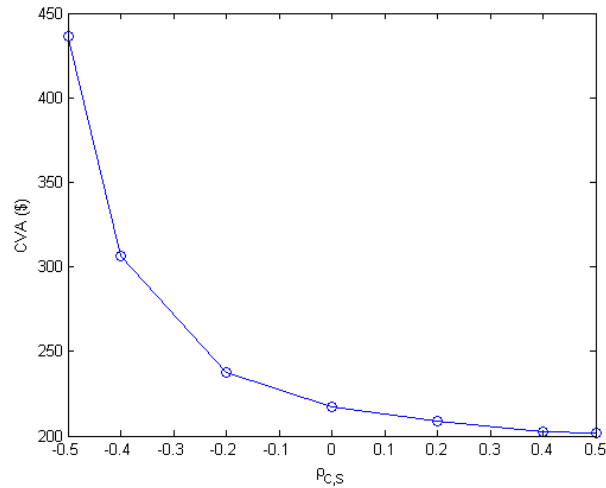


Figure 4.6.10: The CVA of a cash-settled Bermudan swaption with 10-year maturity and 1-year lockout period on 28th April 2014. $K = 1\%$, $N = \$100000$, $\rho_{C,S} = \{-0.5, -0.4, -0.2, 0, 0.2, 0.4, 0.5\}$.

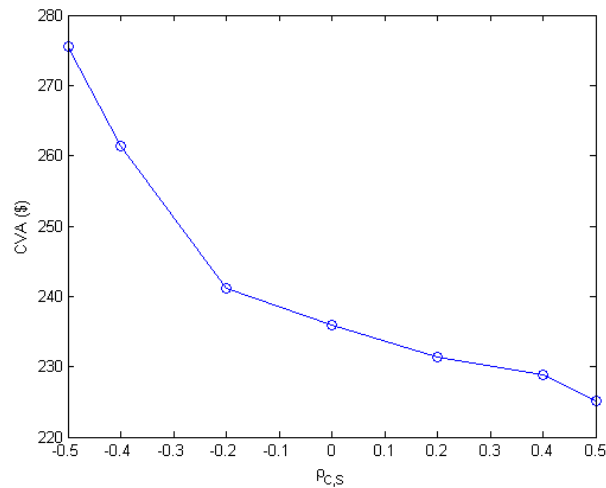


Figure 4.6.11: The CVA of a cash-settled Bermudan swaption with 10-year maturity and 5-year lockout period on 28th April 2014. $K = 1\%$, $N = \$100000$, $\rho_{C,S} = \{-0.5, -0.4, -0.2, 0, 0.2, 0.4, 0.5\}$.

with a constant volatility parameter for all maturities. The standard Least-Square regression method is then used to obtain the optimal exercise boundary of the Bermudan swaptions.

Next, we introduce the counterparty default model which is able to capture wrong way/right way risk in an explicit manner. Specifically, we follow Davis and Pistorius (2010) to model the default time as the first time the credit index process crosses zero, where the

random starting point, the drift and volatility function of the credit index process are properly characterized as the solution to the corresponding inverse first-passage time problem such that the default time distribution implied by the model is consistent with the ones implied from the market CDS quotes. Conditional on default at a particular time, the credit index process can be simulated in terms of a three dimensional Bessel bridge. The asset-credit correlation is imposed onto the evolution of the credit index process and the forward basis spreads. Numerical examples of cash-settle Bermudan swaptions have been studied and it is shown the wrong way/right way risk could lead to significant adjustment in the value of expected positive exposures and CVAs. It can be shown in the numerical examples that when the Libor-OIS spread is high the impact of negative asset-credit correlation is evident and this is a very desirable modelling feature during periods of market stress as the exposure profiles and CVA will be more sensitive to the widening of Libor-OIS spreads. Future extensions of have distinct spread dynamics can be incorporated, which offers a comprehensive approach to capture the impact of Libor-OIS spreads of various tenors. Furthermore, the impact of asset-credit correlation on CVA of Bermudan swaptions of various maturities and lock-out periods under multi-curve framework is analyzed and it is shown that wrong way risk could increase the CVA charge significantly and this is especially true at portfolio level with high notionals of the trades.

Chapter 5

Conclusion

In this thesis, we study counterparty risk modelling of fixed income derivatives with a specific focus on wrong way risk.

In Chapter 2, we have developed a joint model for the exchange rate and counterparty default risk based on Davis and Pistorius (2010), which enables us to capture unilateral wrong way/right way risk of FX forward and cross currency swap trades given an exogenously specified set of exchange rate-credit correlation scenarios. Compared to the canonical Hull and White (2001) approach, our model can be calibrated exactly to the market implied default probabilities without having to numerically bootstrapp a default barrier. Our joint FX-Hull-White hybrid modelling framework can be easily extended to incorporate correlation structures between interest rates and counterparty credit quality. Numerical examples of expected positive exposures and potential future exposures with wrong way/right way risk embedded show that FX-credit correlation can have a significant impact on counterparty risk quantifications than traditional models which treat wrong way/right way risk often implicitly, as they can increase or decrease expected positive exposures and potential future exposures.

In Chapter 3, in light of empirical evidences that both counterparty of a trade may default, we naturally extend our joint FX-credit default model to the bilateral version.

An efficient way of jointly simulating the credit index processes of two counterparties is proposed where no identification of the conditional first-to-default joint distribution of the two-dimensional time-changed Brownian motion with drifts is required. Under the bilateral framework, the FX-credit correlations with both counterparties and the default correlation between the two counterparties can be easily incorporated and their impact can be quantified through EPE calculation of cross currency swaps against a range of correlation scenarios. As shown, based on the perspective of each counterparty, the three correlations may have counterbalancing effects in EPEs and ENEs, which provides a delicate tool for CVA and DVA calculations.

Finally, in Chapter 4, we consider our unilateral default model together with a multi-curve interest rate model with stochastic basis spreads to formulate a framework for Bermudan swaptions CVA calculations with wrong way/right way risk embedded. The interest rate framework is built in terms of a Hull-White short rate dynamics capturing the evolution of the overnight-index-swap (OIS) rate and a one-factor lognormal process with zero drift to model the stochastic Libor-OIS basis spreads, such that the Libor rate is expressed as the sum of the two. Since the Libor-OIS spread is a measure of liquidity and credit risk in the interbank market, the wrong way correlation is imposed between the credit index process and the forward Libor-OIS spread. Our approach is the first to incorporate wrong way/right way risk in the calculation of CVA of Bermudan swaptions under the post-crisis multi-curve interest rate framework. The model is applied to calculate CVAs of Bermudan swaptions with different maturities and lock-out periods and wrong way/right way risk are properly quantified against various correlation scenarios.

Appendix A

Histograms of EPEs and ENEs in Chapter 3

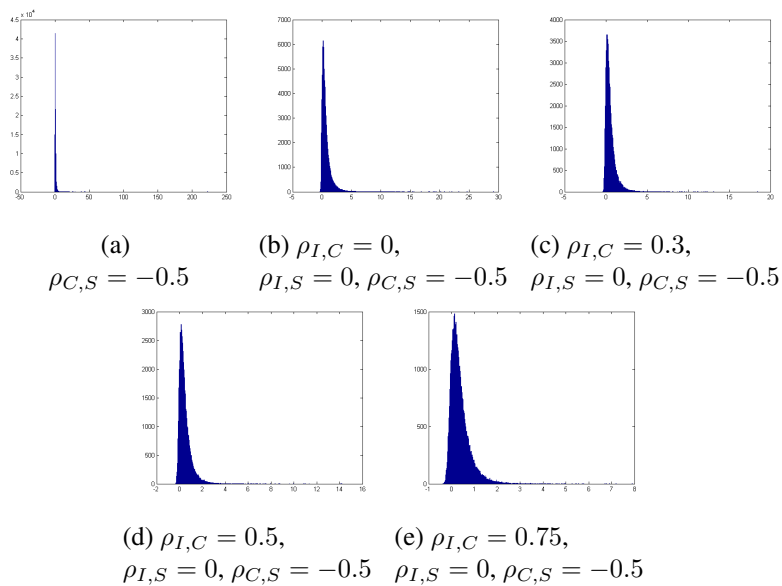


Figure A.0.1: Histograms of the exposures of the 5-year fixed-for-fixed USDJPY cross currency swap from the point of view of Daiwa Securities conditional on first-to-default of Nomura Securities at $t = 2.5$ (years). Unilateral Case: $\rho_{C,S} = -0.5$. Bilateral Case: $\rho_{C,S} = -0.5, \rho_{I,S} = 0, \rho_{I,C} = \{0, 0.3, 0.5, 0.75\}$.

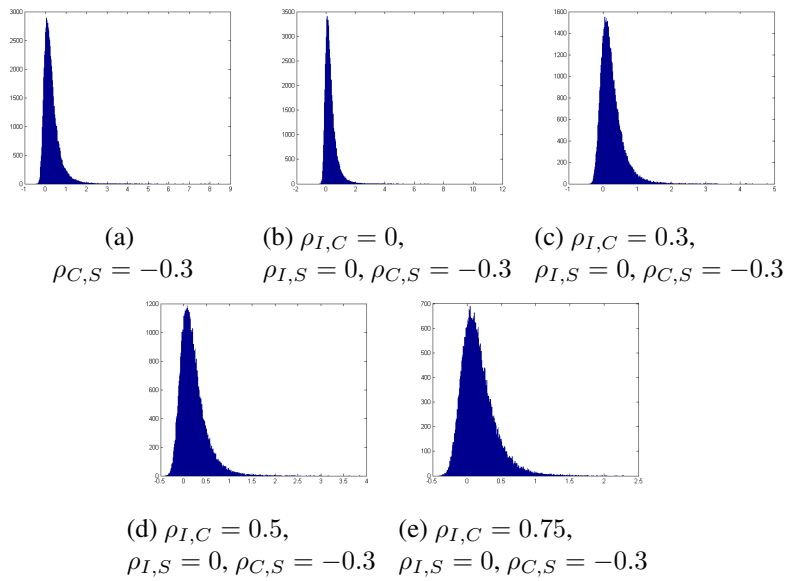


Figure A.0.2: Histograms of the exposures of the 5-year fixed-for-fixed USDJPY cross currency swap from the point of view of Daiwa Securities conditional on first-to-default of Nomura Securities at $t = 2.5$ (years). Unilateral Case: $\rho_{C,S} = -0.3$. Bilateral Case: $\rho_{C,S} = -0.3, \rho_{I,S} = 0, \rho_{I,C} = \{0, 0.3, 0.5, 0.75\}$.

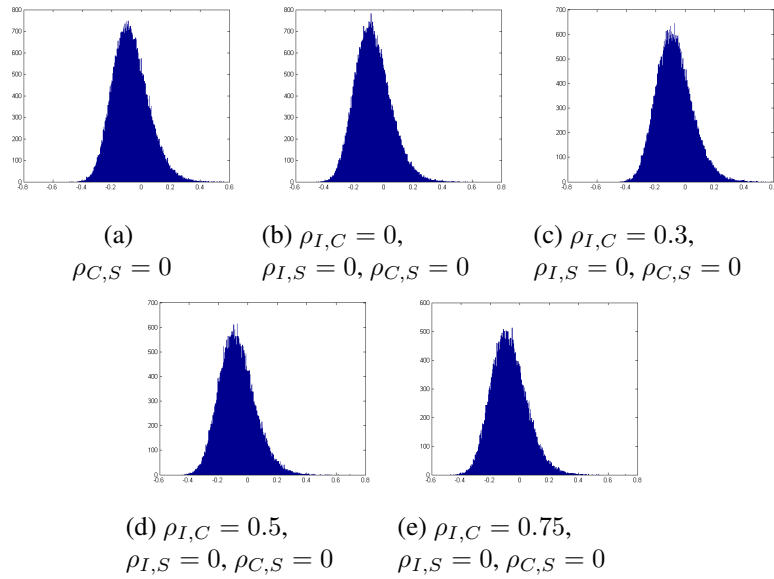


Figure A.0.3: Histograms of the exposures of a 5-year fixed-for-fixed USDJPY cross currency swap conditional on first-to-default of Nomura Securities at $t = 2.5$ (years) observed on 28th April 2014. Unilateral Case: $\rho_{C,S} = 0$. Bilateral Case: $\rho_{C,S} = 0, \rho_{I,S} = 0, \rho_{I,C} = \{0, 0.3, 0.5, 0.75\}$.

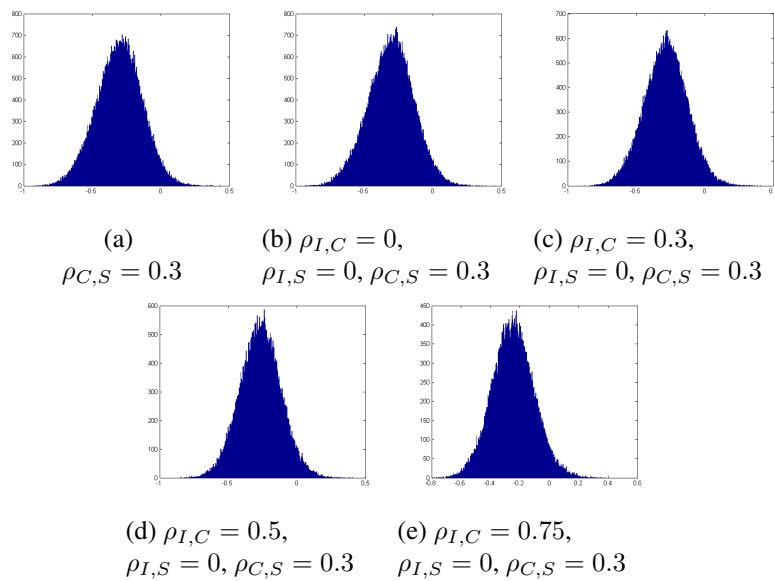


Figure A.0.4: Histograms of the exposures of a 5-year fixed-for-fixed USDJPY cross currency swap conditional on first-to-default of Nomura Securities at $t = 2.5$ (years) observed on 28th April 2014. Unilateral Case: $\rho_{C,S} = 0.3$. Bilateral Case: $\rho_{C,S} = 0.3, \rho_{I,S} = 0, \rho_{I,C} = \{0, 0.3, 0.5, 0.75\}$.

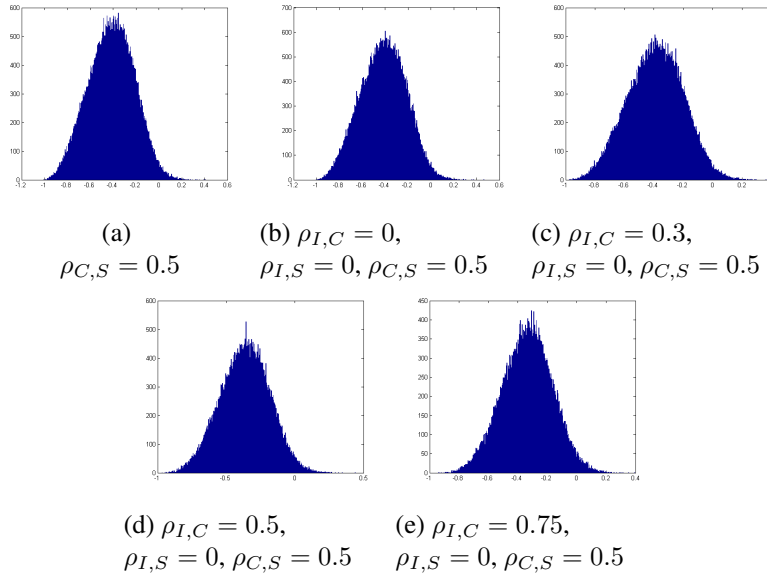


Figure A.0.5: Histograms of the exposures of a 5-year fixed-for-fixed USDJPY cross currency swap conditional on first-to-default of Nomura Securities at $t = 2.5$ (years) observed on 28th April 2014. Unilateral Case: $\rho_{C,S} = 0.5$. Bilateral Case: $\rho_{C,S} = 0.5$, $\rho_{I,S} = 0$, $\rho_{I,C} = \{0, 0.3, 0.5, 0.75\}$.

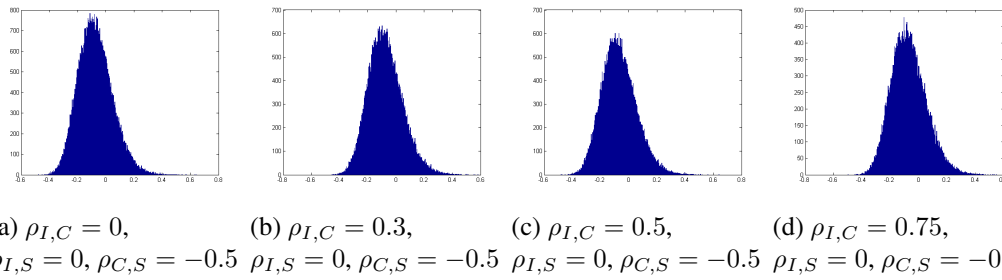


Figure A.0.6: Histograms of the exposures of a 5-year fixed-for-fixed USDJPY cross currency swap conditional on first-to-default of Daiwa Securities at $t = 2.5$ (years) observed on 28th April 2014. $\rho_{C,S} = -0.5$, $\rho_{I,S} = 0$, $\rho_{I,C} = \{0, 0.3, 0.5, 0.75\}$.

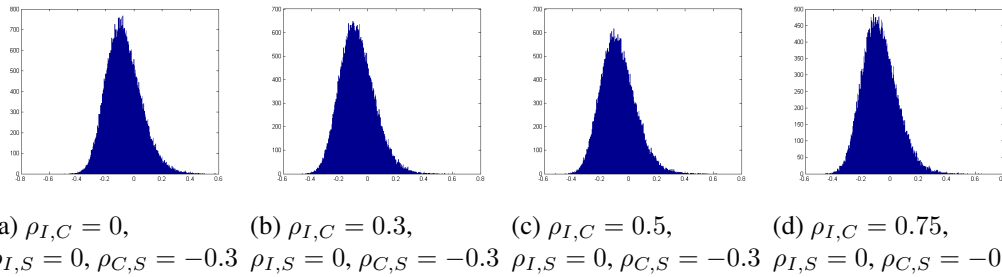
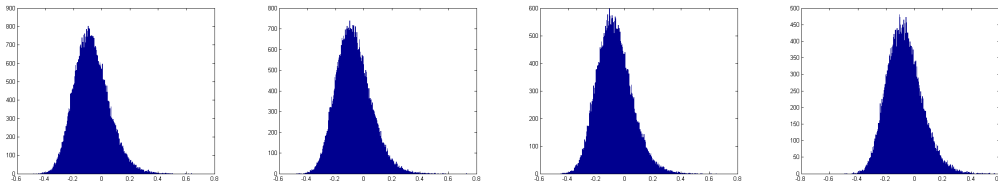
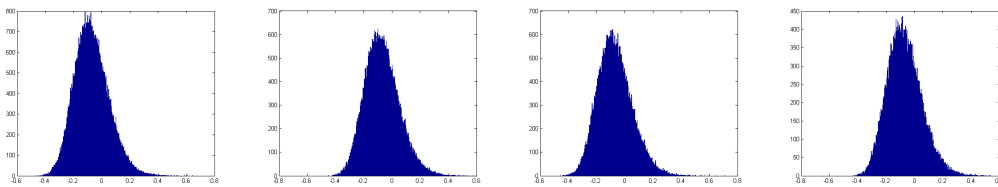


Figure A.0.7: Histograms of the exposures of a 5-year fixed-for-fixed USDJPY cross currency swap conditional on first-to-default of Nomura Securities at $t = 2.5$ (years) observed on 28th April 2014. $\rho_{C,S} = -0.3$, $\rho_{I,S} = 0$, $\rho_{I,C} = \{0, 0.3, 0.5, 0.75\}$.



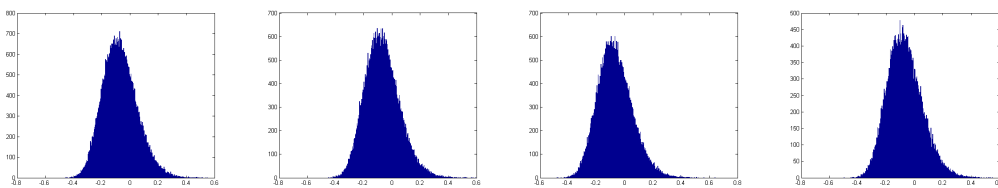
(a) $\rho_{I,C} = 0,$
 $\rho_{I,S} = 0, \rho_{C,S} = 0$ (b) $\rho_{I,C} = 0.3,$
 $\rho_{I,S} = 0, \rho_{C,S} = 0$ (c) $\rho_{I,C} = 0.5,$
 $\rho_{I,S} = 0, \rho_{C,S} = 0$ (d) $\rho_{I,C} = 0.75,$
 $\rho_{I,S} = 0, \rho_{C,S} = 0$

Figure A.0.8: Histograms of the exposures of a 5-year fixed-for-fixed USDJPY cross currency swap conditional on first-to-default of Nomura Securities at $t = 2.5$ (years) observed on 28th April 2014. $\rho_{C,S} = 0, \rho_{I,S} = 0, \rho_{I,C} = \{0, 0.3, 0.5, 0.75\}$.



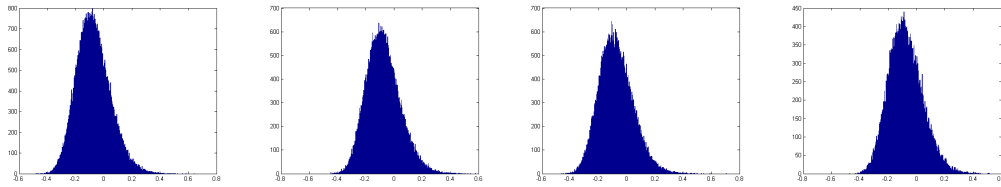
(a) $\rho_{I,C} = 0,$
 $\rho_{I,S} = 0, \rho_{C,S} = 0.3$ (b) $\rho_{I,C} = 0.3,$
 $\rho_{I,S} = 0, \rho_{C,S} = 0.3$ (c) $\rho_{I,C} = 0.5,$
 $\rho_{I,S} = 0, \rho_{C,S} = 0.3$ (d) $\rho_{I,C} = 0.75,$
 $\rho_{I,S} = 0, \rho_{C,S} = 0.3$

Figure A.0.9: Histograms of the exposures of a 5-year fixed-for-fixed USDJPY cross currency swap conditional on first-to-default of Daiwa Securities at $t = 2.5$ (years) observed on 28th April 2014. $\rho_{C,S} = 0, \rho_{I,S} = -0.3, \rho_{I,C} = \{0, 0.3, 0.5, 0.75\}$.



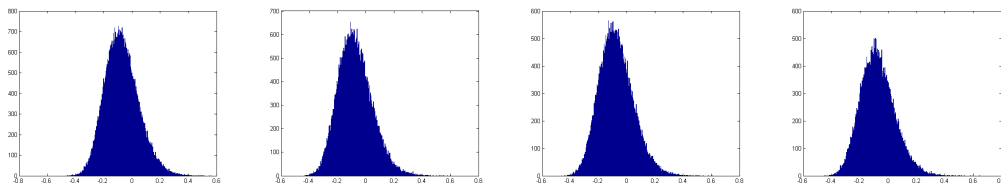
(a) $\rho_{I,C} = 0,$
 $\rho_{I,S} = 0, \rho_{C,S} = 0.5$ (b) $\rho_{I,C} = 0.3,$
 $\rho_{I,S} = 0, \rho_{C,S} = 0.5$ (c) $\rho_{I,C} = 0.5,$
 $\rho_{I,S} = 0, \rho_{C,S} = 0.5$ (d) $\rho_{I,C} = 0.75,$
 $\rho_{I,S} = 0, \rho_{C,S} = 0.5$

Figure A.0.10: Histograms of the exposures of a 5-year fixed-for-fixed USDJPY cross currency swap conditional on first-to-default of Daiwa Securities at $t = 2.5$ (years) observed on 28th April 2014. $\rho_{C,S} = 0, \rho_{I,S} = 0, \rho_{I,C} = \{0, 0.3, 0.5, 0.75\}$.



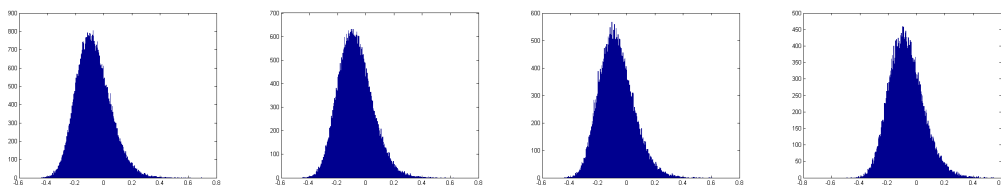
(a) $\rho_{I,C} = 0$, $\rho_{I,S} = -0.5$, $\rho_{C,S} = 0$ (b) $\rho_{I,C} = 0.3$, $\rho_{I,S} = -0.5$, $\rho_{C,S} = 0$ (c) $\rho_{I,C} = 0.5$, $\rho_{I,S} = -0.5$, $\rho_{C,S} = 0$ (d) $\rho_{I,C} = 0.75$, $\rho_{I,S} = -0.5$, $\rho_{C,S} = 0$

Figure A.0.11: Histograms of the exposures of a 5-year fixed-for-fixed USDJPY cross currency swap conditional on first-to-default of Daiwa Securities at $t = 2.5$ (years) observed on 28th April 2014. $\rho_{C,S} = 0$, $\rho_{I,S} = -0.5$, $\rho_{I,C} = \{0, 0.3, 0.5, 0.75\}$.



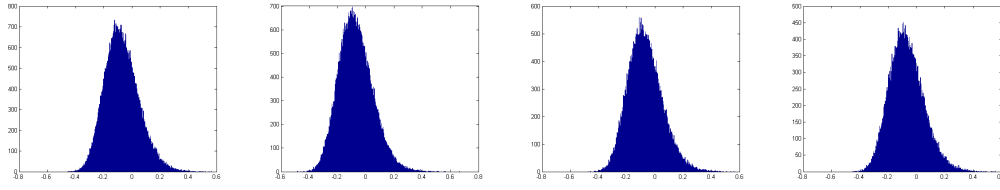
(a) $\rho_{I,C} = 0$, $\rho_{I,S} = -0.3$, $\rho_{C,S} = 0$ (b) $\rho_{I,C} = 0.3$, $\rho_{I,S} = -0.3$, $\rho_{C,S} = 0$ (c) $\rho_{I,C} = 0.5$, $\rho_{I,S} = -0.3$, $\rho_{C,S} = 0$ (d) $\rho_{I,C} = 0.75$, $\rho_{I,S} = -0.3$, $\rho_{C,S} = 0$

Figure A.0.12: Histograms of the exposures of a 5-year fixed-for-fixed USDJPY cross currency swap conditional on first-to-default of Daiwa Securities at $t = 2.5$ (years) observed on 28th April 2014. $\rho_{C,S} = 0$, $\rho_{I,S} = -0.3$, $\rho_{I,C} = \{0, 0.3, 0.5, 0.75\}$.



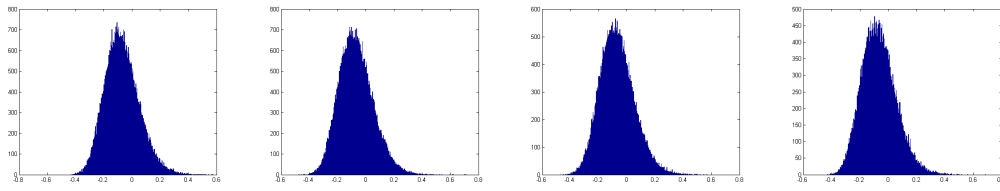
(a) $\rho_{I,C} = 0$, $\rho_{I,S} = 0$, $\rho_{C,S} = 0$ (b) $\rho_{I,C} = 0.3$, $\rho_{I,S} = 0$, $\rho_{C,S} = 0$ (c) $\rho_{I,C} = 0.5$, $\rho_{I,S} = 0$, $\rho_{C,S} = 0$ (d) $\rho_{I,C} = 0.75$, $\rho_{I,S} = 0$, $\rho_{C,S} = 0$

Figure A.0.13: Histograms of the exposures of a 5-year fixed-for-fixed USDJPY cross currency swap conditional on first-to-default of Daiwa Securities at $t = 2.5$ (years) observed on 28th April 2014. $\rho_{C,S} = 0$, $\rho_{I,S} = 0$, $\rho_{I,C} = \{0, 0.3, 0.5, 0.75\}$.



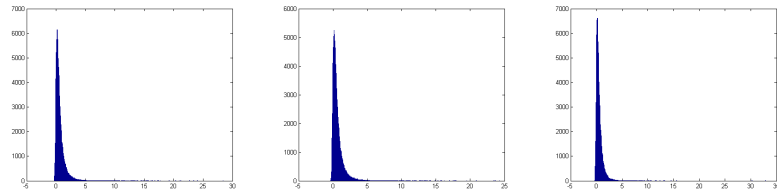
(a) $\rho_{I,C} = 0$, $\rho_{I,S} = 0.3, \rho_{C,S} = 0$ (b) $\rho_{I,C} = 0.3$, $\rho_{I,S} = 0.3, \rho_{C,S} = 0$ (c) $\rho_{I,C} = 0.5$, $\rho_{I,S} = 0.3, \rho_{C,S} = 0$ (d) $\rho_{I,C} = 0.75$, $\rho_{I,S} = 0.3, \rho_{C,S} = 0$

Figure A.0.14: Histograms of the exposures of a 5-year fixed-for-fixed USDJPY cross currency swap conditional on first-to-default of Daiwa Securities at $t = 2.5$ (years) observed on 28th April 2014. $\rho_{C,S} = 0, \rho_{I,S} = 0.3, \rho_{I,C} = \{0, 0.3, 0.5, 0.75\}$.

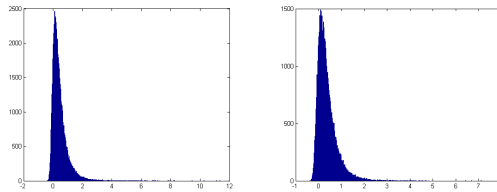


(a) $\rho_{I,C} = 0$, $\rho_{I,S} = 0.5, \rho_{C,S} = 0$ (b) $\rho_{I,C} = 0.3$, $\rho_{I,S} = 0.5, \rho_{C,S} = 0$ (c) $\rho_{I,C} = 0.5$, $\rho_{I,S} = 0.5, \rho_{C,S} = 0$ (d) $\rho_{I,C} = 0.75$, $\rho_{I,S} = 0.5, \rho_{C,S} = 0$

Figure A.0.15: Histograms of the exposures of a 5-year fixed-for-fixed USDJPY cross currency swap conditional on first-to-default of Daiwa Securities at $t = 2.5$ (years) observed on 28th April 2014. $\rho_{C,S} = 0, \rho_{I,S} = 0.5, \rho_{I,C} = \{0, 0.3, 0.5, 0.75\}$.



(a) $\rho_{I,S} = -0.5$ (b) $\rho_{I,C} = 0$, $\rho_{I,S} = -0.5, \rho_{C,S} = 0$ (c) $\rho_{I,C} = 0.3$, $\rho_{I,S} = -0.5, \rho_{C,S} = 0$



(d) $\rho_{I,C} = 0.5$, $\rho_{I,S} = -0.5, \rho_{C,S} = 0$ (e) $\rho_{I,C} = 0.75$, $\rho_{I,S} = -0.5, \rho_{C,S} = 0$

Figure A.0.16: Histograms of the exposures of a 5-year fixed-for-fixed USDJPY cross currency swap conditional on first-to-default of Daiwa Securities at $t = 2.5$ (years) observed on 28th April 2014. Unilateral Case: $\rho_{I,S} = -0.5$. Bilateral Case: $\rho_{C,S} = 0, \rho_{I,S} = -0.5, \rho_{I,C} = \{0, 0.3, 0.5, 0.75\}$.

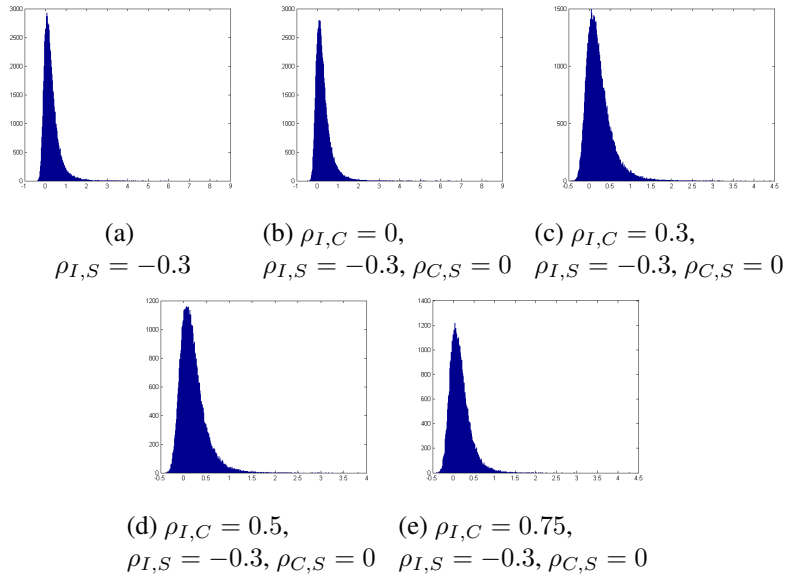


Figure A.0.17: Histograms of the exposures of a 5-year fixed-for-fixed USDJPY cross currency swap conditional on first-to-default of Daiwa Securities at $t = 2.5$ (years) observed on 28th April 2014. Unilateral Case: $\rho_{I,S} = -0.3$. Bilateral Case: $\rho_{C,S} = 0, \rho_{I,S} = -0.3, \rho_{I,C} = \{0, 0.3, 0.5, 0.75\}$.

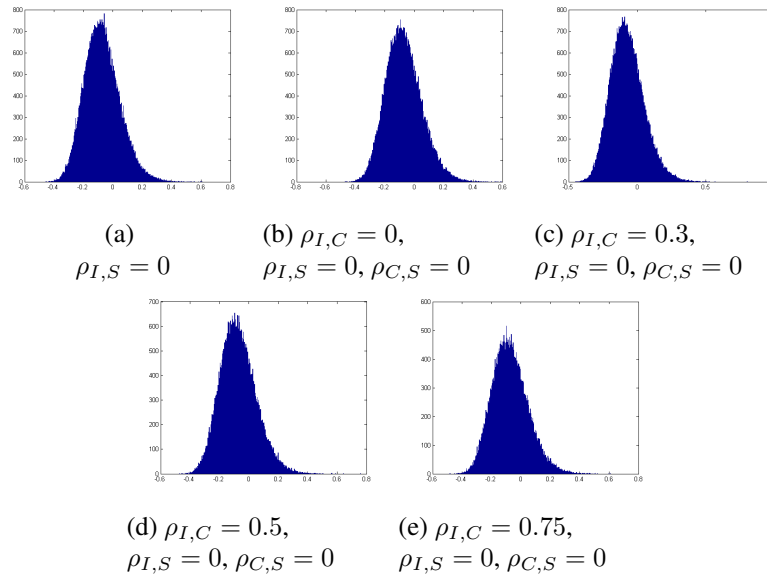


Figure A.0.18: Histograms of the exposures of a 5-year fixed-for-fixed USDJPY cross currency swap conditional on first-to-default of Daiwa Securities at $t = 2.5$ (years) observed on 28th April 2014. Unilateral Case: $\rho_{I,S} = 0$. Bilateral Case: $\rho_{C,S} = 0, \rho_{I,S} = 0, \rho_{I,C} = \{0, 0.3, 0.5, 0.75\}$.

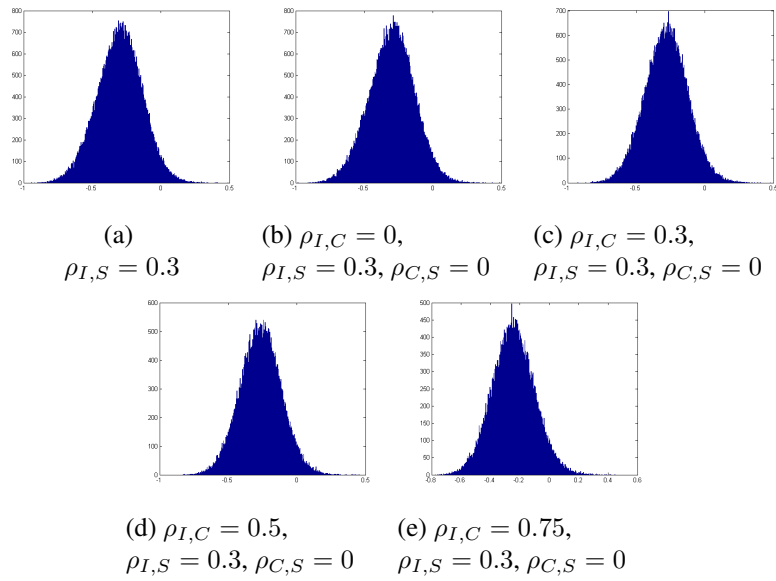


Figure A.0.19: Histograms of the exposures of a 5-year fixed-for-fixed USDJPY cross currency swap conditional on first-to-default of Daiwa Securities at $t = 2.5$ (years) observed on 28th April 2014. Unilateral Case: $\rho_{I,S} = 0.3$. Bilateral Case: $\rho_{C,S} = 0$, $\rho_{I,S} = 0.3$, $\rho_{I,C} = \{0, 0.3, 0.5, 0.75\}$.

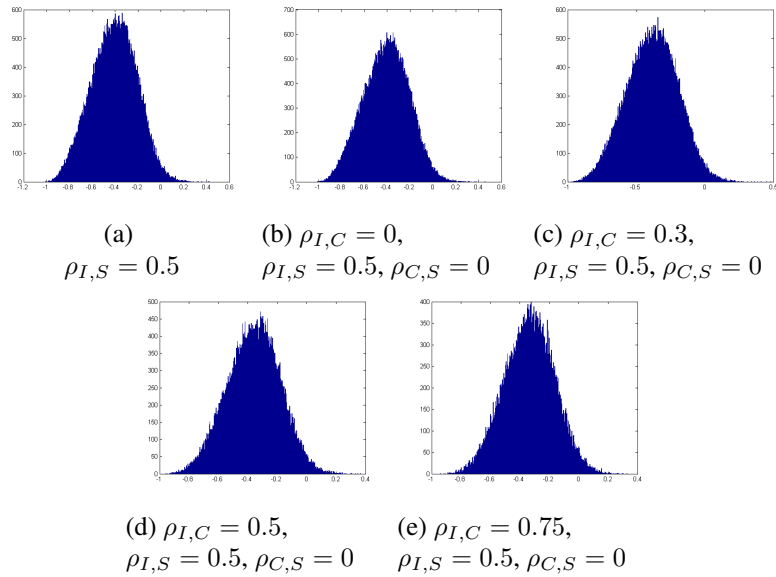


Figure A.0.20: Histograms of the exposures of a 5-year fixed-for-fixed USDJPY cross currency swap conditional on first-to-default of Daiwa Securities at $t = 2.5$ (years) observed on 28th April 2014. Unilateral Case: $\rho_{C,S} = 0.5$. Bilateral Case: $\rho_{C,S} = 0$, $\rho_{I,S} = 0.5$, $\rho_{I,C} = \{0, 0.3, 0.5, 0.75\}$.

Bibliography

- Abramowitz, M. and Stegun, I. A. (1964). *Handbook of mathematical functions: with formulas, graphs, and mathematical tables*, volume 55. Courier Corporation.
- Albanese, C., Bellaj, T., Gimonet, G., and Pietronero, G. (2011). Coherent global market simulations and securitization measures for counterparty credit risk. *Quantitative Finance*, 11(1):1–20.
- Albanese, C., Brigo, D., and Oertel, F. (2013). Restructuring counterparty credit risk. *International Journal of Theoretical and Applied Finance*, 16(02):1350010.
- Ametrano, F. M. and Bianchetti, M. (2009). Bootstrapping the illiquidity: multiple yield curves construction for market coherent forward rates estimation. *Risk Books, Incisive Media*.
- Andersen, L. B. and Piterbarg, V. (2010). *Interest rate modeling*, volume 1. Atlantic Financial Press London.
- Arora, N., Gandhi, P., and Longstaff, F. A. (2012). Counterparty credit risk and the credit default swap market. *Journal of Financial Economics*, 103(2):280–293.
- Avellaneda, M. and Zhu, J. (2001). Distance to default. *Risk*, 14(12):125–129.
- Ballotta, L. and Fusai, G. (2014). Counterparty credit risk in a multivariate structural model with jumps. *Available at SSRN 2212813*.
- Basel (2010). Basel III: A global regulatory framework for more resilient banks and banking systems. *Basel Committee on Banking Supervision, Basel*.

- Baxter, M. (2007). Lévy simple structural models. *International Journal of Theoretical and Applied Finance*, 10(04):593–606.
- Bertoin, J., Pitman, J., and de Chavez, J. R. (1999). Constructions of a Brownian path with a given minimum. *Electron. Comm. Probab*, 4(1999):31–37.
- Bianchetti, M. (2010). Two curves, one price. *Risk*, 23(8):66–72.
- Bielecki, T. R. and Rutkowski, M. (2002). *Credit risk: modeling, valuation and hedging*. Springer Science & Business Media.
- Black, F. and Cox, J. C. (1976). Valuing corporate securities: some effects of bond indenture provisions. *The Journal of Finance*, 31(2):351–367.
- Blanchet-Scalliet, C., Patras, F., Bielecki, T. R., Brigo, D., and Patras, F. (2011). Structural counterparty risk valuation for credit default swaps. *Credit risk frontiers: subprime crisis, pricing and hedging, CVA, MBS, ratings, and liquidity*, pages 437–455.
- Böcker, K. and Brunnbauer, M. (2014). Path-consistent wrong-way risk. *Risk*, 19(1):49–53.
- Boenkost, W. and Schmidt, W. M. (2005). Cross currency swap valuation. *Available at SSRN 1375540*.
- Boenkost, W. and Schmidt, W. M. (2015). CVA/DVA wrong way risk put into practice. *Available at SSRN 2431162*.
- Boukhobza, A. and Maetz, J. (2012). CVA, wrong way risk, hedging and bermudan swaption. *mpra.ub.uni-muenchen.de*.
- Brigo, D. and Alfonsi, A. (2005). Credit default swap calibration and derivatives pricing with the SSRD stochastic intensity model. *Finance and Stochastics*, 9(1):29–42.
- Brigo, D., Buescu, C., and Morini, M. (2011a). Impact of the first to default time on bilateral CVA. *Available at SSRN 1868853*.
- Brigo, D. and Capponi, A. (2010). Bilateral counterparty risk with application to CDSs. *Risk*, 23(3):85–90.

- Brigo, D. and Chourdakis, K. (2009). Counterparty risk for credit default swaps: impact of spread volatility and default correlation. *International Journal of Theoretical and Applied Finance*, 12(07):1007–1026.
- Brigo, D. and Masetti, M. (2006). *Counterparty credit risk modeling: risk management, pricing and regulation*. Risk Books London.
- Brigo, D. and Mercurio, F. (2007). *Interest rate models: theory and practice: with smile, inflation and credit*. Springer Science & Business Media.
- Brigo, D. and Morini, M. (2006). Structural credit calibration. *Risk*, 19(4):78–83.
- Brigo, D., Morini, M., and Pallavicini, A. (2013). *Counterparty credit risk, collateral and funding: with pricing cases for all asset classes*. John Wiley & Sons.
- Brigo, D., Morini, M., Tarengi, M., Bielecki, T. R., and Patras, F. (2011b). Credit calibration with structural models and equity return swap valuation under counterparty risk. *Credit risk frontiers: subprime crisis, pricing and hedging, CVA, MBS, ratings, and liquidity*, pages 457–484.
- Brigo, D. and Pallavicini, A. (2008). Counterparty risk and CCDSs under correlation. *Risk*, 21(2):46–51.
- Brigo, D., Pallavicini, A., and Papatheodorou, V. (2011c). Arbitrage-free valuation of bilateral counterparty risk for interest-rate products: impact of volatilities and correlations. *International Journal of Theoretical and Applied Finance*, 14(06):773–802.
- Brigo, D. and Tarengi, M. (2005). Credit default swap calibration and counterparty risk valuation with a scenario based first passage model. *Available at SSRN 683160*.
- Canabarro, E. and Duffie, D. (2003). Measuring and marking counterparty risk, Chapter 9 of *Asset/Liability Management of Financial Institutions*.
- Cariboni, J. and Schoutens, W. (2007). Pricing credit default swaps under Lévy models. *Journal of Computational Finance*, 10(4):71–91.

- Carr, P. and Ghamami, S. (2015). Derivatives pricing under bilateral counterparty risk. Available at SSRN 2588487.
- Carriere, J. F. (1996). Valuation of the early-exercise price for options using simulations and nonparametric regression. *Insurance: Mathematics and Economics*, 19(1):19–30.
- Cesari, G., Aquilina, J., Charpillon, N., Filipovic, Z., Lee, G., and Manda, I. (2009). *Modelling, pricing, and hedging counterparty credit exposure: a technical guide*. Springer Science & Business Media.
- Cespedes, J. C. G., de Juan Herrero, J. A., Rosen, D., and Saunders, D. (2010). Effective modeling of wrong way risk, counterparty credit risk capital, and alpha in basel II. *The Journal of Risk Model Validation*, 4(1):71–98.
- Chen, X., Cheng, L., Chadam, J., Saunders, D., et al. (2011). Existence and uniqueness of solutions to the inverse boundary crossing problem for diffusions. *The Annals of Applied Probability*, 21(5):1663–1693.
- Cheng, L., Chen, X., Chadam, J., and Saunders, D. (2006). Analysis of an inverse first passage problem from risk management. *SIAM Journal on Mathematical Analysis*, 38(3):845–873.
- Cherubini, U. (2013). Credit valuation adjustment and wrong way risk. *Quantitative Finance Letters*, 1(1):9–15.
- Chibane, M. and Sheldon, G. (2009). Building curves on a good basis. Available at <http://ssrn.com/abstract=1394267>.
- Chung, S.-L., Kao, C.-W., Wu, C., and Yeh, C.-Y. (2015). Counterparty credit risk in the municipal bond market. *The Journal of Fixed Income*, 25(1):7–33.
- Crépey, S., Grbac, Z., Ngor, N., and Skovmand, D. (2015). A Lévy HJM multiple-curve model with application to CVA computation. *Quantitative Finance*, 15(3):401–419.
- Crépey, S., Grbac, Z., and Nguyen, H.-N. (2012). A multiple-curve HJM model of interbank risk. *Mathematics and Financial Economics*, 6(3):155–190.

- Crépey, S., Macrina, A., Nguyen, T. M., and Skovmand, D. (2016). Rational multi-curve models with counterparty-risk valuation adjustments. *Quantitative Finance*, 16(6):847–866.
- D’amico, G., Manca, R., and Salvi, G. (2014). Bivariate semi-Markov process for counterparty credit risk. *Communications in Statistics-Theory and Methods*, 43(7):1503–1522.
- Davis, M. and Pistorius, M. (2010). Quantification of counterparty risk via Bessel bridges. *Available at SSRN 1722604*.
- Davis, M. and Pistorius, M. (2015). Explicit solution of an inverse first-passage time problem for Levy processes and counterparty credit risk. *The Annals of Applied Probability*, 25(5):2383–2415.
- De Graaf, C. S., Feng, Q., Kandhai, D., and Oosterlee, C. W. (2014). Efficient computation of exposure profiles for counterparty credit risk. *International Journal of Theoretical and Applied Finance*, 17(04):1450024.
- Duffie, D. and Zhu, H. (2011). Does a central clearing counterparty reduce counterparty risk? *The Review of Asset Pricing Studies*, 1(1):74–95.
- El Hajjaji, O. and Subbotin, A. (2015). CVA with wrong way risk: sensitivities, volatility and hedging. *International Journal of Theoretical and Applied Finance*, 18(3):155–170.
- Ettinger, B., Evans, S. N., Hening, A., et al. (2014). Killed Brownian motion with a prescribed lifetime distribution and models of default. *The Annals of Applied Probability*, 24(1):1–33.
- Finger, C. C. (2000). Toward a better estimation of wrong-way credit exposure. *The Journal of Risk Finance*, 1(3):43–51.
- Fiorani, F., Luciano, E., and Semeraro, P. (2010). Single and joint default in a structural model with purely discontinuous asset prices. *Quantitative Finance*, 10(3):249–263.
- Frey, R. and Sommer, D. (1996). A systematic approach to pricing and hedging international

- derivatives with interest rate risk: analysis of international derivatives under stochastic interest rates. *Applied Mathematical Finance*, 3(4):295–317.
- Fujii, M., Shimada, Y., and Takahashi, A. (2011). A market model of interest rates with dynamic basis spreads in the presence of collateral and multiple currencies. *Wilmott*, 2011(54):61–73.
- Gençay, R., Signori, D., Xue, Y., Yu, X., and Zhang, K. (2015). Economic links and credit spreads. *Journal of Banking & Finance*, 55:157–169.
- Ghamami, S. and Carr, P. (2015). Derivatives pricing under bilateral counterparty risk. *Available at SSRN 2588487*.
- Ghamami, S. and Goldberg, L. R. (2014). Stochastic intensity models of wrong way risk: wrong way CVA need not exceed independent CVA. *Available at SSRN 2479520*.
- Glasserman, P. and Yang, L. (2015). Bounding wrong-way risk in measuring counterparty risk. *Available at SSRN 2648495*.
- Glasserman, P., Yu, B., et al. (2004). Number of paths versus number of basis functions in American option pricing. *The Annals of Applied Probability*, 14(4):2090–2119.
- Gregory, J. (2009). Being two-faced over counterparty credit risk. *Risk*, 22(2):86–90.
- Gregory, J. (2010). *Counterparty credit risk: the new challenge for global financial markets*, volume 470. John Wiley & Sons.
- Grzelak, L. A. and Oosterlee, C. W. (2011). On the Heston model with stochastic interest rates. *SIAM Journal on Financial Mathematics*, 2(1):255–286.
- Haworth, H., Reisinger, C., and Shaw, W. (2008). Modelling bonds and credit default swaps using a structural model with contagion. *Quantitative Finance*, 8(7):669–680.
- Heath, D., Jarrow, R., and Morton, A. (1992). Bond pricing and the term structure of interest rates: a new methodology for contingent claims valuation. *Econometrica: Journal of the Econometric Society*, 60(1):77–105.

- Henrard, M. (2007). The irony in the derivatives discounting. *Wilmott Magazine*, 1(4):92–98.
- Henrard, M. (2010). The irony in the derivatives discounting part II: the crisis. *Wilmott Magazine*, 2(6):301316.
- Henrard, M. (2013). Multi-curves framework with stochastic spread: a coherent approach to stir futures and their options. *Available at SSRN 2230545*.
- Hull, J. and White, A. (2001). Valuing credit default swaps II: modelling default correlations. *Journal of Derivatives*, 8(3):12–22.
- Hull, J. and White, A. (2012). CVA and wrong way risk. *Financial Analysts Journal*, 68(5):58–69.
- Hunzinger, C. B. and Labuschagne, C. C. (2014). The Cox, Ross and Rubinstein tree model which includes counterparty credit risk and funding costs. *The North American Journal of Economics and Finance*, 29((2014)):200–217.
- Jacobs Jr, M. (2014). Supervisory requirements and expectations for portfolio level counterparty credit risk measurement and management. *Journal of Financial Regulation and Compliance*, 22(3):252–270.
- Jaimungal, S., Kreinin, A., and Valov, A. (2009). Integral equations and the first passage time of Brownian motions. *arXiv:0902.2569*.
- Jarrow, R. A. and Yu, F. (2001). Counterparty risk and the pricing of defaultable securities. *the Journal of Finance*, 56(5):1765–1799.
- Jorion, P. and Zhang, G. (2009). Credit contagion from counterparty risk. *The Journal of Finance*, 64(5):2053–2087.
- Kao, L.-J. (2016). Credit valuation adjustment of cap and floor with counterparty risk: a structural pricing model for vulnerable european options. *Review of Derivatives Research*, 19(1):41–64.

- Karlsson, P., Jain, S., and Oosterlee, C. W. (2014). Counterparty credit exposures for interest rate derivatives using the stochastic grid bundling method. *Available at SSRN 2538173*.
- Kenyon, C. (2010). Post shock short rate pricing. *Risk*, 23(11):83–87.
- Kim, I. J., Ramaswamy, K., and Sundaresan, S. (1993). Does default risk in coupons affect the valuation of corporate bonds?: a contingent claims model. *Financial Management*, 22(3):117–131.
- Kim, J. and Leung, T. (2016). Pricing derivatives with counterparty risk and collateralization: A fixed point approach. *European Journal of Operational Research*, 249(2):525–539.
- Klein, P. (1996). Pricing Black-Scholes options with correlated credit risk. *Journal of Banking & Finance*, 20(7):1211–1229.
- Klein, P. and Yang, J. (2013). Counterparty credit risk and american options. *The Journal of Derivatives*, 20(4):7–21.
- Lee, S. J. and Capriotti, L. (2015). Wrong way risk done right. *Risk*, 39(2):74–79.
- Leung, S. Y. and Kwok, Y. K. (2005). Credit default swap valuation with counterparty risk. *The Kyoto Economic Review*, 74(1):25–45.
- Li, M. and Mercurio, F. (2015). Jumping with default: wrong way risk modeling for credit valuation adjustment. *Available at SSRN 2605648*.
- Liang, X. and Dong, Y. (2014). A Markov chain copula model for credit default swaps with bilateral counterparty risk. *Communications in Statistics-Theory and Methods*, 43(3):498–514.
- Lipton, A. and Savescu, I. (2012). A structural approach to pricing credit default swaps with credit and debt value adjustments. *arXiv:1206.3104*.
- Lipton, A. and Savescu, I. (2013). CDSs, CVA and DVA-a structural approach. *Risk*, 26(4):60–65.

- Lipton, A. and Sepp, A. (2009). Credit value adjustment for credit default swaps via the structural default model. *The Journal of Credit Risk*, 5(2):127–150.
- Lipton, A. and Shelton, D. (2012). Credit default swaps with and without counterparty and collateral adjustments. *Stochastics: An International Journal of Probability and Stochastic Processes*, 84(5-6):603–624.
- Lo, C.-L., Lee, J.-P., and Yu, M.-T. (2013). Valuation of insurers' contingent capital with counterparty risk and price endogeneity. *Journal of Banking & Finance*, 37(12):5025–5035.
- Longstaff, F. A. and Schwartz, E. S. (1995). A simple approach to valuing risky fixed and floating rate debt. *The Journal of Finance*, 50(3):789–819.
- Longstaff, F. A. and Schwartz, E. S. (2001). Valuing American options by simulation: a simple least-squares approach. *Review of Financial studies*, 14(1):113–147.
- Loon, Y. C. and Zhong, Z. K. (2014). The impact of central clearing on counterparty risk, liquidity, and trading: evidence from the credit default swap market. *Journal of Financial Economics*, 112(1):91–115.
- Mahul, O. and David Cummins, J. (2008). Hedging under counterparty credit uncertainty. *Journal of Futures Markets*, 28(3):248–263.
- Meissner, G., Rooder, S., and Fan, K. (2013). The impact of different correlation approaches on valuing credit default swaps with counterparty risk. *Quantitative Finance*, 13(12):1903–1913.
- Mercurio, F. (2009). Interest rates and the credit crunch: new formulas and market models. *Bloomberg Portfolio Research Paper No. 2010-01-FRONTIERS*, (2010-01).
- Mercurio, F. (2010). Libor market models with stochastic basis. *Bloomberg Education and Quantitative Research Paper No. 2010-05-FRONTIERS*, (2010-05).
- Mercurio, F. and Xie, Z. (2012). The basis goes stochastic. *Risk*, 25(12):78–83.

- Merton, R. C. (1974). On the pricing of corporate debt: the risk structure of interest rates*. *The Journal of Finance*, 29(2):449–470.
- Metzler, A. (2010). On the first passage problem for correlated Brownian motion. *Statistics & Probability Letters*, 80(5):277–284.
- Moreni, N. and Pallavicini, A. (2014). Parsimonious HJM modelling for multiple yield curve dynamics. *Quantitative Finance*, 14(2):199–210.
- Morini, M. (2009). Solving the puzzle in the interest rate market. *Available at SSRN 1506046*.
- Musiela, M. and Rutkowski, M. (2006). *Martingale methods in financial modelling*, volume 36. Springer Science & Business Media.
- O’Kane, D. (2011). *Modelling single-name and multi-name credit derivatives*, volume 573. John Wiley & Sons.
- Pallavicini, A. and Tarenghi, M. (2010). Interest rate modeling with multiple yield curves. *Available at SSRN 1629688*.
- Patras, F. (2006). A reflection principle for correlated defaults. *Stochastic Processes and Their Applications*, 116(4):690–698.
- Pelsser, A. (2000). *Efficient methods for valuing interest rate derivatives*. Springer Finance. Springer Science & Business Media, 1 edition.
- Peskir, G. (2002). On integral equation arising in the first-passage problem for Brownian motion. *Journal of Integral Equations and Applications*, 14(4):397–423.
- Picoult, E. (2005). Calculating and hedging exposure, credit value adjustment and economic capital for counterparty credit risk. Risk Books, London.
- Piterbarg, V. (2003). A practitioner’s guide to pricing and hedging callable libor exotics in forward libor models. *Journal of Computational Finance*, 8(2):65–117.
- Piterbarg, V. (2006). Smiling hybrids. *Risk*, 19(5):66–71.

- Pykhtin, M. (2012). General wrong way risk and stress calibration of exposure. *Journal of Risk Management in Financial Institutions*, 5(3):234–251.
- Pykhtin, M. and Rosen, D. (2010). Pricing counterparty risk at the trade level and CVA allocations. *FEDS Working Paper*, 6(4):3–38.
- Pykhtin, M. and Sokol, A. (2012). If a dealer defaulted, would anybody notice? *Global Derivatives Conference 2012*.
- Pykhtin, M. and Zhu, S. H. (2006). Measuring counterparty credit risk for trading products under basel II. *Risk Books*.
- Redon, C. (2006). Wrong way risk modelling. *Risk*, 19(4):90–95.
- Rogers, L. and Williams, D. (2000). Diffusions, Markov processes, and Martingales. Vol. 2. Itô calculus. Reprint of the second (1994) edition. Cambridge Mathematical Library.
- Rosen, D. and Saunders, D. (2012). CVA the wrong way. *Journal of Risk Management in Financial Institutions*, 5(3):252–272.
- Sacerdote, L., Tamborrino, M., and Zucca, C. (2016). First passage times of two-dimensional correlated diffusion processes: analytical and numerical methods. *Journal of Computational and Applied Mathematics*, 296(12):275–292.
- Schönbucher, P. J. (2003). *Credit derivatives pricing models: models, pricing and implementation*. John Wiley & Sons.
- Sengupta, R. and Tam, Y. M. (2008). The Libor-OIS spread as a summary indicator. *Economic Synopses*, 2008.
- Sepp, A. (2006). Extended credit grades model with stochastic volatility and jumps. *Wilmott Magazine*, 2(1):50–62.
- Shreve, S. E. (2004). *Stochastic calculus for finance II: continuous-time models*, volume 11. Springer Science & Business Media.

- Simaitis, S., de Graaf, C., Hari, N., and Kandhai, D. (2016). Smile and default: the role of stochastic volatility and interest rates in counterparty credit risk. *Quantitative Finance*, 16(11):1725–1740.
- Sippel, J. and Ohkoshi, S. (2002). All power to PRDC notes. *Risk*, 15(11):1–3.
- Taylor, J. B. and Williams, J. C. (2009). A black swan in the money market. *American Economic Journal: Macroeconomics*, 1(1):58–83.
- Teng, L., Ehrhardt, M., and Günther, M. (2013). Bilateral counterparty risk valuation of cds contracts with simultaneous defaults. *International Journal of Theoretical and Applied Finance*, 16(07):1350040.
- Thompson, J. R. (2010). Counterparty risk in financial contracts: Should the insured worry about the insurer? *The Quarterly Journal of Economics*, 125(3):1195–1252.
- Thornton, D. L. (2009). What the LIBOR-OIS spread says. *Economic Synopses*.
- Tuckman, B. and Porfirio, P. (2003). Interest rate parity, money market basis swaps, and cross-currency basis swaps. *Fixed income liquid markets research, Lehman Brothers*, 1.
- Turlakov, M. (2013). Wrong way risk, credit and funding. *Risk*, 26(3):69–71.
- Valuzis, M. (2008). On the probabilities of correlated defaults: a first passage time approach. *Nonlinear Analysis: Modeling and Control*, 13(1):117–133.
- Wehn, C., Hoppe, C., and Gregoriou, G. N. (2012). *Rethinking valuation and pricing models: lessons learned from the crisis and future challenges*. Academic Press.
- Zhou, C. (2001a). An analysis of default correlations and multiple defaults. *Review of Financial Studies*, 14(2):555–576.
- Zhou, C. (2001b). The term structure of credit spreads with jump risk. *Journal of Banking & Finance*, 25(11):2015–2040.
- Zucca, C. and Sacerdote, L. (2009). On the inverse first-passage-time problem for a Wiener process. *The Annals of Applied Probability*, 19(4):1319–1346.